Received 14 August 2024; revised 27 August 2024; accepted 3 September 2024. Date of publication 5 September 2024;
date of current version 18 September 2024. The review of this article was arranged by Associate Editor Federico Baronti.

Digital Object Identifier 10.1109/OJIES.2024.3455239

Battery Energy Storage Systems in Microgrids: A Review of SoC Balancing and Perspectives

THALES AUGUSTO FAGUNDES [1], GUILHERME HENRIQUE FAVARO FUZATO [2] (Member, IEEE), LUCAS JONYS RIBEIRO SILVA [1], AUGUSTO MATHEUS DOS SANTOS ALONSO [1] (Member, IEEE), JUAN C. VASQUEZ [3] (Senior Member, IEEE), JOSEP M. GUERRERO [3,4,5] (Fellow, IEEE), AND RICARDO QUADROS MACHADO [1] (Senior Member, IEEE)

[1]Sao Carlos School of Engineering, University of Sao Paulo, Sao Carlos, SP 13566-590, Brazil
[2]Federal Institute of Education, Science and Technology of Sao Paulo, Campinas, SP 01109-010, Brazil
[3]Center for Research on Microgrids (CROM), AAU Energy, Aalborg University, 9220 Aalborg East, Denmark
[4]CROM, Department of Electronic Engineering, Technical University of Catalonia, 08034 Barcelona, Spain
[5]ICREA, 08010 Barcelona, Spain

CORRESPONDING AUTHOR: THALES AUGUSTO FAGUNDES (e-mail: thales.fagundes@usp.br).

This work was supported in part by the Coordination for the Improvement of Higher Education Personnel (CAPES) under Grant PDSE-88881.187771/2018-01, Grant 88881.030370/2013-0, and Grant 88887.482911/2020-00, in part by the National Council for Scientific and Technological Development (CNPq) under Grant 309624/2018-5 and Grant 312664/2021-4, in part by the Sao Paulo Research Foundation (FAPESP) under Grant 2013/20721-4, Grant 2020/05865-3, Grant 2022/02721-6, and Grant 2022/00628-9, and in part by the *PróReitoria de Pesquisa e Inovação da USP* (PRPI) under Grant 2022.1.9345.1.2 - Centro 49000/49053.

ABSTRACT Microgrids (MGs) often integrate various energy sources to enhance system reliability, including intermittent methods, such as solar panels and wind turbines. Consequently, this integration contributes to a more resilient power distribution system. In addition, battery energy storage system (BESS) units are connected to MGs to offer grid-supporting services, such as peak shaving, load compensation, power factor quality, and operation during source failures. In this context, an energy management system (EMS) is necessary to incorporate BESS in MGs. Consequently, state-of-charge (SoC) equalization is a common approach to address EMS requirements and balance the internal load among BESS units in MG operation. In this article, we present a comprehensive review of EMS strategies for balancing SoC among BESS units, including centralized and decentralized control, multiagent systems, and other concepts, such as designing nonlinear strategies, optimal algorithms, and categorizing agents into clusters. Moreover, in this article, we discuss alternatives to improve EMS and strategies regarding the topology of power converters, including redundancy-based topology, modular multilevel converter, cascaded-based converter, and hybrid-type systems. In addition, this article explores optimization processes aimed at reducing operational costs while considering SoC equalization. Finally, second-life BESS units are explored as an emerging topic, focusing on their operation within specific power converters topologies to achieve SoC balance.

INDEX TERMS Battery energy storage system (BESS), centralized control, decentralized control, multiagent system, state-of-charge (SoC) equalization.

NOMENCLATURE

Abbreviations

MG	Microgrid.
NG	Nanogrid.
ESU	Energy storage unit.
ESS	Energy storage system.
HESS	Heterogeneous ESS.
BESS	Battery ESS.
2-BESS	Second-life BESS unit.
FC	Fuel cell.
SoH	State-of-health.
EMS	Energy management system.
SoC	State-of-charge.
FIS	Fuzzy inference system.
p.u.	Per unit.
PV	Photovoltaic.
HIL	Hardware-in-the-loop.
UC	Ultracapacitor.

SC	Supercapacitor.
PI	Proportional–integral.
DoD	Depth of discharge, DoD = 1 − SoC.
GA	Genetic algorithms.
Ah	Ampere-hour.
RAh	Reflected ampere-hour capacity.
LQR	Linear quadratic regulator.
MMC	Modular multilevel converter.
DPP	Differential power processing.
PSO	Particle swarm optimization.

Variables and constants

BESS_i	i−th BESS.
$\mathrm{SoC}(t)$	SoC at time t.
$\mathrm{SoC}(t_0)$	Initial SoC at reference time t_0.
SoC_i	SoC from the ith BESS unit.
$\mathrm{SoC}_{\mathrm{avg}}$	Average value from the SoC of all BESS units.
$\Delta\mathrm{SoC}$	Difference between $\mathrm{SoC}_{\mathrm{avg}}$ and SoC_i.
$\mathrm{SoC}_{\mathrm{avg}i}$	Local SoC average value.
$\mathrm{SoC}_{\mathrm{opti}}$	Optimized SoC for the ith BESS unit.
$\Delta\mathrm{SoC}_{\mathrm{oper}i}$	Operation range of SoC for the ith BESS unit.
$\mathrm{SoC}_{\min}$	Minimum SoC value.
$\mathrm{SoC}_{\max}$	Maximum SoC value.
$\mathrm{SoC}_{\mathrm{avg}\_p}$	Step ahead prediction of $\mathrm{SoC}_{\mathrm{avg}}$.
SoC_{i_p}	Step ahead prediction of SoC_i.
SoC_f	Final SoC value from EMS.
DoD_i	DoD from the ith BESS unit.
$\mathrm{DoD}_{\mathrm{avg}}$	Average value from the DoD of all BESS units.
C_{bat}	BESS capacity.
$C_{\mathrm{bat}i}$	Capacity of i− th BESS unit.
$C_{\mathrm{bat\_max}}$	Maximum capacity of BESS units.
$C_{\mathrm{bat\_avg}}$	Average capacity of BESS units.
i_{BESS}	BESS current.
i_{BESSi}	BESS current from the i− th BESS unit.
v_o	DC-link voltage.
v_{ref}	DC-link voltage reference.
r_d	Virtual resistance.
$k_{\mathrm{SoC}i}$	SoC-based droop parameter from the i -th BESS.
i_{BESS_outi}	Output current from the i -th dc/dc converter.
ω	Output angular frequency.
ω_{ref}	Rated angular frequency.
m_d	Droop coefficient.
P_B	Output power from the i -th BESS unit.
PI_i	PI current control from the i -th BESS unit.
PI_v	PI voltage control from the i -th BESS unit.
i_{refi}	Current reference from the i -th BESS unit.
I_{bat_rated}	Rated BESS current.
Δv_o	Voltage range in the dc-link.
p	Constant value.
$\mathcal{G}$	Communication graph of MG.
$\mathcal{V}$	Nodes set - each BESS unit in $\mathcal{G}$.
$\mathcal{E}$	Edges set - the communication links among BESS.
$\mathcal{A}$	Adjacency matrix, $\mathcal{A} = [a_{ij}] \in \mathbb{R}^{N\times N}$.
$\mathcal{N}_i$	Set of neighbors of the i -th BESS unit.
$\mathcal{D}$	Degree matrix, $\mathcal{D} = \mathrm{diag}\{d_{ii}\} \in \mathbb{R}^{N\times N}$.
$\mathcal{L}$	Laplacian matrix, $\mathcal{L} = \mathrm{diag}\{l_{ij}\} \in \mathbb{R}^{N\times N}$.
γ	State variables.
x	Local input.
κ	Integrator gain from the diffusion algorithm.
χ_i	Virtual state variable.
χ_{avgi}	Average virtual state variables.
σ_i	Transition factors.
ρ	Gain in the range [0-1].
$\Delta v_{\max}$	Maximum Δv.
Δv_{v_i}	Fictitious voltage drop.
K_{opti}	Optimized convergence parameter.
m	Convergence factor.
ψ	Adaptive variables for the BESS units.
μ	Constant step size.
ξ_i	Intermediate variables for $BESS_i$.
ξ_j	Intermediate variables for $BESS_j$.
v_{ref_min}	Minimum value of v_{ref}.
v_{ref_max}	Maximum value of v_{ref}.
α	Constant value.
β	Constant value.
$PI_{\mathrm{SoC}}(s)$	PI controller from SoC.
i_{BESS_avg}	Average value from i_{BESS}.
i_{BESS_total}	Total current value of all BESS units.
i_{BESS_max}	Maximum current value of a BESS unit.
i_{BESS_min}	Minimum current value of a BESS unit.
OCV	Open circuit voltage from BESS.
v_{BESS}	Instantaneous BESS unit voltage.
V_{bat}	Average output BESS voltage.
r_i	Internal resistance of BESS units.
r_0	Initial value of the virtual resistance.
$r_{\min}$	Minimum value of the virtual resistance.
$r_{\max}$	Maximum value of the virtual resistance.
P_{load}	Power from dc load.
P_{PV}	Power from PV.
$P_{\max}$	Maximum power from the MG.
P_{ref}	Power reference from the MG.
P_{rating}	Power rating.
$P_{B\_\max}$	Maximum power of a BESS unit.
N	Total number of BESS units in the MG.
$P_{B\_\min}$	Minimum power of a BESS unit.
P_{B_total}	Total power from all BESS units.
P_{grid}	Power applied on grid.
$P_{grid\_\max}$	Maximum power applied on grid.
k_i	Coefficient factor.
k_0	Initial value from the coefficient factor.
k_{grid}	Coefficient factor from power grid.
$k_{\min}$	Minimum value from the coefficient factor.
$k_{\max}$	Maximum value from the coefficient factor.
k_s	Coefficient factor.
k_λ	Load adjustment factor.
Δk_{FIS}	Coefficient obtained by FIS.
n	Order factor.
f	Frequency parameter.
f_{ref}	Frequency reference.
$f_{\min}$	Minimum value of frequency.
δf_{rest}	Frequency restoration.

$\delta f_{charging}$	Frequency for the charging controller.
δf_{power}	Frequency from the power limit.
τ	Constant time.
$\hat{v}_{dci}$	Output estimated voltage.
k_{pvi}	Control parameter.
k_{ivi}	Control parameter.
k_{is}	Control parameter.
k_{id}	Control parameter.
k_{iP}	Constant parameter.
k_{iB}	Constant parameter.
u_{iB}	Control input for SoC equalization.
$u_{i\omega}$	Control input for frequency recovery.
G_{vi}	Transfer function from voltage controller.
G_{bati}	Transfer function from consensus.
ζ_i	Connection between agents i and j.
ϑ_{ij}	Accumulative SoC error.
i_{dppi}	DPP converter current.
v_{dppi}	DPP converter input voltage.
$i_{fe,\alpha}$	Front-end converter current.
$i_{fe,\beta}$	Front-end converter current.
v_{fe}	Front-end converter input voltage.
v_{dc}	Front-end converter output voltage.
α_{sig}	Constant factor that modifies the sigmoid function.

I. INTRODUCTION

In recent decades, the deployment of microgrids (MGs) has increased as an alternative to traditional thermal power plants, and the implementation of energy storage units (ESUs) has consequently risen striving to improve the efficiency of alternative energy sources and targeting the provision of grid-supporting services [1], [2]. Thus, the benefits of ESUs in the operation of MGs include frequency and voltage regulation, grid management, and the reduction of emissions and costs. For example, some projects [3], such as AURORA by the U.S. Department of Energy, have been implemented to incorporate ESUs. In addition, the government of Singapore invested in the Asia project ACCESS, while France created Grid4EU in Europe, and The Netherlands initiated the 24 MW/48 MWh project. All of these projects have resulted in the integration of ESUs into grid operations. Furthermore, major companies, such as Google, have also introduced ESUs to collaborate with power production [3]. The most applied technology for ESU is the battery energy storage system (BESS) units, due to factors, such as cost, service life, dynamic response time, and the ability to rapidly absorb or deliver power [3]. In this context, according to [4], [5] the importance of BESS units is defined as follows.

1) *Supporting power demand:* Upon operation considering intermittent alternative sources, such as solar systems and wind turbines, BESS units can provide energy dispatch to the grid during periods of low power production from these sources.
2) *Peak shaving:* BESS units can be charged during periods of low demand on the grid and discharged when demand increases. As a result, such an energy service can reduce the cost of MG operation.
3) *Islanded operation:* If there is any issue related to the main grid, such as a fault or maintenance interruptions, BESS units can be responsible for maintaining the delivery of power to local loads and consumers.
4) *Electric power conditioning:* BESS units can regulate voltage and frequency within the MG. As a result, the reliability of the system is improved, and the power quality regulation is enhanced.
5) *Load compensation:* BESS units can be used to mitigate or absorb load transients from the grid. In this context, critical loads can be protected, and sensitive energy systems' components, such as fuel cell (FC) membranes, if integrated into the MG, can also be safeguarded.

To reduce the cost of BESS units, it is necessary to ensure a long cycle life during various operation modes. One of the first actions is to maintain the state-of-charge (SoC) within a specific range, for instance, between 20% and 80% for MGs or 30% and 80% for electric vehicles [6], [7].

Furthermore, as noted in [8], variations in the manufacturing process can lead to different characteristics in BESS units, even when they have the same nominal parameters. In this context, the SoC among all units could diverge during similar charging/discharging operations.

Thus, implementing an energy management system (EMS), also referred to as secondary control, can maintain the SoC of BESS units at the same level, maximizing power capacity and minimizing the risk of any single BESS unit operating outside the desired SoC range [6]. As a result, the BESS units employed in the MG reduce their damage or degradation, thereby extending their lifespan. In this perspective, the EMS can be responsible for avoiding excess charging/discharging and ensuring that the SoC among BESS units is balanced.

In addition, it is important to note that the depth of discharge (DoD) is a parameter of BESS units that is the complement of the SoC. While SoC represents the amount of charge currently in the BESS unit relative to its capacity, DoD refers to the percentage of the BESS's capacity that has been discharged. Therefore, the relationship is defined as DoD = 1 − SoC, meaning that BESS units with high levels of SoC have lower levels of DoD (i.e., the BESS unit is more charged), while BESS units with low SoC have higher levels of DoD (i.e., the BESS unit is more discharged) [9]. In this context, this complementary relationship is crucial for the EMS of BESS units, as effectively managing the SoC helps in controlling the DoD, which impacts the performance of BESS units.

Although the BESS units may operate at different power levels to achieve SoC equalization, after the SoC equalization, the units will operate with similar SoC levels. Consequently, BESS units operating with the same SoC may degrade their state-of-health (SoH) equally, thereby enhancing BESS unit operation in MGs, as indicated in [10] and [11]. Therefore, the main benefits of SoC balance are outlined as follows [12], [13], [14], [15], [16], [17].

1) *Improved voltage condition:* Noting that the voltage terminal for the BESS units are dependent on SoC, achieving balanced SoC condition ensures that the existing BESS units within the MG operate at the same voltage level altogether.
2) *Enhancing BESS operation within EMS:* By considering the SoC, the EMS prevents overcharging and overdischarging, avoiding thermal stress and voltage reduction. The BESS voltage reflects its SoC; that is, a lower SoC indicates a lower output voltage, while a higher SoC results in a higher output voltage. Thus, with an intelligent EMS that avoids overcharging and overdischarging, there is no need to disconnect BESS units that might encounter issues. This approach prevents delays in reconnecting them and minimizes any impact on power demand that depends on BESS power in MG operation.
3) *Improving power delivery:* All BESS units can deliver power according to their capacity and internal charge. Consequently, the reliability of the system is heightened as BESS units provide uniform energy to the MG.

The MG's EMS (i.e., secondary control) topology can be categorized as centralized, decentralized, and distributed multiagent. In a centralized approach, the MG employs a central controller that monitors the entire system using a communication link among sources [18], [19]. Regarding the EMS for SoC balance in BESS units, the central controller possesses information about all BESS units operating in the system, including the real-time dynamics of SoC [20], [21]. In this context, if a new source or BESS is added to the MG configuration, the central controller needs to be reconfigured. In addition, another drawback of centralized control is the occurrence of failure or maintenance, which affects the entire operation of the MG [22], [23].

To address this issue, decentralized control employs EMS based on local information without the need to exchange data among sources [4], [24]. The most common strategy for decentralized EMS is droop control, which is based on a deviation of voltage between the reference and the measured voltage [25], [26]. When applied to a power converter, this deviation is directly proportional to the current from this device, and the proportional term is often referred to as virtual resistance when the strategy is applied to dc MGs [17], [27]. In the case of ac MGs, droop control can adjust the frequency or be applied to adjust the voltage amplitude from the main grid according to the desired power sharing [21], [24], [28].

Regarding SoC equalization, the classic droop control can be modified, which is named SoC-based droop. This approach can then be centralized or decentralized, depending on the droop coefficient, i.e., if the BESS unit provides information that is processed in a central controller (centralized control) or locally (decentralized control) [20], [29].

Aiming at a distributed multiagent system, coordination among sources and BESS units occurs through local information and communication among agents neighbor-to-neighbor to make the best decisions in order to achieve specific goals or tasks, such as power delivery, voltage secondary control, tertiary level (optimal power flow), and SoC equalization for BESS units. In this context, a distributed multiagent system has robustness derived from centralized control and can enhance performance compared to decentralized control [4]. Nevertheless, such a control topology still relies on the effectiveness of communication links [30].

On a different perspective, the topology of power converters also plays an important role in the EMS implementation for MGs. With regards to SoC equalization for BESS units, the most commonly structure involves bidirectional dc/dc converters for dc MGs, and inverters for ac MGs in parallel connection. Furthermore, proposed topologies found in the literature aim to enhance the operation of BESS units and, consequently, the EMS designed for them. Thus, some researchers have introduced the employment of hybrid-types systems and the design of a multiport converter that shares multiple BESS units [11]. As a result, the number of traditional converters is reduced, helping to avoid bulky circuit sizes and reducing the overall configuration cost [31].

An example that can enhance the operation of BESS units is the topology of a MG based on redundancy. Parallel modules play a crucial role in providing increased reliability during uncertain events, such as faults or cyberattacks, and they are also beneficial for maintenance purposes [32]. Redundancy-based MGs, for instance, are vital for alleviating problems in systems that cannot afford to be inoperative, such as military devices, aerospace MGs, medical centers, and shipboard MGs [33], [34]. The redundancy approach aims to maintain SoC balancing in BESS units during the aforementioned events [35].

Moreover, in shipboard MGs, the SoC among BESS units may exhibit discrepancies during system operation. As proposed by Chen et al. [36], the bidirectional modular multilevel converter (MMC) for shipboard MGs can simplify installation, maintenance, and manufacturing processes. In addition, it can provide a high output voltage, a compact structure, flexibility in power control, and fault-tolerant capability. Therefore, when considering SoC among BESS units in a shipboard setting, discrepancies may arise due to navigational uncertainties, the transition of aging BESS units to other devices, fault-tolerant events, and the load variation compensation provided by the BESS, which aims to protect the vessel from pulse strikes [14], [37].

Considering optimization as the tertiary level to improve the EMS (which is the secondary level), the authors from [11] argue that this optimization, operating alongside SoC equalization, is a developing area. Another emerging topic is the handling of second-life BESS (2-BESS) units repurposed for applications in MGs [38]. This review also addresses studies related to power converters that accommodate 2-BESS units and the parameters required for their operation within the SoC equalization methodology in MGs.

Almost all review articles found in the literature are limited to ESU, characteristics, drawbacks, and benefits for MG applications [39]. In addition, the work in [4] and [12] are restricted to control strategies for ESS; however, they provide a brief overview of BESS units and SoC equalization. In [12], the explanation of ESS units regarding communication–centralized, decentralized, and multiagent–is provided, but only a subsection considering SoC-based droop control is elaborated on. In contrast, Saadi et al. [4] focused on SoC-based droop control and power converter topologies but does not take into account centralized SoC-based droop control, optimization performance under SoC equalization, nonlinear functions based on S-shaped functions, and other approaches that achieve SoC equalization, such as reflected ampere-hour (RAh) capacity, fuzzy inference system (FIS) without droop control, proportional power sharing, and adaptive current sharing. In addition, neither review elaborates on the perspective of dividing BESS units in operation into cluster agents, which can be considered an emerging topic regarding BESS units, along with the perspective of incorporating 2-BESS in EMS.

Therefore, this article strives for providing information about the deployment of BESS units in MGs, focusing on the implementation of EMS with SoC equalization, as well as discussing the strategies adopted to enhance the coordination task and system reliability, such as the power converters topology and optimization as tertiary level.

The rest of this article is organized as follows. Section II focuses on the BESS model and SoC estimation as they relate to the EMS. Moreover, Section III provides an overview of the EMS designed for BESS units, including challenges and possible solutions. Then, Section IV presents an overview of centralized control, including the centralized SoC-based droop, while Section V provides information about decentralized control, along with common SoC-based droop without communication, non-linear functions for employing EMS, FIS, and optimal algorithms. Following this, Section VI reviews multiagent system control, including the consensus approach and diffusion algorithm. Section VII focuses on hybrid-type systems, while Section VIII explains how the topology of power converters can enhance the EMS for BESS units. Moreover, Section IX focuses on optimization as tertiary control, and Section X discusses how to handle 2-BESS units to operate in MGs and achieve SoC equalization. Finally, Section XI concludes this article.

II. PRELIMINARIES

A. BESS MODEL

Several models of BESS units have been discussed to define their performance, such as electrochemical model, electric circuit model, and neural networks model [40]. Thus, the EMS from [40], [41], [42], and [43], considered a first-order circuit model, with the output voltage v_{bat} defined as follows:

$$v_{\text{BESS}} = \text{OCV} - i_{\text{BESS}} r_i - i_{\text{BESS}} r_1 \left[1 - \exp\left(-\frac{t}{r_1 C_1} \right) \right] \tag{1}$$

with OCV being the open circuit voltage, i_{bat} the BESS current, r_i the internal resistance, $r_1 C_1$ representing the BESS relaxation process, and t the time. In addition, the Belal et al. [44] considered the equivalent electric model proposed in [45].

Finally, considering MGs and the higher level application of EMS and SoC equalization, the nonlinearities of BESS units could be neglected since a large number of researchers are focusing on studying SoC dynamics under EMS and SoC equalization.

B. SOC ESTIMATION

There are several methods for SoC estimation in the literature, according to [46], [47], and [48]. Usually, when they discuss SoC balancing for MGs, the most common methodology is the Coulomb counting method, as follows:

$$\text{SoC}(t) = \text{SoC}(t_0) + \frac{1}{C_{\text{bat}}} \int_{t_0}^{t} i_{\text{BESS}}(\tau)\, d\tau \tag{2}$$

where $\text{SoC}(t)$ is the SoC at time t, $\text{SoC}(t_0)$ is the initial SoC at the reference time t_0, C_{bat} is the nominal capacity of the battery, $i_{\text{BESS}}(\tau)$ is the current at time τ.

This method assumes that the initial SoC, $\text{SoC}(t_0)$, is known (for lab-scale prototypes, an arbitrary value is usually chosen), and that the current is accurately measured over time. Since this methodology is the simplest for SoC estimation and it is easy to implement, papers on EMS often focus on the dynamics of parameters related to SoC equalization, such as current from BESS units and other sources, power on loads, and voltage levels. Thus, when the study is about EMS, some authors reference other papers that address SoC estimation and discuss its accuracy.

As the review focuses on EMS regarding SoC balancing, most of the literature considers the Coulomb counting method. However, BESS units exhibit nonlinearities that can impact the accuracy of SoC estimation. Consequently, some authors compare the dynamics obtained from experimental results using hardware-based approaches with those from software that accounts for BESS nonlinearities, such as PSIM, MATLAB/Simulink, and PSCAD [17], [28], [49]. Others directly validate the approach using hardware-in-the-loop (HIL) systems that consider BESS nonlinearities, such as Typhoon HIL [11], [50], OPAL-RT [19], [31], [51], and RTDS Technologies, real-time digital simulator [16], [26], [52].

III. ENERGY MANAGEMENT SYSTEM

An EMS is essential for managing renewable energy sources and BESS units in MGs. It coordinates power flow and sustains system stability through load demand monitoring and SoC equalization for BESS units [53]. Consequently, it manages dc-link voltage or ac-link bus operations. The controllers present in the MG face the challenge of managing and equalizing the SoCs of BESS units with the supervision of injected or absorbed current from the dc-link/ac-link, considering additional sources, such as FC and photovoltaic (PV) panels.

The equalization approach should supply more power to BESS units with low SoC while reducing power absorption from units with high SoC. Conversely, during power demand

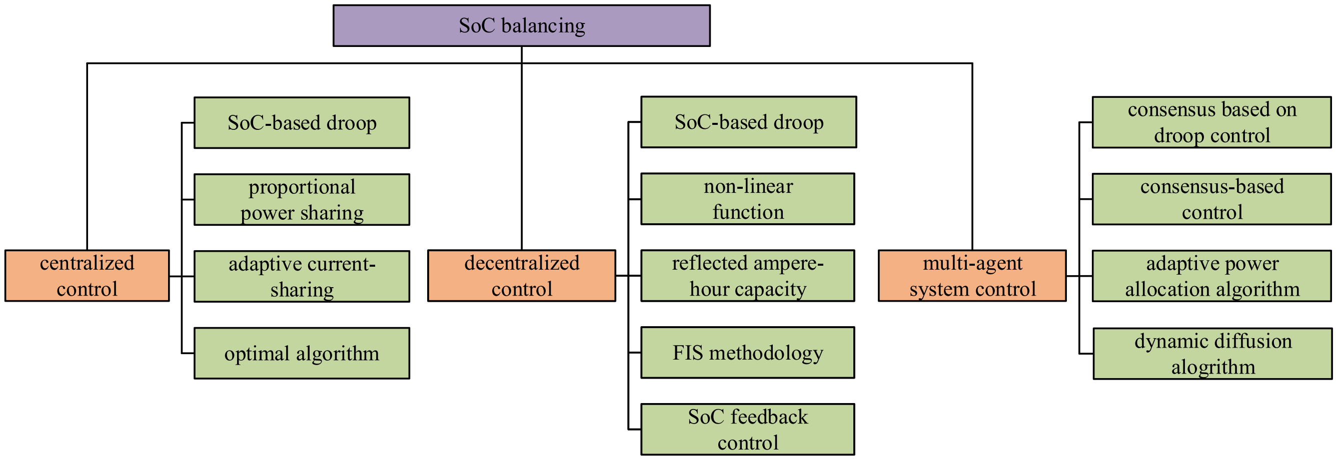

FIGURE 1. **Flowchart of existing methodologies for SoC balancing.**

from the dc-link or ac-link, BESS units with high SoC can provide more power than those with lower SoC. Hence, such a process of charging/discharging leads to the convergence of SoC in BESS units.

The EMS provides efficient coordination among all BESS units and other sources, such as FC and PV panels, whether in a centralized, decentralized manner, or through multiagent system control. It maintains balance in the SoC of BESS units while supplying power to the load connected to the dc-link or ac-link. Thus, the EMS for BESS ensures the balance of SoC in the MG, allowing BESS units to operate with similar charging currents. Since the SoC changes slowly due to BESS capacity, the EMS also handles power and current management effectively.

A. COMPARATIVE SUMMARY: MAIN APPROACHES FROM THE LITERATURE

From the literature, a wide range of methodologies for SoC balancing has been proposed in MGs, as indicated in Fig. 1 and discussed in this study. Therefore, Tables 1, 4, and 8 present a comparative summary of methodologies for MGs, encompassing centralized, decentralized, and multiagent system communication. In this context, the aforementioned tables compare the type of MG (dc, ac, or ac/dc), the topology of power converters composing the MG, the EMS-based type, whether the EMS also operates with voltage or frequency regulation, whether it combines ultracapacitors (UCs) and supercapacitors (SCs) into the MG, and whether it operates at islanded or grid-connected mode. In addition, Tables 2, 5, 9, and 10 provide the strengths and drawbacks of the approaches. Thus, in the following sections the approaches are described in more details.

TABLE 1. **Comparative Summary: Centralized Methodologies**

		Centralized
MG Type	dc	[9], [13], [20], [49], [54], [55], [56], [57], [58], [59], [60], [61], [62], [63], [64], [65], [66], [67]
	ac	[21], [24], [68]
	ac/dc	[69]
Topology of power converters	conventional	[9], [13], [20], [21], [24], [49], [54], [55], [56], [57], [58], [59], [60], [61], [62], [63], [64], [65], [66], [67], [68], [69]
EMS Type	SoC-based droop	[9], [20], [21], [24], [49], [54], [55], [56], [57], [58], [59], [60], [61], [62], [63], [64], [68]
	proportional power sharing	[69]
	adaptive current control	[65]
	optimal algorithm	[13], [66], [67]
voltage or/and frequency regulation	✓	[9], [20], [54], [56], [57], [59], [68], [60], [61], [64], [66], [69]
	X	[49], [55], [58], [62], [13], [21], [24], [63], [65], [67]
combination with UCs/SCs	✓	[54], [67]
	X	[21], [49], [55], [58], [62], [63], [64], [68], [13], [24], [65], [66]
Islanded Mode	✓	[9], [20], [49], [54], [55], [56], [57], [58], [59], [60], [61], [62], [13], [21], [24], [63], [64], [65], [67], [68], [69]
	X	[66]
Grid Connected	✓	[66], [69]
	X	[20], [49], [54], [55], [56], [57], [58], [59], [60], [13], [21], [24], [61], [62], [63], [64], [65], [67], [68]

IV. CENTRALIZED CONTROL

According to [12], the centralized strategy can be implemented for secondary and tertiary control levels. Thus, the operation of all sources is managed through continuous communication among them, providing a comprehensive perception of the entire MG and ensuring that the BESS functions within an acceptable range, as indicated by Fig. 2.

In this context, as the centralized control is dependent on a central control unit, this disadvantage is a single point that can impact all coordination among sources when facing a malfunction, compromising the flexibility and reliability of the system [70]. Thus, centralized control is suitable for sources that are in close proximity to each other because it requires high-bandwidth communication links. This section covers approaches with centralized communication, with Tables 1 and 2 presenting a comparative summary of the literature

TABLE 2. Comparative Summary: Strengths and Drawbacks of Centralized Methodologies

Strategy	Strengths	Drawbacks
[9]	Power sharing among BESS units considering the effect of resistance line in the MGs	This strategy demands a complex and expensive central network to exchange information among BESS units, which can result in a single point of failure. In addition, considerable PI controllers are applied, resulting in a high order of the system, which can impact stability analysis.
[54]	The strategy also operates with failure and considers different capacities of BESS units and line impedance	This strategy demands a complex and expensive central network to exchange information among BESS units for calculating SoC and average current, which can result in a single point of failure.
[55]	Employment of droop parameter weights by SoC	This strategy demands a complex and expensive central network to exchange information among BESS units, which can result in a single point of failure.
[20], [56], [57], [58]	The equalization is achieved thanks to the incorporation of the SoC into a virtual dc machine control	The virtual inertia strategy demands a challenging and complex implementation. Moreover, while the method is suitable for high-frequency converters, providing inertia for a stable dc-link in low switching frequency converters presents a significant difficulty.
[49]	The droop parameter is based on exponential function, allowing faster equalization	The inconsistency of line impedance is not taken into account. This method can cause dc-link voltage deviation and can only identify SoC differences in the later stages of SoC balancing, leading to slower SoC convergence.
[59]	The droop parameter is adjusted by FIS, and the voltage recovery control can correct the error in the dc-link voltage.	The implementation into other dc MGs could be complex.
[60]	The virtual resistance is based on an arc tangent function, which helps to accelerate SoC balancing.	The virtual resistance varies depending on whether the current is charging or discharging and whether the SoC of the ith BESS unit is higher or lower than the average value. Thus, there are four different virtual resistances.
[61]	This approach is able to avoid power distribution deviations and achieve accurate output power.	The droop parameter varies depending on whether the current is charging or discharging and whether the SoC of the ith BESS unit is higher or lower than the average value. Thus, there are four different virtual resistances.
[62]	A sample and holder are introduced for the droop control to be modified in accordance with the load sharing error and SoC error at each sample period	This strategy relies on a communication system, making it impractical for geographically dispersed MGs. Moreover, it involves high costs and complexity, low efficiency and scalability, limited flexibility, and lacks plug-and-play capability.
[63]	It is suitable to balance BESS units with different capacities	This strategy relies on a communication system, making it impractical for geographically dispersed MGs. Moreover, it involves high costs and complexity, low efficiency and scalability, limited flexibility, and lacks plug-and-play capability.
[64]	A reduced-order generalized integrator can suppress output voltage unbalance and 5th and 7th harmonics.	The SoC_{avg} should be calculated in central control, creating a single point of failure.
[21], [68]	The approach can be integrated into active generators, allowing the BESS units to reduce the intermittency of the RES	This strategy relies on a communication system, making it impractical for geographically dispersed MGs. Moreover, it involves high costs and complexity, low efficiency and scalability, limited flexibility, and lacks plug-and-play capability.
[24]	The droop parameter is based on exponential function, allowing faster equalization	The droop control cause variations in the frequency.
[69]	SoC equalization is achieved, in both sides of the grid	Because communication is centralized, extensive deployment in MGs is not practical.
[65]	An adaptive current distribution coefficient is designed to adjust the current reference according to SoC	Due to the arbitrary parameters, the implementation into another approach may be complex.
[13]	GA enables the SoC balancing and reduction of power delivered/absorbed	Implementing three optimizations within an EMS introduces complexity and demands substantial computational effort.
[66]	The EMS takes into account the parameter limits of the BESS units.	The SoC equalization may not be effective in some scenarios.
[67]	The optimal algorithm does not require significant computational effort.	The current from BESS units is oscillatory.

review, including the main characteristics, strengths, and drawbacks.

A. CENTRALIZED SOC-BASED DROOP

The most common strategy for SoC balance in an EMS implemented for MGs is the SoC-based droop, which is derived from the traditional droop with the coefficient modified based on SoC information. Although the droop control is a decentralized strategy, the central information must typically receive the SoC data from all BESS units present in the MG to manage the operation of all sources concerning EMS and primary control. Generally, the SoC-based droop is derived from (3) for dc MGs

$$v_o = v_{\text{ref}} - r_d k_{\text{SoC}} i_{\text{BESS\_out}} \tag{3}$$

with v_o as the dc-link voltage, v_{ref} as the dc-link voltage reference, r_d as the virtual resistance, k_{SoC} as a droop factor, which functions based on the SoC information from all BESS units, taking the common average value from all SoC measurements, and $i_{\text{BESS\_out}}$ representing the output current from the dc/dc converter. Furthermore, Table 3 presents an overview of the equations from the EMS, highlighting some examples based on (3) and modifications thereof.

For the scenario involving dc MGs, the SoC equalization method, as proposed by [9], is centralized. This is because the equivalent droop coefficient is determined by a proportional–integral (PI) controller based on the SoC and DoD for the ith BESS unit, as well as the average value across all BESS units. Similarly, Kewei et al. [54] proposed a polynomial function dependent on the SoC and current from each BESS unit, as well as the average value among all units. This function is then added to the traditional droop control, making it possible for the EMS to achieve SoC equalization due to the additional term, which includes the SoC of the ith BESS unit and the average value among all units.

TABLE 3. Comparison of EMS for DC MGs—Centralized SoC-Based Droop

Strategy	EMS Equations
[9]	$v_o = \begin{cases} v_{\mathrm{ref}} - (k_{\mathrm{SoC}} + PI_{\mathrm{SoC}}(s)(\mathrm{SoC_{avg}} - \mathrm{SoC}_i))\,P_B, & \text{if } P_B > 0 \\ v_{\mathrm{ref}} - (k_{\mathrm{SoC}} + PI_{\mathrm{SoC}}(s)(\mathrm{DoD_{avg}} - \mathrm{DoD}_i))\,P_B, & \text{if } P_B < 0 \end{cases}$
[54]	$v_o = v_{\mathrm{ref}} - k_{\mathrm{SoC}} i_{\mathrm{BESS\_out}} + \cdots$ $\cdots + \sum_{i=1}^{n} \left(a(\mathrm{SoC}_i - \mathrm{SoC_{avg}}) - b(i_{\mathrm{BESS\_out}} - i_{\mathrm{BESS\_avg}})\right)$
[55]	$v_o = v_{\mathrm{ref}} - r_d k_{\mathrm{SoC}} i_{\mathrm{BESS\_out}}$
[49]	$v_o = v_{\mathrm{ref}} - r_d k_{\mathrm{SoC}} i_{\mathrm{BESS\_out}}$, with $k_{\mathrm{SoC}} = \begin{cases} \exp[-p(\mathrm{SoC}_i - \mathrm{SoC_{avg}})], & \text{if } i_{\mathrm{BESS\_out}} > 0 \\ \exp[p(\mathrm{SoC}_i - \mathrm{SoC_{avg}})], & \text{if } i_{\mathrm{BESS\_out}} < 0 \end{cases}$
[59]	$v_o = v_{\mathrm{ref}} - k_{\mathrm{SoC}} i_{\mathrm{BESS\_out}}$, with $k_{\mathrm{SoC}} = \begin{cases} k_{\min}, & \text{if } \lvert \mathrm{SoC}_i - \mathrm{SoC_{avg}} \rvert > 2.5\% \\ \mathrm{SoC}_{abs} k_{\max} + \Delta k_{\mathrm{FIS}}, & \text{if } \lvert \mathrm{SoC}_i - \mathrm{SoC_{avg}} \rvert < 2.5\% \end{cases}$ and $\left\lvert \frac{\mathrm{SoC_{avg}} - \mathrm{SoC}_i}{\mathrm{SoC_{avg}} - \mathrm{SoC_{max}}} \right\rvert$
[60]	$v_o = v_{\mathrm{ref}} - r_d i_{\mathrm{BESS\_out}}$, with $r_d = \begin{cases} r_0 + \frac{r_0 - r_{\min}}{\pi/2} k_{\mathrm{arc}}, & \text{if } \mathrm{SoC}_i > \mathrm{SoC_{avg}} \text{ and } i_{\mathrm{BESS\_out}} > 0 \\ r_0 + \frac{r_{\max} - r_0}{\pi/2} k_{\mathrm{arc}}, & \text{if } \mathrm{SoC}_i < \mathrm{SoC_{avg}} \text{ and } i_{\mathrm{BESS\_out}} > 0 \\ r_0 + \frac{r_{\max} - r_0}{\pi/2} k_{\mathrm{arc}}, & \text{if } \mathrm{SoC}_i > \mathrm{SoC_{avg}} \text{ and } i_{\mathrm{BESS\_out}} < 0 \\ r_0 + \frac{r_0 - r_{\min}}{\pi/2} k_{\mathrm{arc}}, & \text{if } \mathrm{SoC}_i < \mathrm{SoC_{avg}} \text{ and } i_{\mathrm{BESS\_out}} < 0 \end{cases}$ with $k_{\mathrm{arc}} = \arctan(-p(\mathrm{SoC}_i - \mathrm{SoC_{avg}}))$
[61]	$v_o = v_{\mathrm{ref}} - k_i P_B, \quad \text{with } k_i = k_0 + m_d \frac{1}{C_{\mathrm{bat}}} \arctan\left(\frac{\Delta \mathrm{SoC}}{\mathrm{SoC}^n}\right),$ with $m_d = \begin{cases} \frac{k_{\max} - k_0}{\pi/2}, & \text{if } \mathrm{SoC}_i > \mathrm{SoC_{avg}} \text{ and } i_{\mathrm{BESS\_out}} > 0 \\ \frac{k_0 - k_{\min}}{\pi/2}, & \text{if } \mathrm{SoC}_i < \mathrm{SoC_{avg}} \text{ and } i_{\mathrm{BESS\_out}} > 0 \\ \frac{k_0 - k_{\min}}{\pi/2}, & \text{if } \mathrm{SoC}_i < \mathrm{SoC_{avg}} \text{ and } i_{\mathrm{BESS\_out}} < 0 \\ \frac{k_{\max} - k_0}{\pi/2}, & \text{if } \mathrm{SoC}_i < \mathrm{SoC_{avg}} \text{ and } i_{\mathrm{BESS\_out}} < 0 \end{cases}$
[62]	$v_o = v_{\mathrm{ref}} - (k_0 + K_\lambda + k_{\mathrm{SoC}}(\mathrm{SoC}_i - \mathrm{SoC_{avg}}))\, i_{\mathrm{BESS\_out}}$ with $k_\lambda \left(\frac{i_{\mathrm{BESS\_out}}}{C_{\mathrm{bat}i}} - \frac{i_{\mathrm{BESS\_avg}}}{C_{bat\_avg}}\right)$
[63]	$v_o = v_{\mathrm{ref}} - r_d i_{\mathrm{BESS}}$, with $r_d = \begin{cases} 1 - (\mathrm{SoC}_i - \mathrm{SoC_{avg}}) \frac{1}{C_{\mathrm{bat}i}}, & \text{if } i_{\mathrm{BESS}} > 0 \\ 1 - (\mathrm{SoC_{avg}} - \mathrm{SoC}_i) \frac{1}{C_{\mathrm{bat}i}}, & \text{if } i_{\mathrm{BESS}} < 0 \end{cases}$

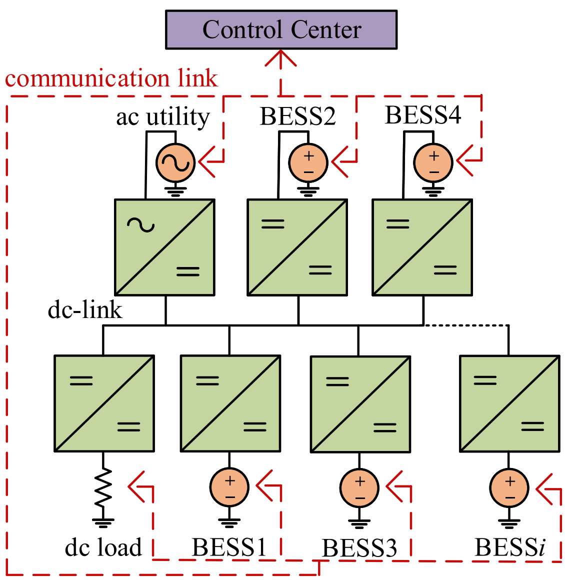

FIGURE 2. Centralized control.

In addition, the approach outlined in [55] is considered centralized because it employs a central controller to define the droop parameter based on SoC in order to modify the droop control and achieve SoC equalization. As proposed in [20], [56], [57], and [58], a centralized control for dc MGs using an SoC-based virtual dc machine can balance the SoC among BESS units, with the works in [20], [56], and [57] also compensating the dc-link with secondary voltage control. In this method, the virtual dc machine can virtually modify the virtual armature resistance when there is a SoC variation. In

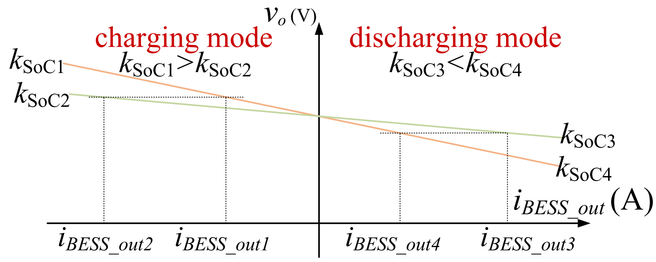

FIGURE 3. Example of SoC-based droop.

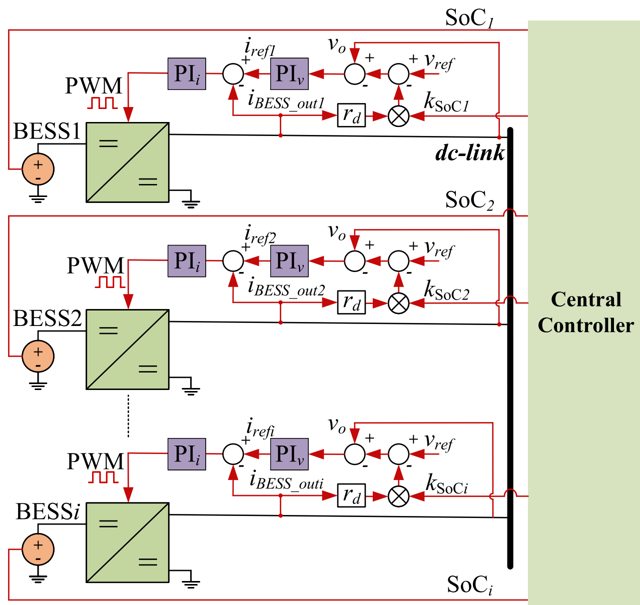

FIGURE 4. Common SoC-based droop control with central controller for dc MG.

addition, an SoC-based droop with a weight factor defined by an exponential function dependent on SoC from the ith BESS unit and the average SoC from all units is elaborated in [49]. Tian et al. [59] proposed a SoC-based droop modified by a FIS. In this method, the inputs of the FIS are parameters dependent on the average SoC and the power released by the BESS units.

Moreover, the authors in [60] and [61] proposed a virtual resistance based on the arc tangent function, which depends on SoC of the ith BESS unit and the average SoC of all units. In addition, in [62], with the employment of a sample and holder, the SoC-based droop parameter is adjusted based on the load sharing error and SoC error (the difference between the average value and the value from the ith BESS unit) at each sampling error. Furthermore, Fig. 3 demonstrates an example of a SoC-based control, with a k_{SoC} being a parameter which depends on SoC from the BESS unit according to it corresponded current $i_{\mathrm{BESS\_out}}$ [63], while Fig. 4 illustrates a common centralized controller for SoC-based droop control in a dc MG. Finally, Chen et al. [64] calculated a value $\Delta i_{\mathrm{ref}} = n(\mathrm{SoC}_i - \mathrm{SoC_{avg}})$ that is added to the current reference from the converter to balance the SoC of the BESS units.

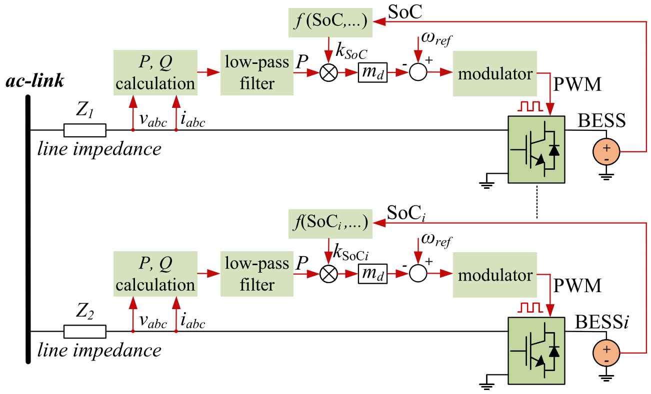

FIGURE 5. Common SoC-based droop control with central controller for ac MG.

With regards to ac MGs, as indicated in [21] and [68], the centralized SoC-based droop approach is derived from the behavior given as follows:

$$\omega = \omega_{\text{ref}} - m_d k_{\text{SoC}} P_B \tag{4}$$

with ω defined as the output frequency, ω_{ref} as the rated frequency, m_d as the droop coefficient, k_{SoC} as the SoC-based droop parameter (which depends on the SoC information from all BESS units), and P_B as the output power from the ith BESS unit.

Regarding certain methods from the literature in ac MGs, Fig. 5 illustrates a common EMS for ac MGs, with $f(\text{SoC},\ldots)$ representing a function defining the droop parameter. The EMS could be centralized, decentralized, or multiagent depending on the approach that processes the SoC and other information within the EMS. For example, the authors in [21] and [68] proposed a centralized control by applying a weight factor similar to (4), which is directly proportional to the BESS unit. Furthermore, Ye et al. [24] achieved SoC equalization with the SoC-based parameter being an exponential function dependent on SoC for the ith BESS unit and the average value among all units, as follows:

$$f = f_{\text{ref}} - \frac{m_d}{C_{\text{bat}}} P_B \exp(-k(\text{SoC}_i - \text{SoC}_{\text{avg}})) \tag{5}$$

where k is a constant, C_{bat} is the BESS unit's capacity, SoC_{avg} is the average SoC of all BESS units, f is the output frequency (Hz), and f_{ref} is the output frequency reference.

Finally, in the case of SoC-based droop in a centralized manner for MGs, a specific parameter should essentially depend on SoC. These parameters include the droop coefficient, virtual resistance, and voltage reference. Most of the presented strategies depend on the average value of SoCs. Although this strategy is simple to implement, a single point of failure in the communication of SoC could impact the SoC balance. This could lead to charging or discharging the BESS units unreliably, causing SoC imbalances and consequently requesting power from BESS units that are more discharged.

B. PROPORTIONAL AND ADAPTIVE POWER SHARING

In this approach, Brandao et al. [69] elaborated on an EMS in a hybrid ac/dc MG, which incorporates BESS units on both sides. The EMS, whose central controller is based on low-bandwidth communication, is designed to facilitate power exchange between the MG buses and the grid. Consequently, proportional power sharing is achieved among the BESS units, operating at a constant SoC in both subgrids. The power charging can be defined as P_{ref} according to (6) for BESS units charging and (7) for discharging mode

$$P_{\text{ref}} = P_{B\_\min}(-\text{SoC}_{\text{avg}})\left(1 + (\text{SoC}_{\text{avg}} - \text{SoC})^p\right) \tag{6}$$

$$P_{\text{ref}} = P_{B\_\max}\text{SoC}_{\text{avg}}\left(1 - (\text{SoC}_{\text{avg}} - \text{SoC})^p\right) \tag{7}$$

with $P_{B_{\min}}$ and $P_{B_{\max}}$ representing the interval of power within which the BESS units operate.

Considering the EMS from [69], it operates as a single controllable entity to provide SoC equalization. However, because time-based signals are used to regulate power flow from various sources, these signals should be synchronized simultaneously.

In [65], an adaptive current-sharing parameter control is used as a function of the SoC from the ith BESS unit and the average SoC from all units. This is determined by the current $i_{\text{BESS}i}$ from the ith BESS unit, which has SoC_i, in a MG with N BESS units

$$i_{\text{BESS}i} = \begin{cases} i_{\text{BESS\_total}} \dfrac{k_s^{p(\text{SoC}_i - \text{SoC}_{\text{avg}})}}{\sum_{j=1}^{N} k_s^{p(\text{SoC}_j - \text{SoC}_{avg})}}, & \text{if charging mode} \\ i_{\text{BESS\_total}} \dfrac{k_s^{p(\text{SoC}_{\text{avg}} - \text{SoC}_i)}}{\sum_{j=1}^{N} k_s^{p(\text{SoC}_{\text{avg}} - \text{SoC}_j)}}, & \text{if discharging mode} \end{cases} \tag{8}$$

where $i_{\text{BESS\_total}}$ is the total current value from the BESS units, and p and k_s are constant parameters. As the value of SoC can dynamically adjust the parameter based on current sharing, SoC balancing can be performed. Compared to droop control, this approach can mitigate problems related to voltage drops on the dc-link and accelerate SoC equalization. However, Qiao et al. [65] operated with arbitrary parameters that could impact the implementation of this EMS in another approach.

C. OPTIMIZATION APPLIED TO BALANCING THE SOC

From the literature, an approach proposed by Ricardo et al. [13] involved operating a MG with genetic algorithms (GA) to ensure balanced SoC for BESS units, while Hosseini et al. [66] proposed a charging station that applies a time-step based optimization to balance the BESS units among the electric vehicles. These techniques are able to achieve BESS unit equalization along with EMS in the MG, which can reduce voltage and frequency variations originating from conventional droop.

In this context, the optimization process obtains parameters from the MG and then provides the optimal current for each BESS unit operate. The process involves the following three steps of optimization in [13].

1) Choosing the SoC and the current from the ith BESS units to minimize the objective function in order

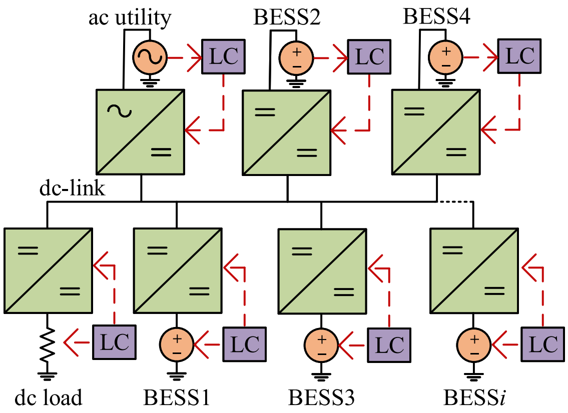

FIGURE 6. Decentralized control.

to achieve SoC equalization with a predefined SoC (SoC_f), as follows:

$$\min_{i_{\mathrm{BESS}i},\, \mathrm{SoC}_i} \frac{C_{\mathrm{bat}}(\mathrm{SoC}_i - \mathrm{SoC}_f)}{i_{\mathrm{BESS}i}}. \tag{9}$$

2) The objective function involves EMS and SoC equalization to minimize the power delivered/absorbed by the grid (P_{grid}), with the maximum value supported being $P_{\mathrm{grid\_max}}$, as follows:

$$\min_{i_{\mathrm{BESS}i}} \left(\frac{P_{\mathrm{grid}}}{P_{\mathrm{grid\_max}}}\right)^2. \tag{10}$$

3) Overcoming the limitations from the second optimization without applying a minimum limit for SoC variation in the constraints, as shown in (11), with k_s and k_{grid} being coefficient factors

$$\min_{i_{\mathrm{BESS}i}} \left(k_s k_{\mathrm{SoC}} |P_B| + k_{\mathrm{grid}} \left|P_{\mathrm{grid}}\right|\right). \tag{11}$$

In addition, applying optimization in the aforementioned approaches could prevent voltage and frequency deviations in droop control. However, the implementation is complex and involves excessive computational effort due to the use of multiple optimizations as part of the EMS. Thus, Pawitan and Kim [67] proposed an optimal charging/discharging EMS for BESS units in a dc MG that includes SoC equalization through quadratic programming, which does not require high computational complexity. However, the current from the BESS units exhibited an oscillatory behavior, which can compromise power quality and stability, and increase losses in the dc MG operation.

V. DECENTRALIZED CONTROL

Decentralized control is responsible for processing decisions based on local information, providing a solution to the drawbacks of centralized strategies. Thus, the sources in the MG can provide load sharing through power converters without requiring communication among each other, as shown in Fig. 6 [17], [18]. Droop control is the most common method for EMS in MGs without implementation of communication links. In this context, when the droop control for BESS units considers SoC equalization and processes only the information from the local BESS units, this SoC-based droop is categorized as decentralized control [73]. In addition, there are other approaches that are not based on droop control but still fall under the decentralized control perspective, including the design of a nonlinear function (for example, sigmoid functions) and FIS [17], [84]. This section focuses on approaches utilizing decentralized communication, with Tables 4 and 5 offering a comparative overview of the literature, highlighting key characteristics, advantages, and limitations.

TABLE 4. Comparative Summary: Decentralized Methodologies

		Decentralized
MG Type	dc	[18], [25], [26], [44], [50], [71], [72], [73], [74], [75], [14], [43], [76], [77], [78], [79], [11], [17], [29], [35], [80], [81], [82], [83], [84], [85]
	ac	[28], [86], [87], [88], [89], [90], [91], [92]
	ac/dc	[93]
Topology of power converters	Conventional	[18], [25], [26], [50], [71], [72], [73], [43], [44], [74], [75], [76], [14], [29], [77], [78], [79], [80], [17], [28], [81], [82], [83], [84], [85], [86], [87], [88], [89], [90], [91], [92], [93]
	Redundancy-based	[11], [35]
EMS Type	SoC-based droop	[18], [25], [26], [50], [71], [72], [73], [43], [44], [74], [75], [76], [77], [78], [14], [28], [29], [79], [80], [86], [87], [88], [89], [90], [91], [92], [93]
	Nonlinear function based	[81]
	sigmoid function	[11], [17], [35]
	RAh-based	[82], [83]
	FIS	[84]
	SoC feedback control	[85]
Voltage or/and frequency regulation	✓	[18], [25], [26], [50], [72], [77], [78], [14], [79], [86], [87], [89], [82], [83], [85], [92]
	X	[44], [71], [73], [74], [75], [28], [29], [43], [76], [80], [11], [17], [35], [81], [84], [93]
Combination with UCs/SCs	✓	-
	X	[18], [25], [26], [50], [71], [72], [73], [14], [43], [44], [74], [75], [76], [77], [78], [79], [28], [29], [80], [86], [87], [88], [89], [90], [91], [11], [17], [35], [81], [82], [83], [84], [85], [92], [93]
Islanded Mode	✓	[9], [18], [25], [26], [50], [14], [43], [44], [71], [72], [73], [74], [75], [76], [77], [79], [80], [11], [17], [28], [29], [35], [81], [82], [83], [84], [85], [86], [87], [88], [89], [90], [91], [92], [93]
	X	-
Grid Connected	✓	[78]
	X	-

A. DECENTRALIZED SOC-BASED DROOP

For SoC-based droop as decentralized control, essentially, the EMS is similar to the strategy derived from centralized control, with the difference that the parameter influenced by SoC is dependent only on the local BESS units, without requiring information about other units or the average SoC from all of them, as indicated in Fig. 7.

In the context of dc MGs, Table 6 presents a comparison of various approaches to decentralized SoC-based droop. Diaz et al. [18] elaborated the virtual resistance (r_d) defined by a FIS, while a filter-based droop control for SoC equalization is elaborated in [25], with a dc-link voltage recovery that is not impacted by the line resistance among power converters.

TABLE 5. Comparative Summary: Strengths and Drawbacks of Decentralized Methodologies

Strategy	Strengths	Drawbacks
[18]	FIS can manage multiple objectives simultaneously.	Due to the lack of exchanged information, achieving precise power scheduling for each unit may be challenging.
[25]	The SoC balancing is based on a high-pass filter, which allows for the mitigation of line impedance effects	The overall performance may be impacted by the application of a high-pass filter algorithm. In addition, it cannot balance a large number of BESS units with different capacities.
[26]	A double-quadrant droop is proposed based on the n-th order of SoC. In addition, the voltage recovery is based on multiagent system	Determining the appropriate value of n can be challenging, as it must balance the trade-off between SoC convergence speed and dc-link voltage deviation.
[50]	Current-source based equalization, with the virtual resistance based on the nth order of SoC	Due to the lack of network communication, the decentralized strategy may lead to excessive active power compensation.
[71]	The droop coefficient is modified linearly based on SoC	The SoC balancing is not effectively achieved.
[72]	The droop coefficient is modified linearly based on SoC	Due to the arbitrary parameters, the implementation into another approach may be complex.
[44], [73], [74], [75]	A double-quadrant droop is proposed based on the nth order of SoC	The power compensation is inadequate, the control accuracy is low, and there are issues with quality and voltage deviation.
[43], [76]	The virtual resistance is based on a function dependent on SoC	It has dc-link voltage variation and inaccurate power sharing
[77]	The FIS added an ac signal to the droop control	It has dc-link voltage variation, inaccurate power sharing and the SoC balancing is not effectively achieved
[78]	A correction term is added to the voltage reference as a function of the nth order of SoC. In addition, a dual active bridge connects the MG to the grid	It has inaccurate power sharing.
[14]	The approach considers communication failure and is implemented for dc shipboard MG	It has inaccurate power sharing, and complexity in tuning droop parameters
[79]	The droop is based on power rating, with a droop coefficient being based on the nth order of SoC	This methodology is not completely decentralized and requires central control. As a result, a single point of failure can impact overall control performance.
[80]	The droop control is based on micro-tuning resistance, which allows the reduction of line resistance effects	It has inaccurate power sharing, and complexity in tuning droop parameters
[29]	The droop line is adjusted longitudinally, and its inclination is also altered	It has dc-link voltage variation and the SoC convergence speed is slow
[86], [87]	FIS implements the droop control parameter based on SoC	It is not applicable on a large scale and it could be complex to apply to another MG.
[28]	The term introduced in the droop is inversely proportional to the capacity of BESS, enabling balancing among different capacities	It lacks flexibility, and frequency regulation is not considered.
[88]	The term introduced in SoC-based droop is obtained through a PI controller	This methodology is not completely decentralized and requires central control. As a result, a single point of failure can impact overall control performance.
[89]	Applies reactive power sharing in the ac MG	It can cause a large frequency offset and fails when the capacities of BESS units are different.
[90]	A function based on SoC modifies the droop coefficient	There is a complexity in tuning droop parameters
[91]	The EMS operates with selective charging/discharging priority.	The BESS unit curve cannot ensure SoC balance.
[92]	The SoC-based droop is modified thanks to a polynomial function based on SoC and power from the BESS unit	There is a complexity in tuning droop parameters
[93]	SoC-balancing in dc and ac subgrids, along with power sharing between subgrids	The SoC balancing is not effectively achieved.
[81]	SoC balancing without droop control	The approach works with different conditions to determine the current reference, which can lead to complexity when implementing it in other systems. Moreover, it is not continuously differentiable, impacting the stability analysis.
[17]	The Sigmoid function can smooth the EMS and also compensates/absorbs load transients	There is a voltage deviation on dc-link
[82], [83]	The operation can also occur during fault ride-through conditions, converter failure, and communication link failure	The methodology is not suitable when operated with no load on the dc-link.
[84]	The FIS is employed without droop control and also compensates/absorbs load transients	It could be complex to extend to another dc MG. Moreover the SoC balance accuracy of the strategy is low
[85]	The SoC is implemented in a PI controller to achieve equalization	As the SoC control operates with average values, a communication failure can disrupt the SoC equalization.
[35]	Battery-to-battery equalization is employed to enhance the EMS	It is not possible to apply BESS units with different capacities in the redundancy-based dc MG
[11]	The optimization can enhance the EMS and reduce the overall cost from the sources	It is not possible to apply BESS units with different capacities in the redundancy-based dc MG
[94]	The structure provides integration among low-voltage and large-scale voltage among BESS units	A failure in communication results in a BESS unit fault, which in turn causes a problem with SoC equalization.

In addition, Xu et al. [26] proposed a double-quadrant SoC consistent adaptive droop control in cooperation with multiagent control that obtains the dc-link referential voltage and BESS units capacities to compensate for voltage changes through the droop control, while the authors in [44], [73], [74], and [75] indicate an autonomous EMS to balance the SoC among BESS units with a droop factor proportional to the nth order of SoC in the charging mode and inversely proportional to the nth order in the discharging mode, with n increasing the speed of the SoC balance operation, as indicated in Table 6. Also in the approach designed by Belal et al. [44], the relative capacity of BESS unit is introduced into the droop factor, achieving SoC equalization of BESS units with different capacities.

In [50], the SoC-based droop is current-source based, i.e., the EMS is changed in order to provide the current reference instead of voltage reference, as proposed in many conventional approaches. Regarding this matter, the power-sharing maintains accuracy with the voltage regulation in the MG. Thus, the voltage-source-based reference from (3) is modified to provide (12), which determines the current reference (i_{ref}) for the BESS units

$$i_{\mathrm{ref}} = \frac{v_{\mathrm{ref}} - v_o}{r_d}. \tag{12}$$

To clarify the difference between an example of voltage source-based droop (the most common SoC-based droop developed) and the current-source-based droop, it is necessary to consider the control diagram in Fig. 8. As indicated, the methodology of voltage-source-based droop defines the term for the voltage PI control followed by a current PI control, while the current-source-based droop considers only the current PI control.

Considering a common approach for decentralized SoC-based droop the parameter k_{SoC} is also a factor dependent on SoC, which can vary according to different researches. Thus,

TABLE 6. Comparison of EMS for DC MGs - Decentralized SoC-Based Droop

Strategy	EMS Equations	Strategy	EMS Equations
[18]	$v_o = v_{\mathrm{ref}} - i_{\mathrm{BESS}i} r_d$ with r_d obtained by FIS	[25]	$v_o = v_{\mathrm{ref}} - k_{\mathrm{SoC}}(\mathrm{SoC}_{\mathrm{ref}} - \mathrm{SoC}_i) - \frac{\Delta v_{\max}}{P_{\mathrm{rating}} C_{\mathrm{bat}}} P_B + \Delta v$ with $\Delta v = PI(s)\left(v_{\mathrm{ref}} - v_o\right)\frac{\tau}{\tau s+1}$
[26], [73], [74], [75]	$v_o = \begin{cases} v_{\mathrm{ref}} - k_{\mathrm{SoC}} \mathrm{SoC}_i^n P_B & \text{for charging mode} \\ v_{\mathrm{ref}} - \frac{k_{\mathrm{SoC}}}{\mathrm{SoC}_i^n} P_B & \text{for discharging mode} \end{cases}$	[44]	$v_o = \begin{cases} v_{\mathrm{ref}} - \frac{C_{\mathrm{bat\_max}}}{C_{\mathrm{bat}i}} k_{\mathrm{SoC}} \mathrm{SoC}_i^n P_B & \text{for charging mode} \\ v_{\mathrm{ref}} - \frac{C_{\mathrm{bat\_max}}}{C_{\mathrm{bat}i}} \frac{k_{\mathrm{SoC}}}{\mathrm{SoC}_i^n} P_B & \text{for discharging mode} \end{cases}$
[50]	$i_{\mathrm{ref}} = \frac{v_{\mathrm{ref}} - v_o}{r_d}$ with $v_{\mathrm{ref}} = \begin{cases} v_o + \alpha_{\mathrm{dc}}(\mathrm{SoC} - \mathrm{SoC}_{\mathrm{avg}}) & \text{if } \mathrm{SoC}_{\mathrm{avg}} < \mathrm{SoC} \\ v_o & \text{if } \mathrm{SoC}_{\min} \leq \mathrm{SoC} \leq \mathrm{SoC}_{\mathrm{avg}} \\ v_{\mathrm{ref\_min}} & \text{if } \mathrm{SoC} < \mathrm{SoC}_{\min} \end{cases}$ with $\alpha_{\mathrm{dc}} = \frac{v_{\mathrm{ref\_max}} - v_o}{\mathrm{SoC}_{\max} - \mathrm{SoC}_{\mathrm{avg}}}$	[71]	$v_o = v_{\mathrm{ref}} - k_{\mathrm{SoC}} P_B, \quad \text{with } k_{\mathrm{SoC}} = \begin{cases} \frac{\mathrm{SoC}_i}{100}, & \text{for charging mode} \\ 1 - \frac{\mathrm{SoC}_i}{100}, & \text{for discharging mode} \end{cases}$
[72]	$v_o = v_{\mathrm{ref}} - \frac{k_{\mathrm{SoC}}}{\exp(\mathrm{SoC}_i^n)} P_B$	[43]	$v_o = \begin{cases} v_{\mathrm{ref}} - \frac{C_{\mathrm{bat}i}}{C_{\mathrm{bat\_max}}} r_o (\mathrm{SoC}_{\mathrm{avg}t})^q i_{\mathrm{BESS}} & \text{for charging mode} \\ v_{\mathrm{ref}} - \frac{C_{\mathrm{bat}i}}{C_{\mathrm{bat\_max}}} r_o (\mathrm{SoC}_{\mathrm{avg}t})^{-q} i_{\mathrm{BESS}} & \text{for discharging mode} \end{cases}$ with $\mathrm{SoC}_{\mathrm{avg}t} = \frac{\mathrm{SoC}_i - \mathrm{SoC}_{\min}}{\mathrm{SoC}_{\mathrm{low}} - \mathrm{SoC}_{\min}}$
[76]	$\begin{cases} v_o = v_{\mathrm{ref}} - k_{\mathrm{SoC}} C_{\mathrm{rel}} \left(1 + \frac{\Delta \mathrm{SoC}_{\mathrm{opt}i}}{\Delta \mathrm{SoC}_{\mathrm{oper}i}}\right)^p i_{\mathrm{BESS}}, & \text{for charging mode} \\ v_o = v_{\mathrm{ref}} - k_{\mathrm{SoC}} C_{\mathrm{rel}} \left(1 - \frac{\Delta \mathrm{SoC}_{\mathrm{opt}i}}{\Delta \mathrm{SoC}_{\mathrm{oper}i}}\right)^p i_{\mathrm{BESS}}, & \text{for discharging mode} \end{cases}$ with $\Delta \mathrm{SoC}_{\mathrm{opt}i} = \mathrm{SoC}_i - \mathrm{SoC}_{\mathrm{opt}i}$, $\Delta \mathrm{SoC}_{\mathrm{oper}i} = \mathrm{SoC}_{maxi} - \mathrm{SoC}_{\mathrm{min}i}$ and $C_{\mathrm{rel}} = \left(\frac{C_{\mathrm{bat}i}}{C_{\mathrm{bat\_max}}}\right)$	[14]	$v_o = v_{\mathrm{ref}} - r_d k_{\mathrm{SoC}} i_{\mathrm{BESS\_out}}$, with $k_{\mathrm{SoC}} = \begin{cases} \frac{\mathrm{SoC}_{\mathrm{avg}}}{C_{\mathrm{bat}i}\mathrm{SoC}_i} \exp\left[-k_{\exp}\right], & \text{if } i_{\mathrm{BESS\_out}} > 0 \\ \frac{\mathrm{SoC}_{\mathrm{avg}}}{C_{\mathrm{bat}i}\mathrm{SoC}_i} \exp\left[k_{\exp}\right], & \text{if } i_{\mathrm{BESS\_out}} < 0 \end{cases}$ with $k_{\exp} = \frac{p}{\alpha\left\|\mathrm{SoC}_i^n - \mathrm{SoC}_{\mathrm{avg}}^n\right\| + \beta}(\mathrm{SoC}_i^n - \mathrm{SoC}_{\mathrm{avg}}^n)$
[79]	$v_o = \begin{cases} v_{\mathrm{ref}} - k_{\mathrm{SoC}} \left(\frac{\mathrm{SoC}_i}{\mathrm{SoC}_{\min}}\right)^m P_B & \text{for charging mode} \\ v_{\mathrm{ref}} - k_{\mathrm{SoC}} \left(\frac{\mathrm{SoC}_{\max}}{\mathrm{SoC}_i}\right)^m P_B & \text{for discharging mode} \end{cases}$	[80]	$v_o = v_{\mathrm{ref}} - r_d i_{\mathrm{BESS}}$, with $r_d = \begin{cases} \frac{r_0}{C_{\mathrm{bat}}} \exp\left(n(\mathrm{SoC}_{\mathrm{avg}} - \mathrm{SoC}_i)\right), & \text{if } i_{\mathrm{BESS}} > 0 \\ \frac{r_0}{C_{\mathrm{bat}}} \exp\left(n(\mathrm{DoD}_{\mathrm{avg}} - \mathrm{DoD}_i)\right), & \text{if } i_{\mathrm{BESS}} < 0 \end{cases}$
[29]	$v_o = v_{\mathrm{ref}} + k_{\mathrm{SoC}} \mathrm{SoC}_i - r_d i_{\mathrm{BESS}}$		

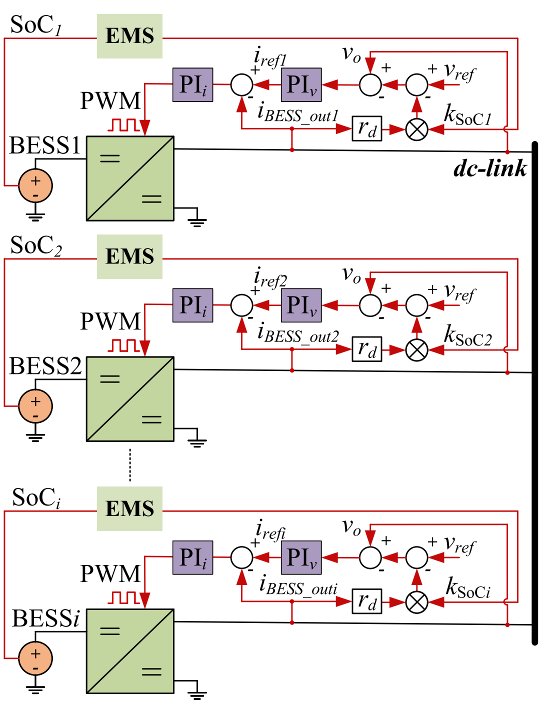

FIGURE 7. Common SoC-based droop control without communication link for dc MG.

droop coefficient from [71], [72] is modified linearly based on the SoC of each BESS unit,

In the method proposed in [43], there is no weight factor; instead, the virtual resistance is defined according to SoC. Thus, the virtual resistance changes while the BESS unit is charging/discharging in order to achieve the same level among all SoCs. Conversely, the approach from [76] considered the weight factor (k_{SoC}), showing similarities with the approach from [43], as shown in Table 6. Eydi and Ghazi [77] injected

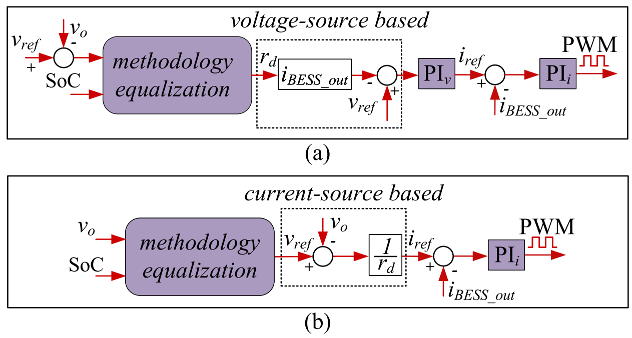

FIGURE 8. Comparison between voltage-source-based droop and current-source-based droop.

an ac signal containing the information about the SoC from the BESS units, with the ac frequency obtained by the FIS using the SoC and current from the BESS units as input, while Yuan et al. [78] added a correction term to the voltage reference as a function of SoC^n.

Furthermore, in [14], when communication is normal, SoC equalization uses a droop approach with control coefficient determined by a distributed algorithm. Then, when any failures occur, the system switches to decentralized control to obtain the coefficient necessary to achieve balance among SoCs. Hence, such an approach can enhance reliability and redundancy for dc shipboard applications. In their study, Hoang and Lee [79] proposed a droop virtual power rating as a function of SoC to achieve equalization and maintain the dc-link voltage without deviation.

In addition, Mi et al. [80] elaborated on an SoC-based droop control system applying the microtuning virtual resistance. In this approach, the influence of line resistance is mitigated, along with the deviation in the dc-link voltage. Finally, the EMS designed by Xia et al. [29] developed an SoC-based

TABLE 7. Comparison of EMS for Ac MGs - Decentralized SoC-Based Droop

Strategy	EMS Equations	Strategy	EMS Equations
[86], [87]	$\omega = \omega_{\text{ref}} - m_d k_{\text{SoC}} P_B$ with k_{SoC} obtained by FIS	[28]	$f = f_{\text{ref}} - \frac{m_d}{C_{\text{bat}}}(P_B - P_{\text{ref}})(1 - k_{\text{SoC}}\text{SoC})$, with m_d and k_{SoC} being a constant
[88]	$f = f_{\text{ref}} - (\frac{f_{\text{ref}} - f_{\text{min}}}{P_{\text{ref}} - P_{\text{max}}} + \delta_{\text{SoC}})(P_B - P_{\text{ref}})$, with δ_{SoC} obtained by PI controller from the $i-$th SoC and the average value of all SoCs	[89]	$f = f_{\text{ref}} - k_s P_B - k_{\text{SoC}}(1 - \text{SoC})$
[90]	$f = \begin{cases} f_{\text{ref}} + m_d(\text{SoC}-1)P_{\text{max}} - m_d\text{SoC}P_B, \text{ if } P_B \geq 0 \\ f_{\text{ref}} + m_d(\text{SoC}-1)P_{\text{max}} - m_d(\text{SoC}-2)\text{SoC}P_B, \text{ if } P_B < 0 \end{cases}$	[91]	$f_{\text{ref}} = f_o + \delta f_{\text{rest}} + \delta f_{\text{charging}} + \delta f_{\text{power}} + m_d(P_{\text{ref}} - P_B)$ with δf_{rest} being frequency restoration, $\delta f_{\text{charging}}$ being frequency from the charging controller and δf_{power} being frequency from the power limit
[92]	$f_{\text{ref}} = f_{\text{max}} - m_d[\alpha P_B + \beta(1 - \text{SoC})]$, with m_d being a constant, $\alpha > 0$ and $\beta > 0$		

droop in which the coefficient changes the inclination, and another parameter is added to the voltage reference to dislocate the droop line longitudinally. Consequently, the SoC balance is enhanced due to the flexibility in changing the voltage and the droop inclination.

Focusing on ac MGs, Table 7 presents a comparison among different strategies for SoC equalization. The authors in [86] and [87] proposed a decentralized SoC equalization method for the islanded mode, which also provided coordination for the existing renewable energy sources. In this case, the droop control adjusts the frequency, with the parameter SoC-dependent being obtained by a FIS, differing for charging and discharging modes. Furthermore, the authors in [28], [88], and [89] achieved SoC balancing within the droop control by introducing a term dependent on SoC, while the authors in [90] and [91] shifted the droop curve along the vertical axis according to a function based on SoC.

The term from [28] is inversely proportional to the BESS units' capacity (C_{bat}), providing equalization among units with different capacities, while the term from [88] is obtained by a PI controller based on the SoC. Moreover, Chen et al. [92] introduced a polynomial term dependent on SoC and power from the ith BESS unit to modify the SoC-based droop and achieve equalization among all units.

In the context of a hybrid ac/dc MG, in [93], a SoC-based droop is used to achieve equalization on both sides of the subgrids by modifying the droop factor, as shown in (3) for the dc side and (4) for the ac side.

Finally, regarding SoC-based droop control for decentralized communication, there are a significant number of approaches that attempt different methods to modify virtual resistance or introduce additional factors to facilitate SoC equalization. These approaches could have simple implementations; however, they could also introduce voltage/frequency deviations, and designers should be cautious because droop control is not continuously differentiable, which impacts the operational limits of MGs.

B. DESIGNING A NONLINEAR FUNCTION TO ACHIEVE EQUALIZATION

In addition to the classical SoC equalization strategy that is based on droop control, it is possible to implement an EMS among BESS units through the employment of a nonlinear function without droop control. A simple example is proposed in [81], wherein the voltage difference from the dc-link and the measured value is modified by a nonlinear function, along with the SoC from the BESS unit, to define the current reference.

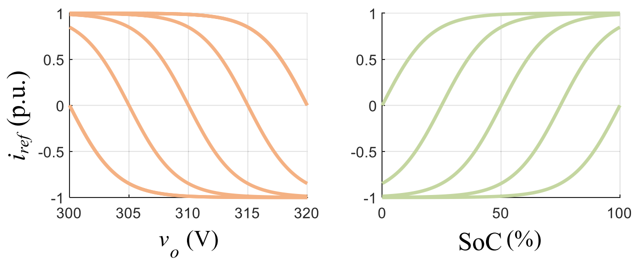

FIGURE 9. Example of Sigmoid function, with i_{ref} given in p.u.

In addition, a Sigmoid function, classified as S-shaped function, is proposed in [17], as indicated by Fig. 9, which operates on a current-source basis, in which the current reference for BESS units is processed by the nonlinear function defined in (13), in which $I_{\text{bat\_rated}}$ represents the rated BESS current, p is the sigmoidal slope, and Δv_o is the voltage range across the dc-link

$$i_{\text{ref}} = I_{\text{bat\_rated}} \left[\frac{2}{1 + e^{\left(\frac{v_o - v_{\text{ref}} - \Delta v_o}{\Delta v_o} - \text{SoC}\right)p}} - 1 \right]. \quad (13)$$

As a result, the current behavior is smoother in comparison to the classical droop control, and the function is continuously differentiable. Therefore, stability analysis can be proven by employing a Lyapunov's function. In addition, if the voltage limit from the dc-link matches that of a droop control, then, in a MG, the Sigmoid function can be designed for the BESS units, while the droop control can coordinate another source, such as PV arrays and FCs. For the application of nonlinear functions and S-shaped functions into EMS operation for SoC equalization, it could introduce a smoother response. This could be an alternative to droop control, which is not continuously differentiable and may cause operational issues for the MG under the limits of droop control. Conversely, voltage deviation is present during operation.

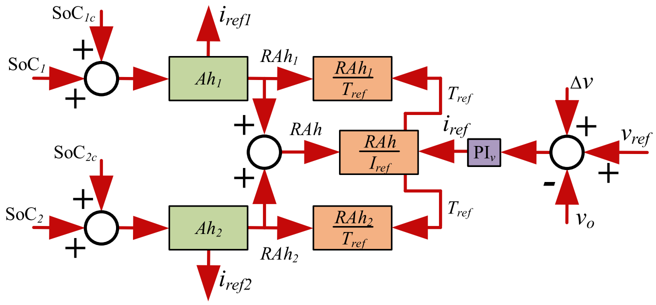

FIGURE 10. Proposed strategy from [82] and [83].

C. EQUALIZATION BASED ON RAH CAPACITY

For this SoC equalization perspective, the authors in [82] and [83] proposed an approach that does not require droop implementation, as shown in the strategy in Fig. 10, with SoC_c being the virtual additional SoCs to regulate v_o within operational limits). Thus, the technique considers the product between "SoC-SoC_c" and Ah rating to obtain the parameter known as RAh capacity for each BESS unit. First, the total reflected capacity from the system is obtained and divided by the current reference by the first local controller to produce the reference time for each BESS unit's charge/discharge.

In sequence, this reference time is processed by the second local controller, then, the RAh for the BESS unit is divided by this reference time (T_{ref}) to provide the reference current for each BESS unit. Later, this current reference is processed by a PI controller. All the information is transmitted via low-bandwidth communication. Finally, this strategy can also facilitate voltage recovery and maintain resilience during a failure in the communication link, being an alternative for droop control.

D. FIS METHODOLOGY

This approach differs from the application that defines the virtual resistance using FIS. In this case, the parameters from each BESS unit and its power converter are processed through FIS, which then provides the current reference for each BESS unit. This coordination helps the MG achieve SoC equalization.

As suggested in [84], the FIS is a decentralized control that takes inputs, such as SoC from the *i*th BESS unit and information about the dc-link voltage to determined the current reference (current-source-based approach). The rules of the FIS determine the equalization, as indicated in the experimental results from [84]. In this context, Fig. 11 illustrates a comparison between the methodology presented in [18] [see Fig. 11(a)] and that in [84] [see Fig. 11(b)], including the differences in control structure between the approaches. Aiming at this approach, it could be beneficial for MGs that require only a current-source-based equalization focusing on current sharing. However, there is a voltage deviation that should be taken into account during operation.

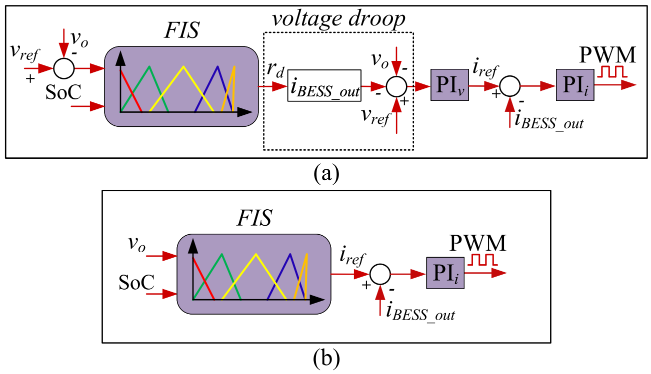

FIGURE 11. Comparison among FIS-based control for SoC equalization (a) with SoC-based droop and (b) without droop control.

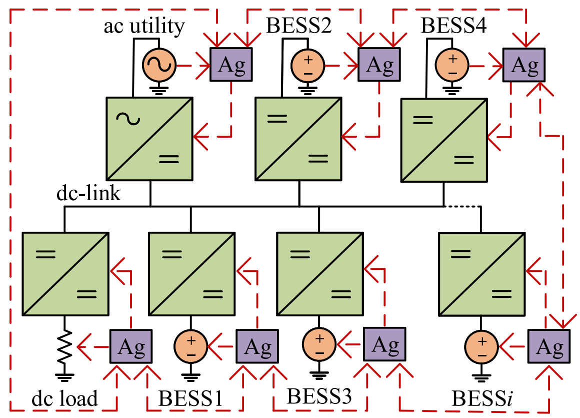

FIGURE 12. Multiagent system.

E. SOC FEEDBACK CONTROL

In [85], SoC equalization can be integrated into a PI controller, where the error is computed as the difference between the SoC of the BESS unit and the average SoC, generating a voltage term, described as follows:

$$v_{ref} = v_o + \Delta v_{\text{SoC}} + \Delta v_{\text{link}} \tag{14}$$

with Δv_{SoC} defined as

$$\Delta v_{\text{SoC}} = (\text{SoC} - \text{SoC}_{\text{avg}})(PI_{\text{SoC}}(s)). \tag{15}$$

It is worth noting that the SoC is obtained through low bandwidth communication. In addition, the authors implement voltage restoration using a PI controller to produce a voltage correction term (Δv_{link}). Subsequently, both terms are incorporated into the voltage reference control. This approach could be an alternative to droop control and voltage regulation. However, the SoC control should operate with the average SoC; thus, any communication failure can impact SoC balancing.

VI. MULTIAGENT SYSTEM CONTROL

Multiagent control is a strategy that does not require communication among sources. As indicated by Fig. 12, all decisions are made locally with information from neighbor-to-neighbor to pursue a specific objective [19]. Due to the information neighbor-to-neighbor, multiagent systems can also be robust as the centralized control and avoid insufficient information from decentralized control. Since multiagent control operates without central communication, this can overcome the drawback of centralized control [4]. Thus, multiagent control is an approach that has been applied to combine decentralization with communication among other units.

For a multiagent system, the consensus algorithm refers to a protocol for achieving a common objective, especially in MGs, where multiple autonomous sources need to reach an agreement or make coordinated decisions (e.g., average consensus and leader-tracking) [12]. As a result, for BESS units, multiagent control entails making decisions to achieve SoC equalization, along with secondary voltage control and heterogeneous coordination for ESUs. In addition, various strategies have been proposed as consensus algorithms altogether with sliding mode control, the adaptive power allocation algorithm and droop control [16], [122]. This section discusses the approaches that utilize centralized communication, with Tables 8, 9, and 10 providing a comparative overview of the literature, highlighting key characteristics, strengths, and weaknesses.

A. GRAPH THEORY

Graph theory is a strategy that can be used to design distributed algorithms for agents to communicate and coordinate their actions effectively [116]. Thus, the methodology can ensure that all agents reach an agreement in decision-making. The graph that represents the communication network of a MG composed by n BESS units is defined as $\mathcal{G} = \{\mathcal{V}, \ \mathcal{E}, \mathcal{A}\}$, where each BESS is a node in the set $\mathcal{V} = \{\text{BESS1}, \ldots, \text{BESS}n\}$ that communicates via the links $\mathcal{E} \subset \mathcal{V} \times \mathcal{V}$. The adjacency matrix is $\mathcal{A} = [a_{ij}] \in \mathbb{R}^{N \times N}$, being $a_{ij} = 1$ if BESS units i and j communicates, and $a_{ij} = 0$ otherwise. The set $\mathcal{N}_i = \{j \mid (v_i, v_j) \in \mathcal{E}\}$ represents the neighbors of the ith BESS, with the number of neighbors given by the matrix $\mathcal{D} = \text{diag}\{d_{ii}\} \in \mathbb{R}^{N \times N}$, where $d_{ii} = \sum_{j \in \mathcal{N}_i} a_{ij}$.

In an undirected graph, if nodes i and j are neighbors, then node i sends its information to node j, and vice versa. However, in a directed graph, it is not necessary for the information to flow in both directions; that is, a_{ij} does not necessarily equal a_{ji}. For an undirected graph, the Laplacian matrix is defined as

$$\mathcal{L} = \left[l_{ij}\right] \in \mathbb{R}^{N \times N} = \mathcal{D} - \mathcal{A} \tag{16}$$

and a common multiagent consensus is represented by

$$\dot{\gamma}_i(t) = \sum_{j \in N_i} a_{ij}[\gamma_i(t) - \gamma_j(t)] + \dot{x}_i(t), \quad i = 1, 2, \ldots, N. \tag{17}$$

In (17), the state variables of node i and j are $\gamma_i(t)$ and $\gamma_j(t)$, respectively, while the local input is $\dot{x}_i(t)$. Then, the global dynamics of the consensus algorithm can be represented as (18), with the state variable and local input being

TABLE 8. Comparative Summary: Multiagent Methodologies

		Multi-Agent
MG Type	dc	[95], [96], [97], [98], [99], [100], [101], [102], [103], [104], [105], [106], [22], [27], [37], [51], [107], [108], [109], [110], [111], [112], [8], [16], [19], [31], [113], [114], [115], [116], [117], [118], [119], [120], [121], [122], [123], [124], [125]
	ac	[3], [6], [41], [42], [52], [126], [127], [128], [129], [130], [131], [132], [133], [134], [135], [136], [137], [138], [139], [140], [141], [142], [143], [144], [145], [146], [147], [148]
	dc NGs	[149]
Topology of power converters	conventional	[22], [27], [37], [95], [97], [98], [99], [100], [101], [102], [103], [104], [105], [106], [107], [108], [109], [111], [16], [51], [112], [113], [114], [147], [148], [3], [6], [19], [115], [116], [126], [127], [128], [129], [117], [118], [119], [120], [130], [131], [132], [133], [134], [135], [137], [138], [121], [125], [149], [41], [42], [122], [124], [139], [140], [141], [142], [143], [144]
	dc electric spring	[96], [110]
	PV and BESS are connected through an inverter to form a distributed PV-BESS system	[136]
	Cascaded multiport	[31]
EMS Type	Consensus based on droop	[95], [96], [97], [98], [99], [100], [101], [22], [27], [37], [102], [103], [104], [105], [106], [107], [108], [109], [110], [111], [112], [16], [19], [51], [113], [114], [115], [3], [6], [116], [126], [127], [128], [129], [130], [131], [132], [133], [134], [135], [136], [148], [52], [137], [138], [146], [147]
	Consensus based control	[31], [117], [118], [119], [120], [121], [125], [139], [149], [41], [42], [140], [141], [142], [143], [144], [145]
	Adaptive power allocation algorithm	[8], [122], [123]
	dynamic diffusion algorithm based on distributed unified controller	[124]
voltage or/and frequency regulation	✓	[95], [96], [97], [98], [99], [100], [101], [102], [104], [106], [107], [22], [37], [51], [108], [109], [110], [111], [112], [16], [19], [113], [114], [115], [116], [126], [147], [148], [3], [6], [127], [128], [129], [130], [131], [132], [31], [117], [133], [134], [135], [136], [137], [142], [52], [121], [124], [144], [145], [146], [149]
	X	[27], [103], [105], [118], [119], [120], [139], [42], [138], [140], [141], [8], [122], [123], [125], [143]
combination with UCs/SCs	✓	[97], [102], [108], [109], [112], [117], [121]
	X	[95], [96], [98], [99], [100], [22], [101], [104], [106], [107], [110], [37], [51], [111], [16], [19], [103], [113], [114], [115], [147], [148], [3], [6], [116], [126], [127], [128], [129], [130], [131], [132], [133], [134], [135], [136], [31], [41], [137], [138], [142], [149], [52], [124], [125], [145], [146]
Islanded Mode	✓	[95], [96], [97], [98], [99], [100], [101], [102], [103], [104], [121], [22], [27], [37], [51], [105], [106], [107], [108], [109], [110], [111], [112], [16], [19], [113], [114], [115], [116], [126], [147], [148], [3], [6], [127], [128], [129], [130], [131], [132], [133], [134], [135], [136], [137], [31], [117], [119], [138], [8], [120], [123], [125], [140], [149], [52], [124], [145], [146]
	X	[42], [118], [139], [141], [41], [122], [143], [144]
Grid Connected	✓	[42], [97], [118], [121], [139], [141], [41], [122], [142], [143], [144]
	X	[22], [27], [95], [96], [98], [99], [100], [101], [102], [103], [104], [105], [106], [107], [108], [109], [110], [111], [16], [37], [51], [112], [113], [114], [115], [3], [6], [19], [116], [126], [127], [128], [129], [130], [147], [148], [131], [132], [133], [134], [135], [136], [31], [117], [119], [137], [138], [120], [125], [140], [149] [8], [52], [123], [124], [145], [146]

TABLE 9. Comparative Summary: Strengths and Drawbacks of Multi-Agent Methodologies (Part 1)

Strategy	Strengths	Drawbacks
[95]	A factor is introduced into the droop control to adjust the SoC equalization speed	Since there are multiple controllers, coordination is required to achieve SoC equalization, current sharing, and voltage recovery.
[96]	The dc electric spring can isolate critical loads from non-critical ones	The SoC balance speed is slow, and multiple controllers increase the system order, compromising stable operation.
[97]	The EMS coordinates the power sharing between BESS and SC	Multiple controllers increase the system order, compromising stable operation.
[98]	A model-free iPI control is responsible for the primary control	The strategy is only suitable for islanded MGs
[99], [127]	A directed-graph-based observer is developed to obtain the current from BESS units more accurate in comparison to the conventional adaptive observer	During charging or discharging mode, the BESS units have to be fully charged or discharged to achieve SoC equalization.
[100]	The approach is designed with three different operation modes, which allow the control of equalization speed	There is a complexity when implementing it in other systems
[101]	Two parameters are designed to improve the SoC convergence speed and precision	The influence of communication delay is not considered. Moreover, the SoC balance is based on droop design and thus still has the limitations of droop control.
[102]	The BESS units delivery power to the low frequency component of loads, while the UCs fed the high frequency component	During charging or discharging mode, the BESS units have to be fully charged or discharged to achieve SoC equalization.
[103]	It accounts for communication delay and information transmitted over a weak communication network.	It only considers BESS units with similar capacities.
[104]	An incremental cost factor is developed to adjust the SoC in all BESS units and increase the power delivery to the MG	The influence of communication delay is not considered.
[105]	The consensus strategy is based on pinning mode, which allocates power among BESS units	During charging or discharging mode, the BESS units have to be fully charged or discharged to achieve SoC equalization.
[106]	A double-quadrant SoC based droop control obtains the information from a consensus protocol	The line impedance is not taken into account. As a result, the average output voltage may not reach the rated value of the MG.
[27]	The consensus strategy is designed to adjust the output power of BESS units according to their SoCs	The dc-link voltage increases with loading increase. Moreover, the strategy can become complex when scaled up
[107]	Two convergence parameters are introduced in a nonsmooth coordination among different time scales, achieving fast recovery performance.	It operates with fixed control parameters, resulting in either redundant or inadequate robustness.
[22]	The fixed-time secondary controller is robust and suitable for BESS units	The fixed-time controller must be combined with parallel distributed control. In addition, it is complex and demands substantial computational effort for applications.
[108], [109]	The BESS units delivery power to the low frequency component of loads, while the UCs fed the high frequency component	Different line resistances may reduce the average power sharing among BESS units, resulting in decreased performance of SoC balancing
[110]	The consensus strategy implements equal priority and control into all power converters	The SoC balance speed is slow, and multiple controllers increase the system order, compromising stable operation.
[111]	The modified voltage reference may result in less impact compared to gain scheduling	The linear consensus protocols employ an undesirable trade-off between the rate of SoC balancing and the utilization of the BESS current capacities.
[37]	A parameter dynamically adjusts the function to accelerate the SoC equalization speed	Communication delay could be a challenge in designing a multi-objective cooperative controller.
[112]	A virtual capacitive control methodology coordinates the power among UCs and BESS units	Different line resistances may reduce the average power sharing among BESS units, resulting in decreased performance of SoC balancing
[51]	A Sigmoid function incorporating an SOC balancing adjustment factor enables both the accuracy and speed of SOC equalization	It has high cost, complex implementation, and communication dependency.
[16]	Sliding mode control operates the distributed average current and secondary current control	The equalization speed is slower when the SoC difference among BESS units is small.
[113]	The approach integrates a multi-agent sliding mode surface alongside the EMS	It is only suitable for dc system
[114]	The approach exhibits tolerance capability for delays in BESS communication	Controller failures could occur if the initial state is not available within the settling time of the designed controller.
[115]	The approach can decrease the communication burden.	The BESS units' current presents a noisy aspect.
[19]	The approach is based on a random packet loss model, incorporating communication failures	There is a complex structure and significant communication variables.
[116]	A voltage shift obtained by a PI controller is responsible for modifying the droop control	There are multiple secondary controllers, which increase the system order. Consequently, this could compromise the stable operation of the MG.
[126]	A leader-follower finite-time multiagent control scheme is proposed for achieving SOC equalization	It is applied in the scenario of optimal scheduling with a long time scale.
[128]	The approach exhibits tolerance capability for delays in BESS communication	Highly sensitive to system parameter variation when the MGs scale up.
[3]	The EMS designs an adaptive frequency droop based on virtual power	During charging or discharging mode, the BESS units have to be fully charged or discharged to achieve SoC equalization.
[6]	The approach designs frequency scheduling to regulate active power	After the SoC equalization, the frequencies from the DG are recovered, which may result in frequency fluctuation when there is a large load variation during the SoC equalization process.
[129]	The approach is designed for low voltage MGs, taking into account the effect of highly resistive line impedances	the SoC balancing is not effectively achieved

defined as $\boldsymbol{\gamma} = [\gamma_1, \gamma_2, \ldots, \gamma_N]^T$ and $\boldsymbol{x} = [x_1, x_2, \ldots, x_N]^T$

$$\dot{\gamma}_i(t) = -\boldsymbol{\mathcal{L}}\gamma(t) + \dot{\boldsymbol{x}}(\boldsymbol{t}). \tag{18}$$

In this context, (17) can satisfy the limit defined by $\lim_{t\to\infty} \left|\gamma_j(t) - \gamma_i(t)\right| = 0$ when the graph still contains a directed spanning tree in the case of a communication failure event. Finally, it is crucial to take into account the convergence speed and communication cost regarding the topology of communication between BESS units [70].

TABLE 10. Comparative Summary: Strengths and Drawbacks of Multiagent Methodologies (Part 2)

Strategy	Strengths	Drawbacks
[130]	The approach has the capability to handle delays and partial communication failures	The SoC equalization is achieved through charging/discharging mode detection.
[131]	The approach is robust during communication failure.	Fault diagnosis is not considered.
[132]	It considers the connection and disconnection of any element, ensuring high scalability.	It is complex to introduce into another approach, and the BESS units have to discharge to equalize the SoC.
[133]	The approach is robust enough to compensate for the unpredictable time-varying power generation from sources	SoC synchronization is not studied in charging mode and it is achieved by tertiary control
[134]	It can operate under changes in the power system, power generation, and load demands.	Communication failure is not considered.
[135]	The EMS has communication delay capability and tolerates aperiodically sampled data	During charging or discharging mode, the BESS units have to be fully charged or discharged to achieve SoC equalization.
[136]	A fixed-time sliding mode control is designed to balance the SoC among BESS units	The convergence time depends on the initial value of the system rather than on the control parameters.
[137]	Due to the event-triggered approach, the BESS units update their own controls at event times	It does not consider communication delays.
[138]	BESS units with different capacities and the communication is needed only with aperiodic information.	The approach depends on small signal analysis, which can result in significant variations in system parameters.
[117]	A dynamic consensus generates the error for the i-th BESS unit to be processed by the PI controller	Under communication failure, there will be a voltage deviation at the dc-link.
[31]	The multi-port converter receives the consensus-based control to coordinate PV and BESS units	It requires a sparse communication network among BESS units for multi-agent communication, resulting in system vulnerabilities such as delays or failures.
[118]	The structure is divided into arrays composed of multiple BESS units and SCs, with the EMS relying on consensus based on model predictive control	It applies multiple control loops, resulting in the complexity of designing the control parameters.
[119]	The approach is based on two lumped parameters obtained from BESS parameters and time-varying values of SoC	A communication delay is neglected. Moreover, the average desired power and SoC are obtained globally rather than locally.
[120]	The approach considered communication failures	The current used to charge the BESS units in charging mode is not taken into account.
[121]	The BESS leader is responsible to maintain the UCs voltage, while the followers achieve the SoC equalization by tracking the value from the BESS leader	There is an additional dc-link voltage recovery strategy, increasing the order of the system and the complexity of its parameters.
[149]	A switching consensus control provides SoC equalization among clustered NGs	BESS unit elements connected to the dc-link may not provide a stable system due to exceeding power limits during load changes or high voltage fluctuations.
[125]	It allows switching ON and OFF of BESS units' operation.	Complexity in implementation across different MGs.
[139]	The coordination among agents is made possible by the application of Riccati control theory	There is a redundant information in the transmission system
[140]	The coordination among agents is made possible by the application LQR-based frequency feedback control	It has high complexity and demands substantial computational effort.
[141]	The coordination among agents is made possible by the reactive power sharing strategy	It neglects the impacts of parameter differences in the distributed BESS.
[41], [42]	The distributed observer defines the desired power output for each BESS unit	It neglects the impacts of parameter differences in the distributed BESS.
[142]	It is reliable against fixed time delays, external disturbances, and uncertainties in the communication links.	Nevertheless, this approach involved discharging the BESS units to achieve SoC balance.
[147]	Resilient against faults and cyber attacks	It neglects communication delays
[148]	It addresses operation under deception attacks and communication delays.	The BESS units are discharged to maintain SoC balance.
[143]	An application for wind farms in conjunction with BESS units.	The complexity in defining the accuracy of the wind distribution.
[144]	It could be applied to remote weak grids for short-term power supply.	It involves a complex communication network, and oscillations among power converters can occur.
[124]	It exhibits a faster dynamic response and a smaller mean square error compared to the consensus strategy.	The results are not elaborated to prove the superiority of the consensus protocol.
[122]	A cooperative adaptive terminal sliding mode is implemented for the BESS units	The sliding mode controller cannot handle fast transients.
[8], [123]	The estimators provide information with any specified precision	The convergence rate of the time observer is impacted by the initial values and specific parameters of the BESS units.
[52], [145], [146]	The BESS units are balanced according to theirs clusters	The aggregated parameters are centralized.
[150]	The structure provides integration among low-voltage and large-scale voltage among BESS units	Increasing the gain of the voltage-shifting term speeds up SoC equalization but also causes circulating currents. Therefore, reducing the gain may affect the rate of SoC balancing.

B. CONSENSUS STRATEGY BASED ON DROOP CONTROL FOR DC MG

A multiagent control consensus can be applied in order to enhance the SoC-based droop. Thus, the EMS is not centralized or decentralized, because the information is processed locally and neighbor-to-neighbor [12], [116], as indicated in Fig. 13.

Thus, there are several strategies based on droop control with parameters estimated by consensus. For example, as indicated in [95], a consensus protocol estimates the global average of SoC, which is then applied in a SoC-based adaptive droop controller, as follows:

$$v_o = v_{\text{ref}} - r_d i_{\text{BESS\_out}} \tag{19}$$

with the virtual resistance r_d obtained by

$$r_d = \begin{cases} \frac{r_0}{C_{\text{bat}}} \left(1 + (\text{SoC}_{\text{avg}i} - \text{SoC}_i)\right)^{\varepsilon_i}, & \text{if } i_{\text{BESS\_out}} > 0 \\ \frac{r_0}{C_{\text{bat}}} \left(1 + (\text{DoD}_{\text{avg}i} - \text{DoD}_i)\right)^{\varepsilon_i}, & \text{if } i_{\text{BESS\_out}} \le 0 \end{cases} \tag{20}$$

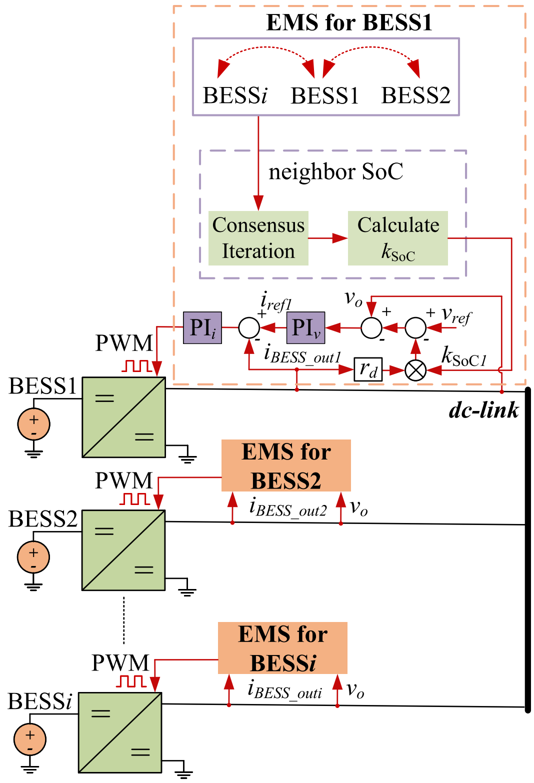

FIGURE 13. Common consensus strategy based on droop control for dc MG.

with ε_i being defined as follows:

$$\varepsilon_i = \begin{cases} \frac{\mathrm{SoC}_{\mathrm{avg}i}}{|\mathrm{SoC}_{\mathrm{avg}i} - \mathrm{SoC}_i| + K_{\mathrm{opt}i}}, & \text{if } i_{\mathrm{BESS\_out}} > 0 \\ \frac{\mathrm{SoC}_{avgi}}{|\mathrm{DoD}_{\mathrm{avg}i} - \mathrm{DoD}_i| + K_{\mathrm{opt}i}}, & \text{if } i_{\mathrm{BESS\_out}} \leq 0 \end{cases} \tag{21}$$

with $K_{\mathrm{opt}i}$ being coefficient factor. Also, in this approach, the virtual voltage drop is also obtained by the consensus strategy, which enables the secondary voltage control to compensate for dc-link variation and avoid the influence of line impedance. Similarly, in [96] and [97], the average estimated SoC, and voltage from the neighbors are considered. Then, both consensus protocols are proposed, including voltage regulation, and SoC regulation, each processed by a PI controller and subsequently used as a parameter for a droop curve. First, the algorithm from (22) defined the droop curve

$$v_o = v_{\mathrm{ref}} + \delta_{1i} + \delta_{2i} \tag{22}$$

with δ_{1i} being defined by a PI controller (gains $k_{\mathrm{pv}i}$ and k_{ivi}) with v_{ref} being the output estimated voltage by consensus from the ith dc/dc converter as follows:

$$\delta_{1i} = k_{\mathrm{pv}i}(v_{\mathrm{ref}} - \hat{v}_{\mathrm{dc}i}) + k_{ivi} \int (v_{\mathrm{ref}} - \hat{v}_{\mathrm{dc}i}). \tag{23}$$

Then, δ_{2i} was obtained by

$$\delta_{2i} = k_{ps} \sum_{j=1}^{N} a_{ij}(\mathrm{SoC}_j - \mathrm{SoC}_i) + k_{is} \sum_{j=1}^{N} a_{ij}(\mathrm{SoC}_j - \mathrm{SoC}_i) \tag{24}$$

with SoC_i being the estimated value from the local ith BESS unit and SoC_j from neighboring BESS units.

Several works have applied SoC-based droop with consensus strategies, as summarized in Table 8. For instance, Hong et al. [98] integrated dynamic consensus for current regulation based on the average BESS unit current, while Xu et al. [99] introduced a SoC-based droop with a coefficient defined by the exponent n (SoC^n).

In [100], [101], [102], and [103], virtual resistance through agreement in a multiagent system enables SoC equalization by processing local and neighbor SoC information. The authors in [104] and [105] utilize consensus-based distributed cooperative control for SoC equalization, with [105] implementing a pinning node for reference values.

Huang et al. [106] presented a double-quadrant SoC-based droop control using an SoC observer for average values, while a hierarchical control structure incorporating dynamic SoC consensus is outlined in [27]. The strategy in [107] enables a multiagent system to access global capacity information, enhancing droop control through a nonsmooth functional design.

In addition, Zeng et al. [22] employed conventional droop for load current sharing and voltage secondary control, using a fixed-time consensus protocol for rapid SoC balancing. The approach in [108] and [109], termed semiconsensus, operates hybrid ESUs with decentralized SCs and distributed BESS communication, adapting the droop controller for real-time SoC balance and voltage restoration.

The authors in [37], [110], and [111] discussed a consensus strategy with voltage and SoC controllers for droop control reference, while Huang et al. [51] employed dynamic average consensus for voltage determination based on average SoC and BESS power. Finally, Morstyn et al. [16] combined neighbor communication for SoC and voltage with distributed average consensus for secondary control, integrating PI controllers for voltage reference in droop control. Practical applications, such as in [116], demonstrate an EMS that balances SoC among BESS units, enhancing load-sharing accuracy and compensating for voltage variations in dc MGs.

Aiming at achieving consensus based on droop control for SoC equalization, the main benefit is the ability to process information neighbor-to-neighbor, thus improving resilience against single points of failure and handling delays effectively. Conversely, increasing the number of nodes can impact efficiency, and the complexity of the algorithm should be considered when implementation is desired.

C. RELIABILITY COMMUNICATION FOR DC MGS

Zhang and Hredzak [114] have proposed a finite-time distributed secondary control for SoC equalization among BESS units and dc-link voltage recovery. Thus, the approach can operate with communication time delays and has plug-and-play capability. First, the voltage secondary control and SoC equalization are processed through feedback linearization. Then, Artstein's Transformation is designed to transform a system with delayed control into a differential control equation. Although the aforementioned approach can tolerate different delays, the communication latency may impact the performance of the controlled approach because the settling time is dependent on the initial system state, causing failure if the initial information is not available. In addition, an event-triggered consensus based on droop is proposed by Huang et al. [115], suitable for delayed communication. However, the BESS units' current presents a noisy aspect.

The finite-time control can guarantee the stability of the dc MG to provide the voltage reference for the droop control. Mi et al. [19] proposed a multiagent distributed secondary control for dc MGs. Thus, the BESS units receive a current-source-based EMS with a term dependent on SoC reference. This SoC reference is obtained by a dynamic-tracking data-compensation consensus strategy, which can operate even in the presence of communication packet loss. Thus, the adaptive current sharing algorithm can achieve SoC balancing and avoid generating circulating current. In addition, a data-driven model-free adaptive control can track voltage and current to improve accuracy in the dc MG. On the other hand, load sharing based on current ratings is not always desirable for MGs, which may comprise alternative sources with different characteristics of generation cost.

D. CONSENSUS STRATEGY BASED ON DROOP CONTROL FOR AC MG

Regarding applications for ac MGs, Li et al. [128] elaborated on SoC equalization by applying a PI controller to adjust the difference between the average SoC among all BESS units and the SoC for the ith unit in a SoC-based droop scheme, as follows:

$$f = f_{\text{ref}} - m_d(P_{Bi} - k_{ps}(\text{SoC}_i - \text{SoC}_{\text{avg}}))\cdots \\ - k_{si}k_{is}\int(\text{SoC}_i - \text{SoC}_{\text{avg}})\,dt \tag{25}$$

where k_{si} depends on a very small threshold (d_{SoC}), as follows:

$$k_{si} = \begin{cases} 1, & \text{if } |\text{SoC}_i - \text{SoC}_{\text{avg}}| \geq d_{\text{SoC}} \\ 0, & \text{if } |\text{SoC}_i - \text{SoC}_{\text{avg}}| < d_{\text{SoC}}. \end{cases} \tag{26}$$

Consequently, as the BESS units operate in the MG, the equalization is achieved. In this approach, the average SoC is obtained using a dynamic consensus technique, then, the EMS is defined as multiagent system. Another example of an algorithm for a multiagent system in ac MGs, is the design presented in [147], where the control input (u_{iB}) for achieving SoC equalization is defined to implement the ω_{ref} for the droop control

$$\omega_{ref} = \int u_{i\omega} + \frac{k_{iP}}{k_{iB}}u_{iB} \tag{27}$$

where u_{iB} is designed as in (28), $u_{i\omega}$ is the control input for frequency recovery, and k_{iP} and k_{iB} are constant parameters

$$u_{iB} = \sum_{j=1}^{N} a_{ij}\left[k_{is}(\text{SoC}_j - \text{SoC}_i) + k_{id}(\dot{\text{SoC}}_j - \dot{\text{SoC}}_i)\right] \tag{28}$$

with k_{is} and k_{id} being the control parameters.

In addition, the authors in [3], [6], [129], [130], [131], and [132] achieved SoC equalization, voltage regulation, and frequency regulation in ac MG. In these proposals, the dynamic average SoC is estimated through a consensus strategy employing graph theory. Subsequently, this value is processed in an adaptive frequency droop based on virtual power. Shotorbani et al. [133] obtained the average values of frequency, power, SoC, and voltage through neighbor-to-neighbor communication. Subsequently, SoC balancing, power sharing, frequency regulation, and voltage regulation are achieved through droop control.

Furthermore, in [126], a leader–follower finite-time consensus strategy approach is able to manage the BESS units, with power tracking and SoC equalization guaranteed in finite-time. First, a virtual leader updates the reference power and energy states according to frequency control in the power system. Subsequently, the reference states are received and transmitted to all BESS units, achieving a consensus steady-state. Moreover, the finite-time fuzzy sliding mode cooperative backstepping scheme, based on a directed graph, improved the voltage tracking operation of the BESS units in the EV, as indicated in [127]. However, during discharging mode, the BESS units have to be fully discharged to achieve SoC equalization. Furthermore, with the rise in cyber attacks, it is important to consider the resilience of MGs, as indicated in [147] for ac MGs. Conversely, this approach did not consider communication delay.

In addition, considering communication delays for ac MGs, the authors in [134] and [135], distributed control for an ac MG with aperiodic sample data control in [134], while Rostami and Hamzeh [135] focused on managing the active and reactive power according to the capacity of BESS units and PV systems. In addition, the approach from [114] is modified in [136], which is based on fixed-time control strategy for frequency and voltage regulation. Later, the average SoC is obtained by a fixed-time observer and is processed through the Artstein's transformation, which can guarantee stability with a time delay. Then, a nonlinear sliding mode is responsible for providing the SoC equalization by generating a frequency reference that will be used in a droop control for the voltage source inverter. However, when considering these approaches, the time delay needs to be smooth and controlled. In addition, Afshari et al. [148] accounted for communication delay and was reliable under deception attacks. Nevertheless, this approach had the BESS units being discharged to achieve SoC balance.

Moreover, the authors in [137] and [138] proposed an event-triggered strategy for controlling ac MGs. Consequently, each BESS unit can update its local control at a determined event by obtaining local information from its own and neighboring units. After the trigger condition, there is a dynamic consensus with an average SoC that provides a power reference to the droop control. Conversely, the approach in [137] neglected communication delays, while approach in [138] is based on small signal analysis, resulting in variations among system parameters.

E. CONSENSUS-BASED CONTROL FOR DC MGS

To mitigate the imbalances caused by droop control, some authors have proposed consensus-based control, as indicated in [117] for hybrid ESS. This approach involves processing a state variable defined as a function of the output power, capacity, and SoC from each BESS unit, as follows:

$$x_i = \frac{P_B}{C_{\text{bat}i} F_{\text{SoC}i}} \tag{29}$$

with $F_{\text{SoC}i}$ defined as follows:

$$F_{\text{SoC}i} = \begin{cases} \text{SoC}_i - 0.4, & \text{for discharging} \\ 0.9 - \text{SoC}_i, & \text{for charging.} \end{cases} \tag{30}$$

Then, all state variables for the ith unit are employed to generate a consensus neighbor-to-neighbor, providing a current reference for the BESS unit, which is processed through a PI controller, as follows:

$$i_{\text{ref}} = -G_{\text{bat}i} \sum_{j=i}^{N} a_{ij}(X_i - X_j) + G_{vi}(v_{\text{ref}} - v_o) \tag{31}$$

with $G_{\text{bat}i}$ and G_{vi} being transfer function from consensus and voltage controller.

Moreover, a proportional current sharing approach has been presented in [31], where the current reference for all BESS units is defined by a PI controller. Subsequently, consensus control for SoC equalization is responsible for providing the proportional current for each ith BESS unit.

As indicated in [118], there is an adaptive power allocation to coordinate SoC equalization among BESS units in a hybrid ESU array. First of all, the upper layer is based on a two time-scale optimization to optimize the power of BESS units and SCs. Then, a weighted discrete consensus algorithm based on model predictive control is designed to allocate the power among the BESS units in the lower layer, named as the distributed control layer. [119], [120] implemented a power allocation strategy that contained information from the SoC for the ith BESS unit.

In addition, an event trigger condition with dynamic average consensus is embedded into the proposal to achieve SoC equalization. As a result, the transmission signal from each BESS unit to its neighbors is transmitted only when requested, leading to a reduction in communication traffic. Furthermore, Xing et al. [120] also applied reliability to consensus against communication failure.

A cooperative controller proposed by Morstyn et al. [121] can coordinate power sharing between the BESS units and UC in a dc MG. In this approach, the BESS leader regulates the UC voltage, while the BESS followers track the SoC from the BESS leader based on neighbor information.

The current reference of each BESS unit is defined by a local cooperative controller based on the difference between its corresponding SoC and the average consensus SoC from neighbors. In addition, as indicated in [125] and [149], a consensus-based approach defines the SoC of all BESS units to be used in distributed power sharing. In the proposal [149], SoC equalization is achieved among clustered dc nanogrids (NGs) in an islanded dc MG. BESS unit components connected to the dc-link may cause system instability due to exceeding power limits during load variations or significant voltage fluctuations.

F. CONSENSUS-BASED CONTROL FOR AC MGS

In the methodology proposed in [139], a distributed control for heterogeneous ESS (HESS), composed of BESS units and building-based ESS with flexible load, can ensure SoC equalization, state of temperature, state of energy, and tracking of the power objective. Thus, an event-triggered communication delivers the strategy and control for the HESS. Finally, an optimal feedback control based on Riccati theory enables proportional power sharing. Similarly to [139], the approach in [140] takes into account event-triggered communication with denial-of-service attacks. This method is also applied in MGs with HESS, investigating frequency regulation and enabling power sharing based on linear quadratic regulator (LQR) control according to SoC and state of temperature. In addition, the approach in [141] focuses on power sharing through multi-agent communication, obtaining SoC, active power, and reactive power to achieve equalization and management among BESS units.

Furthermore, the authors in [41] and [42] designed distributed control for SoC balancing in a grid-connected ac MG, while Raeispour et al. [142] considered an islanded ac MG. In these proposals, the average SoC and power were achieved through neighbor-to-neighbor communication to define the reference power for the ith BESS unit. In addition, Raeispour et al. [142] also accounted for communication delays and external disturbances in the EMS.

Finally, an example of application could be the approach described in [143], which eliminates differences in the SoC and power among all BESS units in a wind farm by defining a consensus condition based on SoC and active power. Another application is proposed in [144], which presented a voltage and frequency regulation for a system composed of PV, BESS units, and wind turbines. The SoC balance is maintained by more than two leaders regulating the BESS units, ensuring that the containment control keeps the EMS stable even if one leader in the consensus protocol withdraws from the formation. However, the approach in [144] demands a complex communication network, increasing the cost, and may also lead to oscillations among power converters.

G. DYNAMIC DIFFUSION ALGORITHM BASED ON DISTRIBUTED UNIFIED CONTROLLER

A distributed unified controller has been proposed by [124] to obtain the voltage reference v_{ref}. Unlike droop control, the unified control directly introduces a correction term v_i without the need of a virtual resistance.

The v_{ref} is obtained as follows:

$$v_{\text{ref}} = v_o + v_i \tag{32}$$

with v_i designed as follows:

$$\dot{v}_i = \kappa \left(v_o - \frac{\chi_{\text{avg}i}}{\sigma_i}. \right) \tag{33}$$

Here, the integrator gain is represented by κ, and $\chi_{\text{avg}i}$ and σ_i are the average virtual state variables and transition factors of BESS units, respectively, determined as follows:

$$\begin{cases} \chi_{\text{avg}i} = \frac{\sum_{i=1}^{n} \chi_i}{n} \\ \chi_i = \sigma_i v_{oi} \\ \sigma_i = 1 - \rho \frac{\Delta v_{v_i}}{\Delta v_{\max}}. \end{cases} \tag{34}$$

The virtual state variable is represented by χ_i. ρ is a gain in the range [0-1] to avoid σ_i being zero. $\Delta v_{\max}$ could be designed as 10% of the rated voltage, and the fictitious voltage drop Δv_{v_i} could be determined as follows:

$$\Delta v_{v_i} = R_{vi} i_{\text{BESS}}. \tag{35}$$

Then, to achieve equalization, the R_{vi} is defined as follows:

$$R_{v_i} = \begin{cases} \frac{1}{C_{\text{bat}}} \left(\frac{\text{SoC}_{\text{avg}i}}{\text{SoC}_i} \right) K_{\text{opt}i}, & i_{\text{BESS}i} > 0 \\ \frac{1}{C_{\text{bat}}} \left(\frac{\text{DoD}_{\text{avg}i}}{\text{DoD}_i} \right) K_{\text{opt}i}, & i_{\text{BESS}i} < 0 \end{cases} \tag{36}$$

with K_{opti} being the optimized convergence parameter, defined as follows:

$$K_{\text{opti}} = \frac{1}{|\text{SoC}_{\text{avg}i} - \text{SoC}_i| + m} \tag{37}$$

with m being a convergence factor.

1) DYNAMIC DIFFUSION ALGORITHM

As the consensus strategy has two time scales–the first to collect the average state variable of neighboring nodes and the second to calculate the average state variables of neighboring nodes locally–this approach can result in slow estimation and may lead to instability in the control system. Thus, the dynamic diffusion strategy is an alternative to distributed average estimation that overcomes the drawbacks of the consensus algorithm methodology [151].

First, a time varying quadratic function is determined as follows:

$$J[x_i(k)] = \frac{1}{2} \|x_i(k) - r_i(k)\|^2 \tag{38}$$

with J being strongly convex and differentiable, $r_i(k) = [\chi_{\text{avg}i}(k), \text{SoC}_{\text{avg}i}]$ being the initial state variables, and $x_i(k) = [\chi_{\text{avg}i}(k), \text{SoC}_{\text{avg}i}]$ being the average state of BESS units at kth iteration.

In sequence the average cost in (39) should be minimized as follows:

$$J[x_i(k)] \triangleq \frac{1}{n} \sum_{i=1}^{n} J[x_i(k)] \tag{39}$$

$$x_{\min}(k) \triangleq \arg\min J[x(k)] = r_{\text{avg}i}(k) \triangleq \frac{1}{n} \sum_{i=1}^{n} r_i(k) \tag{40}$$

Algorithm 1: Iterative Update Algorithm.

1: Initialize $x_i(0)$ randomly, $x_i(0) = \xi_i(0)$
2: **for** k = 1, 2, 3, ... **do**
3: $\quad \psi_i(k) = x_i(k-1) + \mu[r_i(k) - x_i(k-1)]$
4: $\quad \xi_i(k) = x_i(k-1) + \psi_i(k) - \psi_i(k-1)$
5: $\quad x_i(k) = \sum_{j \in N_i} a_{ij} \xi_j(k)$
6: $\quad$ **if** stop criteria is met **then**
7: $\quad\quad$ **break**
8: $\quad$ **end if**
9: **end for**

with the minimum value of $J[x(k)]$ represented by $x_{\min}(k)$ and the average value of $r_i(k)$ being $r_{\text{avg}i}(k)$. Thus, the algorithm of dynamic diffusion strategy for each node is defined as follows.

The adaptive variables for the BESS units at iterations $k-1$ and k are represented by $\psi_i(k)$, where μ is a constant step size (chosen as a small value). $\xi_i(k)$ and $\xi_j(k)$ are the intermediate variables for BESS$_i$ and BESS$_j$, respectively, and a_{ij} is obtained as follows:

$$a_{ij} = \begin{cases} \frac{1}{\max(N_j, N_i)}, & \text{if } i \neq j \text{ and } i \in N_j \\ 1 - \sum_{i \in N_j} a_{ij}, & \text{if } i = j \\ 0, & \text{if } i \notin N_j. \end{cases} \tag{41}$$

Thus, according to the defined algorithm, the intermediate variable is transferred to the neighboring BESS units without the need for another iterative calculation. Later, a new round of data are processed, ensuring that the methodology operates with a continuous data flow on a single time scale. However, the approach described in [124] does not elaborate on a significant result to exemplify the superiority of the diffusion algorithm.

H. ADAPTIVE POWER ALLOCATION ALGORITHM

From a different perspective, the adaptive power allocation proposed by [122] is evaluated. First, a dynamic average consensus to obtain the estimated SoC is assessed, as defined as follows:

$$\begin{cases} \text{SoC}_{\text{avg}i}(k+1) = \text{SoC}_i(k) + \zeta_i \sum_{j=1}^{n} \vartheta_{ij}(k+1) \\ \vartheta_{ij}(k+1) = \vartheta_{ij}(k) + a_{ij} \left[\text{SoC}_{\text{avg}j}(k) - \text{SoC}_{\text{avg}i}(k) \right] \end{cases} \tag{42}$$

where $\vartheta_{ij}(k)$ is the accumulative SoC error between BESS unit i and j and ζ_i is the connection between agents i and j. Later, the adaptive power allocation algorithm is represented as follows:

$$P_{\text{refi}} = \frac{C_{\text{bat}i} P_{\text{ref}}}{\sum_{i=1}^{n} C_{\text{bat}i}} + \Delta P_i \tag{43}$$

with P_{ref} being the power reference from BESS unit, and ΔP_i the adjustment power responsible for achieving SoC equalization, defined as follows:

$$\Delta P_i = \alpha \left(\frac{\text{SoC}_i - \text{SoC}_{\text{avg}}}{\text{SoC}_{\text{avg}}} \right) P_{\text{ref}} \tag{44}$$

where α denotes the adjustment factor. In addition, when all SoCs have the same value, $\text{SoC}_i = \text{SoC}_{\text{avg}}$, it results in $\Delta P_i = 0$.

In sequence, cooperative adaptive terminal sliding mode designs the controller for each BESS unit. According to [122], in this method, multiagent control operating along with sliding mode control can enhance the control system.

The proposal by the authors of [8] and [123] elaborates on an adaptive power allocation for BESS units based on SoC. First, the average power and average unit state (based on SoC) are obtained asymptotically by a consensus protocol for each BESS unit. In the approach from [8], the dynamics SoC is defined as follows:

$$\dot{\text{SoC}}_i = -\frac{1}{C_{\text{bat}i} V_{\text{bat}i}} P_{\text{bat}i}. \quad (45)$$

Then, the rules to regulate SoC variation during the charging and discharging processes, as outlined in (46) and (47) respectively, are as follows:

$$\frac{\dot{\text{SoC}}_1}{\text{SoC}_1} = \frac{\dot{\text{SoC}}_2}{\text{SoC}_2} = \cdots = \frac{\dot{\text{SoC}}_n}{\text{SoC}_n} \quad (46)$$

$$\frac{\dot{\text{SoC}}_1}{1-\text{SoC}_1} = \frac{\dot{\text{SoC}}_2}{1-\text{SoC}_2} = \cdots = \frac{\dot{\text{SoC}}_n}{1-\text{SoC}_n}. \quad (47)$$

Later, the power of each BESS unit is defined as in (48) and (49) for charging and discharging mode, respectively

$$P_{Bi} = \frac{C_{\text{bat}i} V_{\text{bat}i} \text{SoC}_i}{\sum_{i=i}^{N} C_{\text{bat}i} V_{\text{bat}i} \text{SoC}_i} P_{B\_\text{total}} \quad (48)$$

$$P_{Bi} = \frac{C_{\text{bat}i} V_{\text{bat}i} (1-\text{SoC}_i)}{\sum_{i=i}^{N} C_{\text{bat}i} V_{\text{bat}i} (1-\text{SoC}_i)} P_{B\_\text{total}}. \quad (49)$$

Later, also in the approach from [8], a finite-time estimation provides the parameters to achieve SoC equalization. However, the rate at which the time observer converges is influenced by the initial values and specific parameters of the BESS units, which limits its applicability.

I. DISTRIBUTED CLUSTERING ALGORITHM

Distributed clustering enables the division of cluster agents into specific groups, such as those based on power demands and capacities for BESS units [145]. Thus, as proposed by the authors in [145] and [146], these cluster agents can reduce line currents and consequently power losses in the MG. Initially, average parameters are defined and subsequently separated into clusters. Therefore, after aggregating the BESS units into groups, balance in the SoC is achieved within each cluster.

In this context, each cluster accomplishes SoC equalization through a distributed sliding mode control, which includes a term added to droop control. Furthermore, the approach in [52] classifies the clusters according to bulk power demand by providing a high-frequency component. After the division into groups, a consensus-based protocol defines a term to keep the SoC from BESS units balanced that is introduced into the droop control. In addition, Jena and Padhy et al. [152] has introduced cybersecurity into the dc MG clusters under manipulation attacks. This is a significant topic because the interconnected system could have an EMS to achieve SoC equalization among BESS units and maintain consistency against cyberattacks.

In addition, the clustering algorithm can serve as an approach to classify distributed energy resources into a virtual power plant. Finally, classifying the BESS units under operation into clusters could be an emerging topic. The units could be divided according to specific parameters, such as SoH and capacity. In sequence, each group could then follow a different EMS for SoC equalization designed for each cluster.

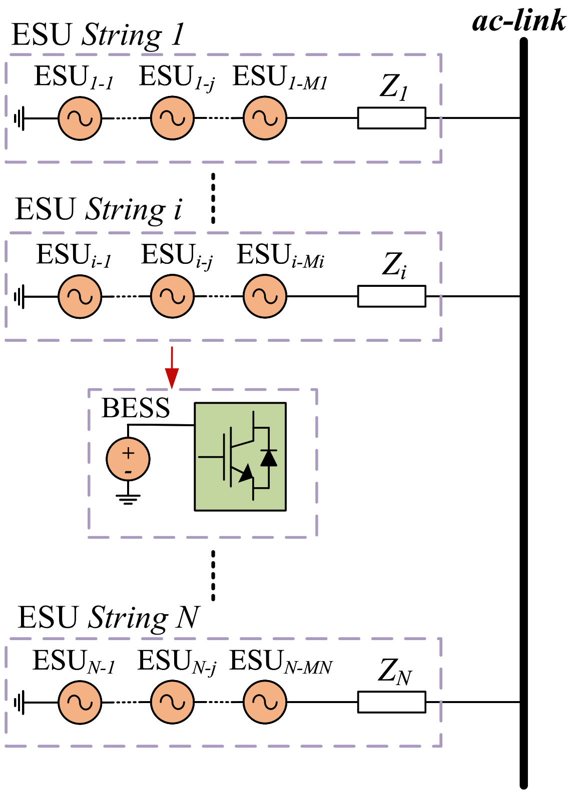

FIGURE 14. Example of hybrid series-parallel topology.

VII. HYBRID-TYPES SYSTEMS

Some approaches involve system configurations composed of N parallel strings, each formed by series-connected BESS, as depicted in Fig. 14 [150], where ESU represents the BESS connected to the H-Bridge topology. Thus, the local EMS among strings can be implemented differently compared to the series-connected BESS.

A. LOCAL-CENTRALIZED AND GLOBAL DECENTRALIZED

In [94], the hybrid-type system receives SoC equalization among BESS in each string by implementing a locally centralized control, which receives voltage and frequency data from global communication. This information is then adjusted locally based on the SoC of each unit in the string. For global control, it operates through a decentralized SoC-based droop, which relies on the SoC of each string.

However, a failure in communication may lead to a fault in the BESS unit and result in a crash of SoC balancing. In addition, without effective communication, achieving SoC equalization through a decentralized method is not possible due to transmission characteristic incompatibilities between parallel-type and cascaded-type topologies.

B. LOCAL-DISTRIBUTED AND GLOBAL DECENTRALIZED

Han et al. [150] implemented a SoC equalization method in a hybrid series-parallel system. Thus, within a local BESS string, distributed SoC balancing is achieved, utilizing both local and neighbor-to-neighbor information to define the voltage amplitude based on SoC using dynamic consensus. Later, when considering the strings, the system can be analyzed as a parallel ac MG, which will employ a SoC-based droop strategy to balance the BESS among strings.

In addition, a voltage-shifting term is applied to achieve SoC equalization. However, a term with high gain increases the SoC equalization speed but generates circulating currents. Therefore, the gain should be reduced, which can impact the rate of SoC balancing.

VIII. TOPOLOGY OF POWER CONVERTER

Most SoC equalization approaches are implemented in either a common dc MG or an ac MG. In a common dc MG, bidirectional boost converters are tied to a common dc-link. For an ac MG, boost converters are connected to inverters, which are then tied to a common ac-link. However, there are power converter topologies that can enhance the operation of BESS units, such as redundancy-based power converters, bidirectional MMCs and cascaded multiport converter and cascaded-type.

The topology of power converters can also be important for improving the operation among BESS units, regardless of whether the strategy is multiagent control, centralized, or decentralized control.

As defined in [35], redundant modules in a dc/dc converter can improve its reliability when a fault or maintenance event occurs. Therefore, if a redundancy-based MG receives an algorithm responsible for balancing the SoC among BESS units, the overall efficiency of the system can be increased. Fig. 15 shows an example of a redundant topology.

The MMC is a topology capable of controlling BESS units to enhance power quality, reliability, and fault-tolerance capability. For instance, an approach to balance BESS units, as described in [153] and shown in Fig. 16, was applied in a modular multilevel dc/dc converter using a SoC-based droop with low-bandwidth communication. In this method, the droop control is current-source based, operating alongside a current correction to mitigate the control deviation caused by droop. In addition, a SoC slope term is introduced, which depends on the average SoC from all BESS units.

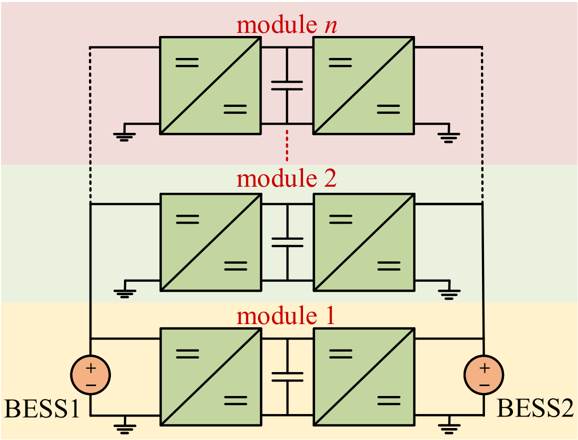

FIGURE 15. Example of redundant modules to enhance the SoC balancing.

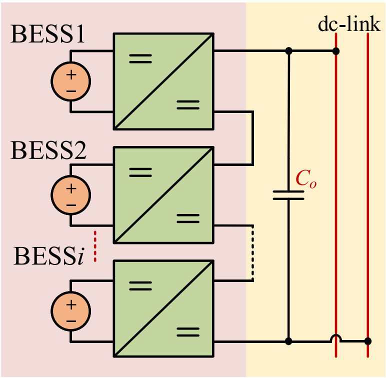

FIGURE 16. Example of MMC to interface BESS units.

Moreover, the topology proposed in [36] is a bidirectional MMC with a compact structure, flexible power control, and fault-tolerant capability, making it ideal for shipboard applications. Furthermore, the authors in [154], [155], [156], [157], and [158] employed PI control to balance the SoC in the MMC-BESS, with the work in [154], [155], and [156] connected to the ac grid. Another example is the single-phase cascaded H-bridge multilevel converter proposed in [159], which elaborates on a gain scheduling-based adaptive SoC balancing.

In addition, a consensus-based control approach for SoC equalization, as introduced in [40], is applied in a differential power processing (DPP) converter to accommodate BESS units, as shown in Fig. 17 with a front-end converter. Meanwhile, Wang et al. [31] proposed a cascaded multiport (see Fig. 18) converter that enables the integration of multiple BESS units in a dc MG. This setup allows the dc/dc converter to balance the power mismatch between PV generation and load dissipation in the dc MG.

Furthermore, Shi et al. [15] has proposed a decentralized SoC balancing method in a cascaded-type ESS. The topology, indicated in Fig. 19, is suitable for large-scale applications, with middle-level and high-level voltages, because the semiconductor switches can provide low output-voltage harmonic

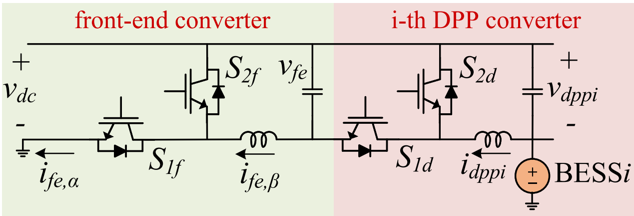

FIGURE 17. Structure of front-end converter and DPP converter: currents from the DPP converter are denoted as $i_{\text{dpp}i}$, while $v_{\text{dpp}i}$ is the input voltage. Currents from the front-end converter are $i_{\text{fe},\alpha}$ and $i_{\text{fe},\beta}$, with v_{fe} and v_{dc} representing the input and output voltages, respectively.

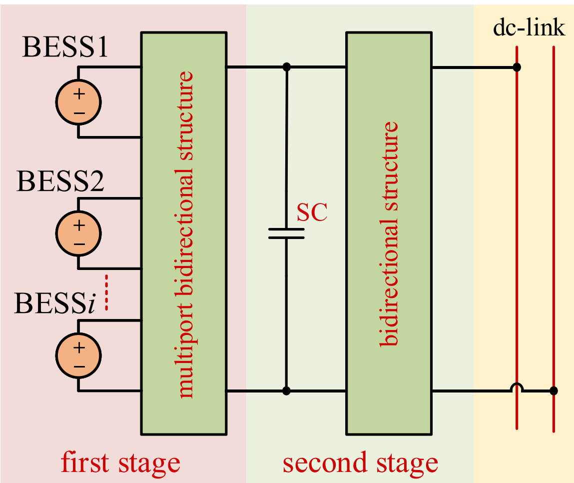

FIGURE 18. Multiport converter (first stage) connected to a bidirectional structure (second stage) through a SC.

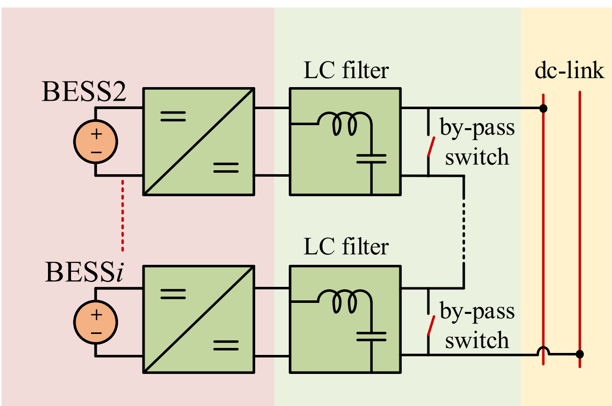

FIGURE 19. Cascaded-type converter with *LC* filter and by-pass switch.

distortion. In addition, it provides the capability to operate an SoC balancing strategy among BESS units without requiring additional balancing circuits. In this sense, Table 11 presents the pros and cons of power converter topologies for SoC equalization among BESS units. Finally, the study of different topologies from the conventional structure of a common ac MG or dc MG could be beneficial. These studies could increase reliability, implement fault-tolerant capabilities, and introduce higher voltage levels in the operation of the MG.

IX. OPTIMIZATION STRATEGY AS TERTIARY CONTROL ALONGSIDE EMS FOR SOC EQUALIZATION

Several methodologies have been studied to optimize the operation of MGs, considering objectives, such as improving load balance, reducing economic costs, and minimizing energy losses. Agnoletto et al. [160] proposed an optimization method based on the ϵ-constraint method for ac MGs. However, this approach assumes only a single BESS unit pack, and consequently, SoC equalization is not taken into account. Similarly, Parisio et al. [161] applied mixed-integer linear programming to reduce the total cost of MGs, but did not address SoC equalization. In addition, a GA was developed for a six-bus dc MG operating under droop control to provide a cost-effective solution. However, it also did not take SoC equalization for BESS units into account.

Although optimization is an important strategy for MG operation, according to [11], there is a lack of consideration for the optimization process as tertiary level control with SoC balancing among BESS units as secondary level. Only a few works have taken optimal parameters for MG operation with SoC balancing into account. For example, the EMS in [118] considered real-time power optimization for a hybrid energy storage array system with SoC equalization. In addition, Fagundes et al. [11] examined an EMS with optimal parameters to reduce the total operating cost of a redundancy-based dc MG and balance the SoC among BESS units. Thus, the EMS uses particle swarm optimization (PSO) to optimize its parameters from the current reference, as shown in (50) for an S-shaped function, with the objective function defined to minimize the operating costs of the alternative sources and BESS units by modifying the parameter α_{sig} and the minimum dc-link voltage reference $v_{\text{ref\_min}}$

$$\begin{cases} i_{\text{ref}} = \overbrace{\alpha_{\text{sig}}}^{\text{PSO}} \underbrace{\left(\dfrac{2}{1 + e^{(e_{\text{factor}} - \text{SoC})p}} - 1\right)}_{\text{term in p.u.}} \\ e_{\text{factor}} = \dfrac{v_o - \overbrace{v_{\text{ref\_min}}}^{\text{PSO}}}{\Delta v_o}. \end{cases} \tag{50}$$

These approaches have significant interest in the field of MGs because they not only involve MG operation to provide EMS but also entail optimization strategies that can benefit the overall operational result of the MG by considering the SoC balancing strategy.

X. 2-BESS UNITS

As there are more and more applications for BESS units, concerns about how to handle them after their useful life have arisen because a significant number of BESS units are disposed in landfills without recycling [38]. However, several studies have indicated that BESS units, after reaching the end of their useful life, can be used for other applications. Most of the BESS units that become obsolete are originally from EV applications and can be reused for utility sector applications [162].

TABLE 11. Pros and Cons Regarding SoC Equalization for Different Topologies of Power Converter

	Pros	Cons
Traditional Topology	Easy implementation of EMS	No fault-tolerant capability
Redundant Modules	Easy implementation of EMS, fault-tolerant capability (BESS unit continues to operate)	BESS units should have similar capacities
MMC	Fault-tolerant capability, high voltage output	Complex implementation of EMS, usually requires PI for SoC balancing, when a fault occurs, the submodule with BESS unit is isolated
Cascaded Multiport Converter	Reduced number of converters	No fault-tolerant capability
Cascaded-Type	High voltage output, reliability on communication	No fault-tolerant capability
DPP Converter	The power rating is reduced	No fault-tolerant capability

Thus, the term "second-life battery" has emerged to describe retired BESS units that can be repurposed. According to the US Advanced Battery Consortium, the end of EV battery life occurs when there is a decrease of 20% in rated capacity [163]. As a result, the application of second-life batteries for different purposes could significantly reduce environmental impact and economic costs.

In addition, several studies have been conducted to estimate the SoH, which is important for handling second-life batteries [164]. In addition, Cheng et al. [165] presented a study that considers the degradation of second-life batteries with online SoH estimation, while Yang et al. [166] estimated second-life battery capacity.

Moreover, a study regarding the operation of 2-BESS units in MGs has been conducted in [167], showing that an average reduction of 60% in maximum peak demand and 39% in peak energy consumption, with 164.5 kW of PV and 262 kWh of 2-BESS, was achieved in the MG. Thus, the challenge is to aggregate 2-BESS units in MGs with fresh BESS units of different capacities and power limits, i.e., heterogeneous batteries, to receive an EMS and operate together [168]. In the approach from [168], the tasks for operating a 2-BESS unit are described as follows.

1) Reduction of the aggregate power rating from power converters: it is the sum of the ratings of the individual power converters, which constitutes the overall electrical power required for normal operation of a power converter.
2) Reduction of the amount of power converters.
3) Reduction of different types of converters.
4) Increase the overall performance, including power capability.

Considering 2-BESS units for SoC balancing, there is limited research on this topic. However, some authors are beginning to take into account the operation of 2-BESS units in various power converter structures. Mukherjee and Strickland [169] elaborated a study suggesting a MMC to integrate 2-BESS units with different characteristics (voltage level, maximum capacity, and degradation levels). In addition, the authors in [170] and [171] proposed a control strategy that takes into account the SoC and the capacity of 2-BESS units in a cascaded H-bridge converter. Furthermore, a SoC balancing strategy in a cascaded H-bridge converter is proposed in [172], considering active power constraints that could be applied to 2-BESS units operated asymmetrically. Moreover, Mukherjee and Strickland [173] proposed a modular boost-multilevel buck dc/dc converter to interface 2-BESS units to an inverter dc-link, providing flexible performance to handle different battery voltages and power levels.

Furthermore, Liang et al. [155] proposed a control methodology to regulate power and balance the SoC among different 2-BESS unit capacities interfaced by a MMC, which is a three-port power converter connected to a dc-link with the midpoint connected to an ac grid. In this approach, the SoC balance occurs at three different levels considering the power converter structure: 1) phase legs, 2) upper and lower arms, and 3) individual submodules. An essential feature of all SoC balancing is that the methodology considers the 2-BESS units' capacity.

Finally, parameter estimation has been conducted, as well as the design of power converter structures to accommodate 2-BESS units. The application of 2-BESS units in MGs concerning SoC and other parameters to operate in EMS and SoC balance presents challenges to be solved and analyzed as a potential emerging topic.

XI. CONCLUSION

In this article, we propose a review of strategies for EMS applied to balance the SoC among BESS units. The EMS can be categorized into centralized control, decentralized control, and multiagent systems. In this context, the latest approaches from the literature are discussed, including centralized and decentralized SoC-based droop methods, with a comparison of several approaches that obtain the droop factor differently to weight the SoC. In addition, optimal algorithm can provide SoC balancing in a centralized approach. Furthermore, the designed of nonlinear function and FIS can achieve BESS units operating with the same SoC level without communication among each other.

In addition, the multiagent system addresses a combination of local information with neighbor-to-neighbor communication without requiring a central controller, including the most applied strategy, which is consensus control. This can operate alongside other strategies, such as sliding mode control and adaptive power allocation. Given the overview of the techniques, the SoC balance operation can be centralized, decentralized, or a multiagent system according to the needs of the MGs, which is important due to factors, such as size, number of sources, and BESS units. Moreover, a meticulous comparison of strategies considering MG type (ac, dc, or ac/dc), topology of power converters, voltage/frequency regulation, combination with UCs or SCs, operation as islanded or grid-connected, strengths and drawbacks, and main equations from the EMS can address the initiatives that can be enhanced for further research.

In this article, we also discussed techniques that can enhance SoC equalization, including a comparison of the topologies of power converters, the employment of redundant modules, MMC, cascaded-based converters, and DPP converters and hybrid-type systems. For instance, shipboard MGs can incorporate redundant modules to improve reliability and tolerance capability, thereby enhancing the operation among BESS units. In addition, a distributed clustering strategy is another significant approach to categorize the agents into specific groups. Finally, emerging topics, such as optimization, at the tertiary level alongside SoC equalization and the application of 2-BESS units in MGs are gaining attention. These areas should include the consideration of BESS units operating with balanced SoC as a potential and interesting research topic.

REFERENCES

[1] S. Choudhury, "Review of energy storage system technologies integration to microgrid: Types, control strategies, issues, and future prospects," *J. Energy Storage*, vol. 48, 2022, Art. no. 103966, doi: 10.1016/j.est.2022.103966.

[2] M. H. Saeed, W. Fangzong, B. A. Kalwar, and S. Iqbal, "A review on microgrids' challenges & perspectives," *IEEE Access*, vol. 9, pp. 166502–166517, 2021, doi: 10.1109/ACCESS.2021.3135083.

[3] S. V. M. Ouoba, A. Houari, and M. Machmoum, "A resilient control for distributed energy storage units in an islanded AC microgrid," *IEEE Trans. Emerg. Sel. Topics Power Electron.*, vol. 12, no. 2, pp. 1446–1455, Apr. 2024, doi: 10.1109/JESTPE.2023.3261669.

[4] M. A. Saadi, M. Al-Greer, and M. Short, "Strategies for controlling microgrid networks with energy storage systems: A review," *Energies*, vol. 14, no. 21, 2021, Art. no. 7234, doi: 10.3390/en14217234.

[5] X. Tan, Q. Li, and H. Wang, "Advances and trends of energy storage technology in microgrid," *Int. J. Elect. Power Energy Syst.*, vol. 44, no. 1, pp. 179–191, 2013, doi: 10.1016/j.ijepes.2012.07.015.

[6] C. Li, E. A. A. Coelho, T. Dragicevic, J. M. Guerrero, and J. C. Vasquez, "Multiagent-based distributed state of charge balancing control for distributed energy storage units in AC microgrids," *IEEE Trans. Ind. Appl.*, vol. 53, no. 3, pp. 2369–2381, May/Jun. 2017, doi: 10.1109/TIA.2016.2645888.

[7] R. R. Kumar, C. Bharatiraja, K. Udhayakumar, S. Devakirubakaran, K. S. Sekar, and L. Mihet-Popa, "Advances in batteries, battery modeling, battery management system, battery thermal management, SoC, SOH, and charge/discharge characteristics in EV applications," *IEEE Access*, vol. 11, pp. 105761–105809, 2023, doi: 10.1109/ACCESS.2023.3318121.

[8] T. Meng, Z. Lin, and Y. A. Shamash, "Distributed cooperative control of battery energy storage systems in DC microgrids," *IEEE/CAA J. Automatica Sinica*, vol. 8, no. 3, pp. 606–616, Mar. 2021, doi: 10.1109/JAS.2021.1003874.

[9] K. D. Hoang and H.-H. Lee, "Accurate power sharing with balanced battery state of charge in distributed DC microgrid," *IEEE Trans. Ind. Electron.*, vol. 66, no. 3, pp. 1883–1893, Mar. 2019, doi: 10.1109/TIE.2018.2838107.

[10] N. Li, F. Gao, T. Hao, Z. Ma, and C. Zhang, "SOH balancing control method for the MMC battery energy storage system," *IEEE Trans. Ind. Electron.*, vol. 65, no. 8, pp. 6581–6591, Aug. 2018, doi: 10.1109/TIE.2017.2733462.

[11] T. A. Fagundes et al., "Economic operation optimization under real-time pricing for an energy management system in a redundancy-based microgrid," *IEEE Trans. Ind. Electron.*, vol. 71, no. 8, pp. 8872–8882, Aug. 2024, doi: 10.1109/TIE.2023.3325566.

[12] T. Morstyn, B. Hredzak, and V. G. Agelidis, "Control strategies for microgrids with distributed energy storage systems: An overview," *IEEE Trans. Smart Grid*, vol. 9, no. 4, pp. 3652–3666, Jul. 2018, doi: 10.1109/TSG.2016.2637958.

[13] C. H. Ricardo, L. H. Adriana, and D. A. Nelson, "Energy management supported on genetic algorithms for the equalization of battery energy storage systems in microgrid systems," *J. Energy Storage*, vol. 72, 2023, Art. no. 108510, doi: 10.1016/j.est.2023.108510.

[14] Y. Zeng et al., "State-of-charge dynamic balancing strategy for distributed energy storage system in dc shipboard microgrid," *Int. J. Elect. Power Energy Syst.*, vol. 133, 2021, Art. no. 107094, doi: 10.1016/j.ijepes.2021.107094.

[15] G. Shi, H. Han, Y. Sun, Z. Liu, M. Zheng, and X. Hou, "A decentralized SoC balancing method for cascaded-type energy storage systems," *IEEE Trans. Ind. Electron.*, vol. 68, no. 3, pp. 2321–2333, Mar. 2021, doi: 10.1109/TIE.2020.2973889.

[16] T. Morstyn, A. V. Savkin, B. Hredzak, and V. G. Agelidis, "Multi-agent sliding mode control for state of charge balancing between battery energy storage systems distributed in a DC microgrid," *IEEE Trans. Smart Grid*, vol. 9, no. 5, pp. 4735–4743, Sep. 2018, doi: 10.1109/TSG.2017.2668767.

[17] T. A. Fagundes, G. H. F. Fuzato, C. R. De Aguiar, K. D. A. Ottoboni, M. Biczkowski, and R. Q. Machado, "Management and equalization of energy storage devices for DC microgrids using a SoC-sharing function," *IEEE Access*, vol. 8, pp. 78576–78589, 2020, doi: 10.1109/ACCESS2020.2990191.

[18] N. L. Diaz, T. Dragičević, J. C. Vasquez, and J. M. Guerrero, "Intelligent distributed generation and storage units for DC microgrids–A new concept on cooperative control without communications beyond droop control," *IEEE Trans. Smart Grid*, vol. 5, no. 5, pp. 2476–2485, Sep. 2014, doi: 10.1109/TSG.2014.2341740.

[19] Y. Mi, J. Deng, X. Wang, S. Lin, X. Su, and Y. Fu, "Multiagent distributed secondary control for energy storage systems with lossy communication networks in DC microgrid," *IEEE Trans. Smart Grid*, vol. 14, no. 3, pp. 1736–1749, May 2023, doi: 10.1109/TSG.2022.3214745.

[20] N. Zhi, K. Ding, L. Du, and H. Zhang, "An SoC-based virtual DC machine control for distributed storage systems in DC microgrids," *IEEE Trans. Energy Convers.*, vol. 35, no. 3, pp. 1411–1420, Sep. 2020, doi: 10.1109/TEC.2020.2975033.

[21] N. L. Díaz, A. C. Luna, J. C. Vasquez, and J. M. Guerrero, "Centralized control architecture for coordination of distributed renewable generation and energy storage in islanded AC microgrids," *IEEE Trans. Power Electron.*, vol. 32, no. 7, pp. 5202–5213, Jul. 2017, doi: 10.1109/TPEL.2016.2606653.

[22] Y. Zeng et al., "Fixed-time secondary controller for rapid state-of-charge balancing and flexible bus voltage regulation in DC microgrids," *IEEE Trans. Power Syst.*, vol. 39, no. 3, pp. 5393–5407, May 2024, doi: 10.1109/TPWRS.2023.3323986.

[23] T. Wu, Y. Xia, L. Wang, and W. Wei, "Multiagent based distributed control with time-oriented SoC balancing method for DC microgrid," *Energies*, vol. 13, no. 11, 2020, Art. no. 2793.

[24] X. Ye, Y. Jia, J. Zhang, W. Zhang, C. Yang, and D. Jiang, "SoC balancing strategy of multi energy storage system in islanded microgrids considering acceleration factor setting," in *2023 8th Asia Conf. Power Elect. Eng.*, 2023, pp. 2603–2608, doi: 10.1109/ACPEE56931.2023.10135866.

[25] X. Lin, R. Zamora, and C. A. Baguley, "A fully filter-based decentralized control with state of charge balancing strategy for battery energy storage systems in autonomous DC microgrid applications," *IEEE Access*, vol. 9, pp. 15028–15040, 2021, doi: 10.1109/ACCESS.2021.3052924.

[26] D. Xu, A. Xu, C. Yang, and P. Shi, "A novel double-quadrant SoC consistent adaptive droop control in DC microgrids," *IEEE Trans. Circuits Syst. II: Exp. Briefs*, vol. 67, no. 10, pp. 2034–2038, Oct. 2020, doi: 10.1109/TCSII.2019.2945009.

[27] W. Jiang, C. Yang, Z. Liu, M. Liang, P. Li, and G. Zhou, "A hierarchical control structure for distributed energy storage system in DC micro-grid," *IEEE Access*, vol. 7, pp. 128787–128795, 2019, doi: 10.1109/ACCESS.2019.2939626.

[28] Q. Wu, R. Guan, X. Sun, Y. Wang, and X. Li, "SoC balancing strategy for multiple energy storage units with different capacities in islanded microgrids based on droop control," *IEEE Trans. Emerg. Sel. Topics Power Electron.*, vol. 6, no. 4, pp. 1932–1941, Dec. 2018, doi: 10.1109/JESTPE.2018.2789481.

[29] Y. Xia, M. Yu, P. Yang, Y. Peng, and W. Wei, "Generation-storage coordination for islanded DC microgrids dominated by PV generators," *IEEE Trans. Energy Convers.*, vol. 34, no. 1, pp. 130–138, Mar. 2019, doi: 10.1109/TEC.2018.2860247.

[30] Z. Cheng, J. Duan, and M. Chow, "To centralize or to distribute: That is the question: A comparison of advanced microgrid management systems," *IEEE Ind. Electron. Mag.*, vol. 12, no. 1, pp. 6–24, Mar. 2018, doi: 10.1109/MIE.2018.2789926.

[31] B. Wang et al., "Consensus-based control of hybrid energy storage system with a cascaded multiport converter in DC microgrids," *IEEE Trans. Sustain. Energy*, vol. 11, no. 4, pp. 2356–2366, Oct. 2020, doi: 10.1109/TSTE.2019.2956054.

[32] W. Zhang, D. Xu, P. N. Enjeti, H. Li, J. T. Hawke, and H. S. Krishnamoorthy, "Survey on fault-tolerant techniques for power electronic converters," *IEEE Trans. Power Electron.*, vol. 29, no. 12, pp. 6319–6331, Dec. 2014, doi: 10.1109/TPEL.2014.2304561.

[33] S. Fang, Y. Xu, H. Wang, C. Shang, and X. Feng, "Robust operation of shipboard microgrids with multiple-battery energy storage system under navigation uncertainties," *IEEE Trans. Veh. Technol.*, vol. 69, no. 10, pp. 10531–10544, Oct. 2020, doi: 10.1109/TVT.2020.3011117.

[34] R. Faraji, L. Ding, T. Rahimi, and M. Kheshti, "Application of soft-switching cell with inherent redundancy properties for enhancing the reliability of boost-based DC–DC converters," *IEEE Trans. Power Electron.*, vol. 36, no. 11, pp. 12342–12354, Nov. 2021, doi: 10.1109/TPEL.2021.3081722.

[35] T. A. Fagundes et al., "A modified redundancy-based energy management system for microgrids: An SoC enhancement approach," *IEEE Trans. Ind. Electron.*, vol. 71, no. 10, pp. 12379–12388, Oct. 2024, doi: 10.1109/TIE.2023.3342325.

[36] P. Chen, F. Xiao, J. Liu, Z. Zhu, and Q. Ren, "Unbalanced operation principle and fast balancing charging strategy of a cascaded modular multilevel converter–bidirectional DC–DC converter in the shipboard applications," *IEEE Trans. Transport. Electrific.*, vol. 6, no. 3, pp. 1265–1278, Sep. 2020, doi: 10.1109/TTE.2020.3016029.

[37] Y. Liu et al., "Multi-objective cooperative controller design for rapid state-of-charge balancing and flexible bus voltage regulation in shipboard DC microgrids," *ISA Trans.*, vol. 146, pp. 421–436, 2024.

[38] J. Li, S. He, Q. Yang, Z. Wei, Y. Li, and H. He, "A comprehensive review of second life batteries toward sustainable mechanisms: Potential, challenges, and future prospects," *IEEE Trans. Transport. Electrific.*, vol. 9, no. 4, pp. 4824–4845, Dec. 2023, doi: 10.1109/TTE.2022.3220411.

[39] M. Faisal, M. A. Hannan, P. J. Ker, A. Hussain, M. B. Mansor, and F. Blaabjerg, "Review of energy storage system technologies in microgrid applications: Issues and challenges," *IEEE Access*, vol. 6, pp. 35143–35164, 2018, doi: 10.1109/ACCESS.2018.2841407.

[40] J. Su and K. Li, "Differential power processing based control framework for multiple battery energy storage systems in DC microgrids," *IEEE Trans. Sustain. Energy*, early access, Jul. 01, 2024, doi: 10.1109/TSTE.2024.3421358.

[41] H. Cai and G. Hu, "Consensus-based distributed package-level state-of-charge balancing for grid-connected battery energy storage system," in *2016 12th IEEE Int. Conf. Control Autom.*, 2016, pp. 365–370, doi: 10.1109/ICCA.2016.7505304.

[42] H. Cai and G. Hu, "Distributed control scheme for package-level state-of-charge balancing of grid-connected battery energy storage system," *IEEE Trans. Ind. Informat.*, vol. 12, no. 5, pp. 1919–1929, Oct. 2016, doi: 10.1109/TII.2016.2601904.

[43] D. N. Huu, "An innovative adaptive droop control based on available energy for DC micro distribution grids," *Energies*, vol. 13, no. 11, 2020, Art. no. 2983.

[44] E. K. Belal, D. M. Yehia, and A. M. Azmy, "Adaptive droop control for balancing SoC of distributed batteries in DC microgrids," *IET Generation, Transmiss. Distrib.*, vol. 13, no. 20, pp. 4667–4676, 2019.

[45] M. Chen and G. Rincon-Mora, "Accurate electrical battery model capable of predicting runtime and I-V performance," *IEEE Trans. Energy Convers.*, vol. 21, no. 2, pp. 504–511, Jun. 2006, doi: 10.1109/TEC.2006.874229.

[46] M. Naguib, P. Kollmeyer, and A. Emadi, "Lithium-ion battery pack robust state of charge estimation, cell inconsistency, and balancing: Review," *IEEE Access*, vol. 9, pp. 50570–50582, 2021, doi: 10.1109/ACCESS.2021.3068776.

[47] D. N. T. How, M. A. Hannan, M. S. Hossain Lipu, and P. J. Ker, "State of charge estimation for lithium-ion batteries using model-based and data-driven methods: A review," *IEEE Access*, vol. 7, pp. 136116–136136, 2019, doi: 10.1109/ACCESS.2019.2942213.

[48] R. Xiong, J. Cao, Q. Yu, H. He, and F. Sun, "Critical review on the battery state of charge estimation methods for electric vehicles," *IEEE Access*, vol. 6, pp. 1832–1843, 2018, doi: 10.1109/ACCESS.2017.2780258.

[49] T. R. Oliveira, W. W. A. G. Silva, and P. F. Donoso-Garcia, "Distributed secondary level control for energy storage management in DC microgrids," *IEEE Trans. Smart Grid*, vol. 8, no. 6, pp. 2597–2607, Nov. 2017, doi: 10.1109/TSG.2016.2531503.

[50] J. Su, K. Li, Y. Li, C. Xing, and J. Yu, "A novel state-of-charge-based droop control for battery energy storage systems to support coordinated operation of DC microgrids," *IEEE Trans. Emerg. Sel. Topics Power Electron.*, vol. 11, no. 1, pp. 312–324, Feb. 2023, doi: 10.1109/JESTPE.2022.3149398.

[51] Z. Huang, Y. Li, X. Cheng, and M. Ke, "A voltage-shifting-based state-of-charge balancing control for distributed energy storage systems in islanded DC microgrids," *J. Energy Storage*, vol. 69, 2023, Art. no. 107861.

[52] R. Zhang and B. Hredzak, "Distributed dynamic clustering algorithm for formation of heterogeneous virtual power plants based on power requirements," *IEEE Trans. Smart Grid*, vol. 12, no. 1, pp. 192–204, Jan. 2021, doi: 10.1109/TSG.2020.3020163.

[53] K. M. Bhargavi, N. S. Jayalakshmi, D. N. Gaonkar, A. Shrivastava, and V. K. Jadoun, "A comprehensive review on control techniques for power management of isolated DC microgrid system operation," *IEEE Access*, vol. 9, pp. 32196–32228, 2021, doi: 10.1109/ACCESS.2021.3060504.

[54] C. Kewei, L. Qinfen, and X. Zhanpeng, "Control strategy research on charge balancing of hybrid energy storage units with islanded operation mode of DC microgrid," in *2023 IEEE 6th Student Conf. Electric Mach. Syst.*, 2023, pp. 1–7, doi: 10.1109/SCEMS60579.2023.10379414.

[55] N. L. Díaz, A. C. Luna, J. C. Vásquez, and J. M. Guerrero, "Energy management system with equalization algorithm for distributed energy storage systems in pv-active generator based low voltage DC microgrids," in *2015 IEEE 1st Int. Conf. DC Microgrids*, 2015, pp. 293–298, doi: 10.1109/ICDCM.2015.7152057.

[56] S. Wang, Z. Wang, X. Liu, and X. Ye, "An SoC-based bidirectional virtual DC machine control for energy storage systems in offshore isolated island DC microgrids," *J. Mar. Sci. Eng.*, vol. 11, no. 8, 2023, Art. no. 1502, doi: 10.3390/jmse11081502.

[57] G. Kang, W. Fang, and M. Li, "Energy balance control of energy storage system based on improved virtual DC motor," *J. Phys.: Conf. Ser.*, vol. 2625, no. 1, 2023, Art. no. 012021.

[58] G. Lin et al., "An inertia-emulation-based cooperative control strategy and parameters design for multi-parallel energy storage system in islanded DC microgrids," *IET Gener., Transmiss. Distrib.*, vol. 16, no. 21, pp. 4370–4385, 2022.

[59] G. Tian, Y. Zheng, G. Liu, and J. Zhang, "SoC balancing and coordinated control based on adaptive droop coefficient algorithm for energy storage units in DC microgrid," *Energies*, vol. 15, no. 8, 2022, Art. no. 2943, doi: 10.3390/en15082943.

[60] C. Wu, C. Wu, J. Zou, and L. Yan, "SoC balance control strategy for distributed energy storage system in DC microgrid," *J. Phys.: Conf. Ser.*, vol. 2655, no. 1, Nov. 2023, Art. no. 012014, doi: 10.1088/1742-6596/2655/1/012014.

[61] Y. Mi, J. Guo, Y. Fu, C. Wang, and P. Wang, "Accurate power allocation of multienergy storage island DC microgrid based on virtual power rating," *IEEE Trans. Power Electron.*, vol. 38, no. 1, pp. 261–270, Jan. 2023, doi: 10.1109/TPEL.2022.3201373.

[62] Y. Mi et al., "An optimised state-of-charge balance control strategy for distributed energy storage units in islanded DC microgrid," *IET Gener., Transmiss. Distrib.*, vol. 15, no. 6, pp. 1021–1030, 2021.

[63] N. Ghanbari, M. Mobarrez, and S. Bhattacharya, "A review and modeling of different droop control based methods for battery state of the charge balancing in DC microgrids," in *Proc. IECON 2018-44th Annu. Conf. IEEE Ind. Electron. Soc.*, 2018, pp. 1625–1632, doi: 10.1109/IECON.2018.8591739.

[64] X. Chen, R. Tian, S. Xu, W. Jiang, Y. Wang, and S. Hashimoto, "A novel voltage-current dual-drop control method for shipboard DC micro-grid with energy storage systems," *IEEE Access*, vol. 12, pp. 62912–62925, 2024, doi: 10.1109/ACCESS.2024.3395451.

[65] S. Qiao et al., "SoC balancing control strategy based on improved adaptive current distribution coefficient algorithm for multi-energy storage units in DC microgrid," in *2023 3rd New Energy Energy Storage Syst. Control Summit Forum*, 2023, pp. 169–173, doi: 10.1109/NEESSC59976.2023.10349318.

[66] A. Z. Hosseini, G. Joós, and B. Boulet, "Control design for effective usage of electric vehicles in V2G-enabled DC charging stations," *IEEE Trans. Power Del.*, vol. 38, no. 6, pp. 4335–4346, Dec. 2023, doi: 10.1109/TPWRD.2023.3317804.

[67] G. A. H. Pawitan and J.-S. Kim, "MPC-based power management of renewable generation using multi-ESS guaranteeing SoC constraints and balancing," *IEEE Access*, vol. 8, pp. 12897–12906, 2020, doi: 10.1109/ACCESS.2019.2962807.

[68] N. L. Díaz, J. G. Guarnizo, M. Mellado, J. C. Vasquez, and J. M. Guerrero, "A robot-soccer-coordination inspired control architecture applied to islanded microgrids," *IEEE Trans. Power Electron.*, vol. 32, no. 4, pp. 2728–2742, Apr. 2017, doi: 10.1109/TPEL.2016.2572262.

[69] D. I. Brandao, R. P. d. Santos, W. W. A. G. Silva, T. R. Oliveira, and P. F. Donoso-Garcia, "Model-free energy management system for hybrid alternating current/direct current microgrids," *IEEE Trans. Ind. Electron.*, vol. 68, no. 5, pp. 3982–3991, May 2021, doi: 10.1109/TIE.2020.2984993.

[70] Y. Guan, L. Meng, C. Li, J. C. Vasquez, and J. M. Guerrero, "A dynamic consensus algorithm to adjust virtual impedance loops for discharge rate balancing of AC microgrid energy storage units," *IEEE Trans. Smart Grid*, vol. 9, no. 5, pp. 4847–4860, Sep. 2018, doi: 10.1109/TSG.2017.2672882.

[71] R. K. Chauhan et al., "Droop control based battery management system for automated DC microgrid," in *2020 Int. Conf. Contemporary Comput. Appl.*, 2020, pp. 81–86, doi: 10.1109/IC3A48958.2020.233274.

[72] H. Zhang, X. Tong, L. Zhang, and H. Fu, "Fast state-of-charge balancing control strategies for battery energy storage systems to maximize capacity utilization," *J. Energy Storage*, vol. 57, 2023, Art. no. 106269.

[73] X. Lu, K. Sun, J. M. Guerrero, J. C. Vasquez, and L. Huang, "Double-quadrant state-of-charge-based droop control method for distributed energy storage systems in autonomous DC microgrids," *IEEE Trans. Smart Grid*, vol. 6, no. 1, pp. 147–157, Jan. 2015, doi: 10.1109/TSG.2014.2352342.

[74] X. Lu, K. Sun, J. M. Guerrero, J. C. Vasquez, and L. Huang, "State-of-charge balance using adaptive droop control for distributed energy storage systems in DC microgrid applications," *IEEE Trans. Ind. Electron.*, vol. 61, no. 6, pp. 2804–2815, Jun. 2014, doi: 10.1109/TIE.2013.2279374.

[75] N. Ghanbari and S. Bhattacharya, "SoC balancing of different energy storage systems in DC microgrids using modified droop control," in *Proc. IECON 2018-44th Annu. Conf. IEEE Ind. Electron. Soc.*, 2018, pp. 6094–6099, doi: 10.1109/IECON.2018.8592890.

[76] D. Nguyen Huu and H. T. Nam, "Adaptive coordinated droop control for multi-battery storage," in *Proc. IEEE EUROCON 2015 - Int. Conf. Comput. Tool*, 2015, pp. 1–6, doi: 10.1109/EUROCON.2015.7313703.

[77] M. Eydi and R. Ghazi, "A novel communication-less fuzzy based control method to improve SoC balancing, current-sharing, and voltage restoration in a widespread DC microgrid," *Int. J. Elect. Power Energy Syst.*, vol. 135, 2022, Art. no. 107578, doi: 10.1016/j.ijepes.2021.107578.

[78] L. Yuan, S. Gao, B. Liu, F. Xiao, C. Kang, and Z. Zhao, "Hierarchical control of electric energy router system integrated with PV and energy storage," in *2020 23rd Int. Conf. Elect. Mach. Syst.*, 2020, pp. 1052–1057, doi: 10.23919/ICEMS50442.2020.9291101.

[79] K. D. Hoang and H.-H. Lee, "State of charge balancing for distributed battery units based on adaptive virtual power rating in a DC micro-grid," *J. Elect. Eng. Technol.*, vol. 15, no. 5, pp. 2121–2131, Sep. 2020, doi: 10.1007/s42835-020-00482-x.

[80] Y. Mi et al., "State of charge balancing strategy for energy storage system in islanded DC microgrid based on micro-tuning virtual resistance," *Electric Power Syst. Res.*, vol. 209, 2022, Art. no. 107921, doi: 10.1016/j.epsr.2022.107921.

[81] R. Sauer, L. J. R. Silva, M. Von Rondow Campos, C. R. De Aguiar, and R. Q. Machado, "State of charge balancing in primary control for DC/DC microgrids," in *2023 IEEE 8th Southern Power Electron. Conf. 17th Braz. Power Electron. Conf.*, 2023, pp. 1–6, doi: 10.1109/SPEC56436.2023.10407928.

[82] R. Bhosale, R. Gupta, and V. Agarwal, "A novel control strategy to achieve SoC balancing for batteries in a DC microgrid without droop control," *IEEE Trans. Ind. Appl.*, vol. 57, no. 4, pp. 4196–4206, Jul./Aug. 2021, doi: 10.1109/TIA.2021.3073376.

[83] R. Bhosale and V. Agarwal, "A novel control strategy to share power among dispatchable battery sources and achieve SoC balancing without a droop control in a DC microgrid," in *2019 IEEE Ind. Appl. Soc. Annu. Meeting*, 2019, pp. 1–6, doi: 10.1109/IAS.2019.8912464.

[84] T. A. Fagundes, G. H. F. Fuzato, P. G. B. Ferreira, M. Biczkowski, and R. Q. Machado, "Fuzzy controller for energy management and SoC equalization in DC microgrids powered by fuel cell and energy storage units," *IEEE J. Emerg. Sel. Topics Ind. Electron.*, vol. 3, no. 1, pp. 90–100, Jan. 2022, doi: 10.1109/JESTIE.2021.3088419.

[85] X. Ding et al., "Feedback control strategy for state-of-charge balancing and power sharing between distributed battery energy storage units in DC microgrid," *IET Power Electron.*, vol. 16, no. 6, pp. 1063–1076, 2023.

[86] N. L. Díaz, J. C. Vasquez, and J. M. Guerrero, "A communication-less distributed control architecture for islanded microgrids with renewable generation and storage," *IEEE Trans. Power Electron.*, vol. 33, no. 3, pp. 1922–1939, Mar. 2018, doi: 10.1109/TPEL.2017.2698023.

[87] N. L. Díaz, D. Wu, T. Dragičević, J. C. Vásquez, and J. M. Guerrero, "Stored energy balance for distributed PV-based active generators in an AC microgrid," in *2015 IEEE Power Energy Soc. Gen. Meeting*, 2015, pp. 1–5, doi: 10.1109/PESGM.2015.7286330.

[88] O. Palizban and K. Kauhaniemi, "Power sharing for distributed energy storage systems in AC microgrid: Based on state-of-charge," in *2015 IEEE PES Asia-Pacific Power Energy Eng. Conf.*, 2015, pp. 1–5, doi: 10.1109/APPEEC.2015.7381023.

[89] X. Sun, Y. Hao, Q. Wu, X. Guo, and B. Wang, "A multifunctional and wireless droop control for distributed energy storage units in islanded AC microgrid applications," *IEEE Trans. Power Electron.*, vol. 32, no. 1, pp. 736–751, Jan. 2017, doi: 10.1109/TPEL.2016.2531379.

[90] J. V. M. Caracas, G. C. Farias, J. G. de Matos, F. Simões, and L. A. d. S. Ribeiro, "Adaptative droop control for balancing the state of charge of multiple energy storage systems in decentralized microgrids," in *Proc. IECON 2018-44th Annu. Conf. IEEE Ind. Electron. Soc.*, 2018, pp. 1658–1663, doi: 10.1109/IECON.2018.8591697.

[91] H. Mahmood and F. Blaabjerg, "Autonomous power management of distributed energy storage systems in islanded microgrids," *IEEE Trans. Sustain. Energy*, vol. 13, no. 3, pp. 1507–1522, Jul. 2022, doi: 10.1109/TSTE.2022.3156393.

[92] F. Chen, H. Deng, and Z. Shao, "Decentralised control method of battery energy storage systems for SoC balancing and reactive power sharing," *IET Gener., Transmiss. Distrib.*, vol. 14, no. 18, pp. 3702–3709, 2020.

[93] M. Eydi and R. Ghazi, "A novel communication-less control method to improve proportional power-sharing and SoCs balancing in a geographically dispersed hybrid AC/DC microgrid," *Electric Power Syst. Res.*, vol. 209, 2022, Art. no. 107989.

[94] H. Wang, Z. Wu, G. Shi, and Z. Liu, "SoC balancing method for hybrid energy storage system in microgrid," in *2019 IEEE 3rd Int. Conf. Green Energy Appl.*, 2019, pp. 141–145, doi: 10.1109/ICGEA.2019.8880766.

[95] Y. Zeng, Q. Zhang, Y. Liu, X. Zhuang, and H. Guo, "Hierarchical cooperative control strategy for battery storage system in islanded DC microgrid," *IEEE Trans. Power Syst.*, vol. 37, no. 5, pp. 4028–4039, Sep. 2022, doi: 10.1109/TPWRS.2021.3131591.

[96] D. Zha, Q. Wang, M. Cheng, F. Deng, and G. Buja, "Distributed cooperative control for multiple DC electric springs with novel topologies applied in DC microgrid," in *2019 IEEE 10th Int. Symp. Power Electron. Distrib. Gener. Syst.*, 2019, pp. 648–652, doi: 10.1109/PEDG.2019.8807459.

[97] X. Lin, R. Zamora, and C. A. Baguley, "A comprehensive multi-functional controller for hybrid energy storage systems in DC microgrids," *IEEE Trans. Ind. Appl.*, vol. 59, no. 3, pp. 2985–2994, May/Jun. 2023, doi: 10.1109/TIA.2023.3243601.

[98] Y. Hong, D. Xu, W. Yang, B. Jiang, and X.-G. Yan, "A novel multi-agent model-free control for state-of-charge balancing between distributed battery energy storage systems," *IEEE Trans. Emerg. Topics Comput. Intell.*, vol. 5, no. 4, pp. 679–688, Aug. 2021, doi: 10.1109/TETCI.2020.2978434.

[99] D. Xu, W. Zhang, B. Jiang, P. Shi, and S. Wang, "Directed-graph-observer-based model-free cooperative sliding mode control for distributed energy storage systems in DC microgrid," *IEEE Trans. Ind. Informat.*, vol. 16, no. 2, pp. 1224–1235, Feb. 2020, doi: 10.1109/TII.2019.2933227.

[100] B. Li, C. Yu, X. Lu, and F. Wang, "A novel adaptive droop control strategy for SoC balance in PV-based DC microgrids," *ISA Trans.*, vol. 141, pp. 351–364, 2023, doi: 10.1016/j.isatra.2023.07.008.

[101] Q. Zhang et al., "An improved distributed cooperative control strategy for multiple energy storages parallel in islanded DC microgrid," *IEEE Trans. Emerg. Sel. Topics Power Electron.*, vol. 10, no. 1, pp. 455–468, Feb. 2022, doi: 10.1109/JESTPE.2021.3072701.

[102] R. Zhang, B. Hredzak, and T. Morstyn, "Cooperative control of distributed heterogeneous energy storage devices with virtual impedance," in *2017 IEEE Innov. Smart Grid Technol.-Asia*, 2017, pp. 1–6, doi: 10.1109/ISGT-Asia.2017.8378318.

[103] H. Yang, L. Yin, Q. Li, W. Chen, and L. Zhou, "Multiagent-based coordination consensus algorithm for state-of-charge balance of energy storage unit," *Comput. Sci. Eng.*, vol. 20, no. 2, pp. 64–77, 2018, doi: 10.1109/MCSE.2017.3301217.

[104] S. Chen, X. Lu, and Q. Gong, "SoC balance and economic dispatch using distributed cooperative control for distributed energy storage systems in DC microgrid applications," in *Proc. IECON 2020 46th Annu. Conf. IEEE Ind. Electron. Soc.*, 2020, pp. 3371–3376, doi: 10.1109/IECON43393.2020.9254280.

[105] H. Yang, S. Li, Q. Li, and W. Chen, "Hierarchical distributed control for decentralized battery energy storage system based on consensus algorithm with pinning node," *Protection Control Modern Power Syst.*, vol. 3, no. 1, pp. 1–9, 2018, doi: 10.1186/s41601-018-0081-5.

[106] B. Huang, S. Zheng, R. Wang, H. Wang, J. Xiao, and P. Wang, "Distributed optimal control of DC microgrid considering balance of charge state," *IEEE Trans. Energy Convers.*, vol. 37, no. 3, pp. 2162–2174, Sep. 2022, doi: 10.1109/TEC.2022.3169462.

[107] J. Lang, C. Zhang, F. Xia, G. Wang, and X. Wang, "Self-disciplined nonsmooth coordination control for battery energy storage system in autonomous DC microgrids toward large-signal stability," *IEEE Trans. Smart Grid*, vol. 14, no. 2, pp. 928–938, Mar. 2023, doi: 10.1109/TSG.2022.3206336.

[108] P. Lin, T. Zhao, B. Wang, Y. Wang, and P. Wang, "A semi-consensus strategy toward multi-functional hybrid energy storage system in DC microgrids," *IEEE Trans. Energy Convers.*, vol. 35, no. 1, pp. 336–346, Mar. 2020, doi: 10.1109/TEC.2019.2936120.

[109] P. Lin, C. Deng, Y. Yang, C. H. T. Lee, and W. P. Tay, "Resilience-oriented control for cyber-physical hybrid energy storage systems using a semiconsensus scheme: Design and practice," *IEEE Trans. Ind. Electron.*, vol. 70, no. 3, pp. 2508–2519, Mar. 2023, doi: 10.1109/TIE.2021.3102397.

[110] X. Chen, M. Shi, H. Sun, Y. Li, and H. He, "Distributed cooperative control and stability analysis of multiple DC electric springs in a DC microgrid," *IEEE Trans. Ind. Electron.*, vol. 65, no. 7, pp. 5611–5622, Jul. 2018, doi: 10.1109/TIE.2017.2779414.

[111] C. Li, T. Dragicevic, M. G. Plaza, F. Andrade, J. C. Vasquez, and J. M. Guerrero, "Multiagent based distributed control for state-of-charge balance of distributed energy storage in DC microgrids," in *Proc. IECON 2014-40th Annu. Conf. IEEE Ind. Electron. Soc.*, 2014, pp. 2180–2184, doi: 10.1109/IECON.2014.7048804.

[112] R. Zhang, B. Hredzak, and T. Morstyn, "Distributed control with virtual capacitance for the voltage restorations, state of charge balancing, and load allocations of heterogeneous energy storages in a DC datacenter microgrid," *IEEE Trans. Energy Convers.*, vol. 34, no. 3, pp. 1296–1308, Sep. 2019, doi: 10.1109/TEC.2018.2889065.

[113] D. Xu, A. Xu, C. Yang, and P. Shi, "Uniform state-of-charge control strategy for plug-and-play electric vehicle in super-ups," *IEEE Trans. Transport. Electrific.*, vol. 5, no. 4, pp. 1145–1154, Dec. 2019, doi: 10.1109/TTE.2019.2939930.

[114] R. Zhang and B. Hredzak, "Distributed finite-time multiagent control for DC microgrids with time delays," *IEEE Trans. Smart Grid*, vol. 10, no. 3, pp. 2692–2701, May 2019, doi: 10.1109/TSG.2018.2808467.

[115] Z. Huang, Y. Li, M. Ke, and J. Deng, "Distributed secondary control with an event-triggered consensus-based observer for energy storage systems in islanded DC microgrids," *IEEE Trans. Sustain. Energy*, vol. 15, no. 2, pp. 1167–1179, Apr. 2024, doi: 10.1109/TSTE.2023.3329950.

[116] Y. Zeng, Q. Zhang, Y. Liu, X. Zhuang, X. Lv, and H. Wang, "An improved distributed secondary control strategy for battery storage system in DC shipboard microgrid," *IEEE Trans. Ind. Appl.*, vol. 58, no. 3, pp. 4062–4075, May/Jun. 2022, doi: 10.1109/TIA.2022.3153755.

[117] X. Chen et al., "Distributed cooperative control of multiple hybrid energy storage systems in a DC microgrid using consensus protocol," *IEEE Trans. Ind. Electron.*, vol. 67, no. 3, pp. 1968–1979, Mar. 2020, doi: 10.1109/TIE.2019.2898606.

[118] H. Zhao and W. Guo, "Hierarchical distributed coordinated control strategy for hybrid energy storage array system," *IEEE Access*, vol. 7, pp. 2364–2375, 2019, doi: 10.1109/ACCESS.2018.2886595.

[119] L. Xing et al., "Distributed state-of-charge balance control with event-triggered signal transmissions for multiple energy storage systems in smart grid," *IEEE Trans. Syst., Man, Cybern. Syst.*, vol. 49, no. 8, pp. 1601–1611, Aug. 2019, doi: 10.1109/TSMC.2019.2916152.

[120] L. Xing et al., "Robust event-triggered dynamic average consensus against communication link failures with application to battery control," *IEEE Trans. Control Netw. Syst.*, vol. 7, no. 3, pp. 1559–1570, Sep. 2020, doi: 10.1109/TCNS.2020.2986515.

[121] T. Morstyn, B. Hredzak, and V. G. Agelidis, "Cooperative multi-agent control of heterogeneous storage devices distributed in a DC microgrid," *IEEE Trans. Power Syst.*, vol. 31, no. 4, pp. 2974–2986, Jul. 2016, doi: 10.1109/TPWRS.2015.2469725.

[122] Y. Yang, D. Xu, T. Ma, and X. Su, "Adaptive cooperative terminal sliding mode control for distributed energy storage systems," *IEEE Trans. Circuits Syst. I: Reg. Papers*, vol. 68, no. 1, pp. 434–443, Jan. 2021, doi: 10.1109/TCSI.2020.3027376.

[123] T. Meng, Z. Lin, Y. Wan, and Y. A. Shamash, "State-of-charge balancing for battery energy storage systems in DC microgrids by distributed adaptive power distribution," *IEEE Contr. Syst. Lett.*, vol. 6, pp. 512–517, May 20, 2021, doi: 10.1109/LCSYS.2021.3082103.

[124] Y. Zeng, Q. Zhang, Y. Liu, H. Guo, F. Zhang, and S. You, "Distributed unified controller design for parallel battery storage system in DC shipboard microgrid," *IEEE Trans. Power Syst.*, vol. 39, no. 1, pp. 546–563, Jan. 2024, doi: 10.1109/TPWRS.2023.3244967.

[125] H. Cai, "Power tracking and state-of-energy balancing of an energy storage system by distributed control," *IEEE Access*, vol. 8, pp. 170261–170270, 2020, doi: 10.1109/ACCESS.2020.3024714.

[126] Y. Wang et al., "Aggregated energy storage for power system frequency control: A finite-time consensus approach," *IEEE Trans. Smart Grid*, vol. 10, no. 4, pp. 3675–3686, Jul. 2019, doi: 10.1109/TSG.2018.2833877.

[127] Y. Dai, L. Zhang, K. Yan, Q. Chen, Z. Zhou, and K. Zhou, "An integrated cooperative control strategy for EVs accessed community uninterruptible power system," *IEEE Trans. Intell. Veh.*, vol. 8, no. 3, pp. 2482–2493, Mar. 2023, doi: 10.1109/TIV.2022.3163147.

[128] D. Li, Z. Wu, B. Zhao, and L. Zhang, "An improved droop control for balancing state of charge of battery energy storage systems in AC microgrid," *IEEE Access*, vol. 8, pp. 71917–71929, 2020, doi: 10.1109/ACCESS.2020.2987098.

[129] R. Zhang, B. Hredzak, and D. Chen, "Bi-level control structure with accurate real and reactive powers sharing for low voltage microgrids with highly resistive line impedances," in *2020 IEEE 9th Int. Power Electron. Motion Control Conf.*, 2020, pp. 1210–1215, doi: 10.1109/IPEMC-ECCEAsia48364.2020.9368181.

[130] S. V. Ouoba, A. Houari, M. Machmoum, and J. M. Guerrero, "A novel resilient state of charge balancing method for distributed storage systems based autonomous microgrids," *J. Energy Storage*, vol. 55, 2022, Art. no. 105439.

[131] M. C. Merchán-Riveros and C. Albea, "Hybrid dynamical control for discharging rate consensus in AC-bus microgrids," *IEEE Contr. Syst. Lett.*, vol. 7, pp. 2323–2328, Jun. 15, 2023, doi: 10.1109/LCSYS.2023.3286579.

[132] M. C. Merchán-Riveros and C. Albea, "Three time-scale singular perturbation hybrid control and large-signal analysis stability in AC-microgrids," *IEEE Trans. Circuits Syst. I: Reg. Papers*, vol. 70, no. 8, pp. 3373–3386, Aug. 2023, doi: 10.1109/TCSI.2023.3273814.

[133] A. M. Shotorbani, B. Mohammadi-Ivatloo, L. Wang, S. Ghassem-Zadeh, and S. H. Hosseini, "Distributed secondary control of battery energy storage systems in a stand-alone microgrid," *IET Gener., Transmiss. Distrib.*, vol. 12, no. 17, pp. 3944–3953, 2018.
[134] R. Zhang, B. Hredzak, and G. Konstantinou, "Distributed control for microgrid batteries communicating over network with aperiodically sampled data with time delays," in *2019 10th Int. Conf. Power Electron. ECCE Asia*, 2019, pp. 2629–2634, doi: 10.23919/ICPE2019-ECCEAsia42246.2019.8797106.
[135] S. M. Rostami and M. Hamzeh, "An adaptive multi-functional control strategy for power management and voltage-frequency regulation of PV, BESS, and hybrid units in a microgrid," *IEEE Trans. Smart Grid*, vol. 15, no. 4, pp. 3446–3458, Jul. 2024, doi: 10.1109/TSG.2023.3345741.
[136] R. Zhang and B. Hredzak, "Nonlinear sliding mode and distributed control of battery energy storage and photovoltaic systems in AC microgrids with communication delays," *IEEE Trans. Ind. Informat.*, vol. 15, no. 9, pp. 5149–5160, Sep. 2019, doi: 10.1109/TII.2019.2896032.
[137] C. Yu, X. Lu, J. Lai, and L. Chai, "Distributed frequency restoration and SoC balancing control for AC microgrids," *Int. J. Elect. Power Energy Syst.*, vol. 136, 2022, Art. no. 107557.
[138] J. Lu, X. Liu, X. Hou, and P. Wang, "A distributed control strategy for state-of-charge balance of energy storage without continuous communication in AC microgrids," *IEEE Trans. Sustain. Energy*, vol. 14, no. 1, pp. 206–216, Jan. 2023, doi: 10.1109/TSTE.2022.3206327.
[139] W. Kang et al., "Distributed event-triggered optimal control method for heterogeneous energy storage systems in smart grid," *IEEE Trans. Sustain. Energy*, vol. 13, no. 4, pp. 1944–1956, Oct. 2022, doi: 10.1109/TSTE.2022.3176741.
[140] W. Kang, Y. Guan, B. YunYu, J. C. V. Q. A. Zavar, and J. M. Guerrero, "Distributed event-triggered secondary frequency regulation by sharing HESS power in microgrids," *IEEE Trans. Smart Grid*, vol. 15, no. 4, pp. 3375–3389, Jul. 2024, doi: 10.1109/TSG.2024.3357772.
[141] W. Kang et al., "Distributed reactive power control and SoC sharing method for battery energy storage system in microgrids," *IEEE Access*, vol. 7, pp. 60707–60720, 2019, doi: 10.1109/ACCESS.2019.2910352.
[142] M. Raeispour, H. Atrianfar, H. R. Baghaee, and G. B. Gharehpetian, "Resilient H_∞ consensus-based control of autonomous AC microgrids with uncertain time-delayed communications," *IEEE Trans. Smart Grid*, vol. 11, no. 5, pp. 3871–3884, Sep. 2020, doi: 10.1109/TSG.2020.2992646.
[143] J. Han et al., "Optimization of communication network for distributed control of wind farm equipped with energy storages," *IEEE Trans. Sustain. Energy*, vol. 14, no. 4, pp. 1933–1949, Oct. 2023, doi: 10.1109/TSTE.2023.3264656.
[144] L. Xiong et al., "Voltage and frequency regulation with WT-PV-BESS in remote weak grids via fixed-time containment control," *IEEE Trans. Power Syst.*, vol. 38, no. 3, pp. 2719–2735, May 2023, doi: 10.1109/TPWRS.2022.3190847.
[145] R. Zhang, B. Hredzak, and J. Fletcher, "Dynamic aggregation of energy storage systems into virtual power plants using distributed real-time clustering algorithm," *IEEE Trans. Ind. Electron.*, vol. 68, no. 11, pp. 11002–11013, Nov. 2021, doi: 10.1109/TIE.2020.3038074.
[146] R. Zhang, Z. Liu, Z. Bie, and B. Hredzak, "Dynamic clusters supported bi-level control system with lower communication requirements for a distribution network with distributed battery and photovoltaic systems," *IEEE Trans. Smart Grid*, vol. 15, no. 4, pp. 3824–3838, Jul. 2024, doi: 10.1109/TSG.2024.3379455.
[147] C. Deng, Y. Wang, C. Wen, Y. Xu, and P. Lin, "Distributed resilient control for energy storage systems in cyber–physical microgrids," *IEEE Trans. Ind. Informat.*, vol. 17, no. 2, pp. 1331–1341, Feb. 2021, doi: 10.1109/TII.2020.2981549.
[148] A. Afshari, M. Karrari, H. R. Baghaee, and G. B. Gharehpetian, "Resilient synchronization of voltage/frequency in AC microgrids under deception attacks," *IEEE Syst. J.*, vol. 15, no. 2, pp. 2125–2136, Jun. 2021, doi: 10.1109/JSYST.2020.2992309.
[149] S. A. G. K. Abadi, T. Khalili, S. I. Habibi, A. Bidram, and J. M. Guerrero, "Adaptive control and management of multiple nano-grids in an islanded DC microgrid system," *IET Gener., Transmiss. Distrib.*, vol. 17, no. 8, pp. 1799–1815, 2023.
[150] H. Han, Y. Zhu, G. Shi, M. Su, and Y. Sun, "A local-distributed and global-decentralized SoC balancing method for hybrid series-parallel energy storage system," *IEEE Syst. J.*, vol. 16, no. 2, pp. 2289–2299, Jun. 2022, doi: 10.1109/JSYST.2021.3068167.
[151] B. Zhang, F. Gao, D. Liao, D. Liu, and P. W. Wheeler, "A dynamic diffusion algorithm for discrete-time cooperative control for DC microgrids," *IEEE Trans. Power Electron.*, vol. 39, no. 8, pp. 9399–9414, Aug. 2024, doi: 10.1109/TPEL.2024.3395998.
[152] S. Jena and N. P. Padhy, "Cyber-secure global energy equalization in DC microgrid clusters under data manipulation attacks," *IEEE Trans. Ind. Appl.*, vol. 59, no. 5, pp. 5488–5505, Sep./Oct. 2023, doi: 10.1109/TIA.2023.3287969.
[153] K. Bi, S. Zhang, Y. Zhu, W. Huang, W. Lu, and Q. Fan, "An improved SoC balancing strategy for HVDC modular energy storage system based on low bandwidth communication with enhanced current regulation accuracy," *IEEE Trans. Energy Convers.*, vol. 36, no. 4, pp. 3355–3364, Dec. 2021, doi: 10.1109/TEC.2021.3082300.
[154] Z. Wang, H. Lin, and Y. Ma, "A control strategy of modular multilevel converter with integrated battery energy storage system based on battery side capacitor voltage control," *Energies*, vol. 12, no. 11, 2019, Art. no. 2151, doi: 10.3390/en12112151. [Online]. Available: https://www.mdpi.com/1996-1073/12/11/2151
[155] H. Liang, L. Guo, J. Song, Y. Yang, W. Zhang, and H. Qi, "State-of-charge balancing control of a modular multilevel converter with an integrated battery energy storage," *Energies*, vol. 11, no. 4, 2018, Art. no. 873, doi: 10.3390/en11040873. [Online]. Available: https://www.mdpi.com/1996-1073/11/4/873
[156] M. Vasiladiotis and A. Rufer, "Analysis and control of modular multilevel converters with integrated battery energy storage," *IEEE Trans. Power Electron.*, vol. 30, no. 1, pp. 163–175, Jan. 2015, doi: 10.1109/TPEL.2014.2303297.
[157] Q. Wang, "State of charge equalization control strategy of modular multilevel converter with battery energy storage system," in *2020 5th Int. Conf. Power Renewable Energy*, 2020, pp. 316–320, doi: 10.1109/ICPRE51194.2020.9233136.
[158] N. Li et al., "Optimal group charging method for battery integrated modular multilevel converter," in *2020 IEEE 9th Int. Power Electron. Motion Control Conf.*, 2020, pp. 2618–2621, doi: 10.1109/IPEMC-ECCEAsia48364.2020.9367916.
[159] F. Eroğlu, M. Kurtoğlu, A. Eren, and A. M. Vural, "A novel adaptive state-of-charge balancing control scheme for cascaded h-bridge multilevel converter based battery storage systems," *ISA Trans.*, vol. 135, pp. 339–354, 2023, doi: 10.1016/j.isatra.2022.09.044.
[160] E. J. Agnoletto, D. Silva de Castro, R. V. A. Neves, R. Quadros Machado, and V. A. Oliveira, "An optimal energy management technique using the ϵ-constraint method for grid-tied and stand-alone battery-based microgrids," *IEEE Access*, vol. 7, pp. 165928–165942, 2019, doi: 10.1109/ACCESS.2019.2954050.
[161] A. Parisio, E. Rikos, and L. Glielmo, "A model predictive control approach to microgrid operation optimization," *IEEE Trans. Control Syst. Technol.*, vol. 22, no. 5, pp. 1813–1827, Sep. 2014, doi: 10.1109/TCST.2013.2295737.
[162] E. Hossain, D. Murtaugh, J. Mody, H. M. R. Faruque, M. S. H. Sunny, and N. Mohammad, "A comprehensive review on second-life batteries: Current state, manufacturing considerations, applications, impacts, barriers & potential solutions, business strategies, and policies," *IEEE Access*, vol. 7, pp. 73215–73252, 2019, doi: 10.1109/ACCESS.2019.2917859.
[163] S. J. Tong, A. Same, M. A. Kootstra, and J. W. Park, "Off-grid photovoltaic vehicle charge using second life lithium batteries: An experimental and numerical investigation," *Appl. Energy*, vol. 104, pp. 740–750, 2013, doi: 10.1016/j.apenergy.2012.11.046. [Online]. Available: https://www.sciencedirect.com/science/article/pii/S0306261912008495
[164] J. S. Edge et al., "Lithium ion battery degradation: What you need to know," *Phys. Chem. Chem. Phys.*, vol. 23, no. 14, pp. 8200–8221, 2021.
[165] M. Cheng, X. Zhang, A. Ran, G. Wei, and H. Sun, "Optimal dispatch approach for second-life batteries considering degradation with online soh estimation," *Renewable Sustain. Energy Rev.*, vol. 173, 2023, Art. no. 113053, doi: 10.1016/j.rser.2022.113053. [Online]. Available: https://www.sciencedirect.com/science/article/pii/S1364032122009340

[166] J. Yang, M. Beatty, D. Strickland, M. Abedi-Varnosfaderani, and J. Warren, "Second-life battery capacity estimation and method comparison," *Energies*, vol. 16, no. 7, 2023, Art. no. 3244, doi: 10.3390/en16073244. [Online]. Available: https://www.mdpi.com/1996-1073/16/7/3244

[167] J. Lacap, J. W. Park, and L. Beslow, "Development and demonstration of microgrid system utilizing second-life electric vehicle batteries," *J. Energy Storage*, vol. 41, 2021, Art. no. 102837.

[168] X. Cui et al., "Lite-sparse hierarchical partial power processing for second-use battery energy storage systems," *IEEE Access*, vol. 10, pp. 90761–90777, 2022, doi: 10.1109/ACCESS.2022.3201132.

[169] N. Mukherjee and D. Strickland, "Analysis and comparative study of different converter modes in modular second-life hybrid battery energy storage systems," *IEEE Trans. Emerg. Sel. Topics Power Electron.*, vol. 4, no. 2, pp. 547–563, Jun. 2016, doi: 10.1109/JESTPE.2015.2460334.

[170] C. Liu, X. Cai, and Q. Chen, "Self-adaptation control of second-life battery energy storage system based on cascaded h-bridge converter," *IEEE Trans. Emerg. Sel. Topics Power Electron.*, vol. 8, no. 2, pp. 1428–1441, Jun. 2020, doi: 10.1109/JESTPE.2018.2886965.

[171] C. Liu, N. Gao, X. Cai, and R. Li, "Differentiation power control of modules in second-life battery energy storage system based on cascaded h-bridge converter," *IEEE Trans. Power Electron.*, vol. 35, no. 6, pp. 6609–6624, Jun. 2020, doi: 10.1109/TPEL.2019.2954577.

[172] G. Liang et al., "A constrained intersubmodule state-of-charge balancing method for battery energy storage systems based on the cascaded h-bridge converter," *IEEE Trans. Power Electron.*, vol. 37, no. 10, pp. 12669–12678, Oct. 2022, doi: 10.1109/TPEL.2022.3170062.

[173] N. Mukherjee and D. Strickland, "Control of second-life hybrid battery energy storage system based on modular boost-multilevel buck converter," *IEEE Trans. Ind. Electron.*, vol. 62, no. 2, pp. 1034–1046, Feb. 2015, doi: 10.1109/TIE.2014.2341598.

THALES AUGUSTO FAGUNDES was born in Jundiai, Brazil. In 2014, he studied abroad with the University of New South Wales Sydney, NSW, Australia, focusing on courses related to alternative energy sources. He received the B.S. degree in electrical engineering and the M.S. degree in power electronics and dynamic systems from the University of Sao Paulo, Sao Carlos, Brazil, in 2017 and 2020, respectively, where he is currently working toward the Ph.D. degree in electrical engineering.

From 2022 to 2023, he was a Visiting Researcher with Aalborg University, Aalborg, Denmark. His main research interests include the fields of microgrids, energy management, and dc–dc converters for renewable energy sources and storage systems.

GUILHERME HENRIQUE FAVARO FUZATO (Member, IEEE) was born in Varginha, Brazil, in 1989. He received the B.S. in electrical engineering in 2011, the M.S. degree in power electronics and dynamic systems in 2015, and the Ph.D. degree in microgrids from the University of Sao Paulo, Sao Carlos, Brazil, in 2011, 2015, and 2019, respectively.

From 2018 to 2019, he was a Visiting Researcher with the University of Aalborg, Aalborg, Denmark. From 2012 to 2013, he worked at Siemens as a field service engineer in automation area. From 2014 to 2015, he worked at Bosch with power electronics in automotive applications as a temporary Researcher. Since 2016, he has been working as a Lecturer with the Federal Institute of Education, Science and Technology of Sao Paulo, Campinas, Brazil. His main research interests include the fields of microgrids, energy management, and dc/dc converter for renewable energy sources and storage systems.

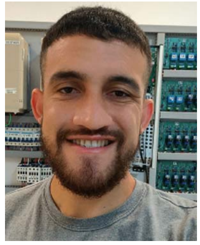

LUCAS JONYS RIBEIRO SILVA received the B.S. in electrical engineering from The Federal University of Viçosa, Viçosa MG, USA, in 2020, and the M.S. degree in 2022 from the University of Sao Paulo, Sao Carlos, Brazil, where he is currently working toward the Ph.D. degree in electrical engineering.

His main research interest are in the fields of microgrids, electric and hybrid vehicles, energy management, and dc/dc converters for renewable energy sources and storage systems.

AUGUSTO MATHEUS DOS SANTOS ALONSO (Member, IEEE) received the double Ph.D. degrees in electric power engineering from the Sao Paulo State University (UNESP), Sao Paulo, Brazil, and the Norwegian University of Science and Technology (NTNU), Norway, in 2021.

He was a Postdoctoral Researcher with the University of Campinas, Campinas, Brazil, until June 2022. In 2015, he was with Whirlpool Latin America/IEL/CNPq as an R&D engineer under the InovaTalentos Fellowship. Currently, he is an Assistant Professor with the Department of Electrical and Computer Engineering, University of Sao Paulo. His main interests are digital control of power converters, microgrid control, power quality, electric vehicles, and smart grids.

Dr. Alonso was the recipient of the FAPESP fund for postdoctoral research, and the Brazilian Power Electronics Society (SOBRAEP) award for the best M.S. dissertation and best Ph.D. thesis of the year, in 2019 and 2022, respectively. He is a Member SOBRAEP.

JUAN C. VASQUEZ (Senior Member, IEEE) received the B.S. degree in electronics engineering from the Autonomous University of Manizales, Manizales, Colombia, in 2002, and the M.Sc. and Ph.D. degrees in automatic control, robotics, and computer vision from the Technical University of Catalonia, Barcelona, Spain, in 2004 and 2009, respectively.

In 2019, he was a Professor of energy internet and microgrids. He is currently the Codirector of the Villum Center for Research on Microgrids. He has authored or coauthored more than 450 journal articles cited more than 30 000 times. His research interests include operation, control, energy management applied to ac/dc microgrids, the integration of IoT, energy internet, digital twin, and blockchain solutions.

Dr. Vasquez was the recipient of the Highly Cited Researcher, since 2017, and the Young Investigator Award, in 2019.

JOSEP M. GUERRERO (Fellow, IEEE) received the B.S. degree in telecommunications engineering, the M.S. degree in electronics engineering, and the Ph.D. degree from the Technical University of Catalonia, Barcelona, Spain, in 1997, 2000, and 2003, respectively.

In 2019, he was a Villum Investigator with the Villum Fonden, which supports the Center for Research on Microgrids (CROM), Aalborg University, Aalborg, Denmark, where since 2011, he has been a Full Professor with the Department of Energy Technology. His research interests include different microgrid aspects, including applications as remote communities, energy prosumers, and maritime and space microgrids.

RICARDO QUADROS MACHADO (Senior Member, IEEE) was born in Santa Maria, Brazil. He received the B.S. degree in electrical engineering from the University of Santa Maria, Santa Maria, Brazil, in 1997, the M.S. and the Ph.D. degrees in electrical engineering from the University of Campinas, Campinas, Brazil, in 2000 and 2005, respectively.

From 2002 to 2003, he was a Visiting Researcher with the University of Padova, Padova, Italy, and from 2005 to 2007, he was a Postdoctorate with the Federal University of Santa Maria, Santa Maria. From 2013 to 2014, he was a Visiting Professor with the University of Toronto, Toronto, ON, Canada. Additionally, from 2007 to 2018, he was Assistant Professor with the University of Sao Paulo, Sao Carlos, Brazil, where he is currently an Associate Professor. His main research interests include processing of energy in dc/dc and dc/ac converters, digital control of power converters, distributed generation systems, smart grids, and control of renewable energy sources.